Investigation of the “Plastic-Behavior” Region in Leak-Off Tests

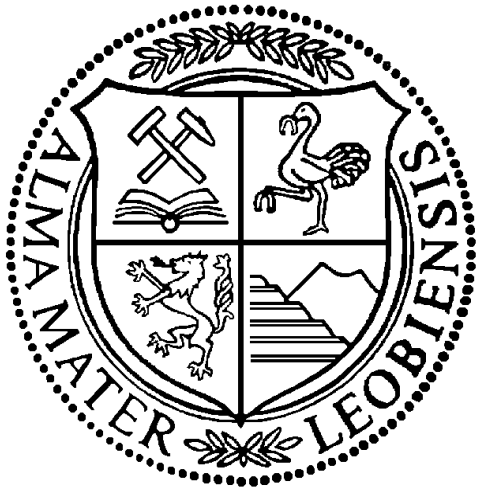

MASTER THESIS

Department of Mineral Resources and Petroleum Engineering

MONTANUNIVERSITÄT LEOBEN, AUSTRIA

Christian Allerstorfer

Leoben, October 2011

DEDICATED TO MY FAMILY AND FRIENDS

Affidavit

I declare in lieu of oath, that I wrote this thesis myself and have not used any sources other than quoted at the end of the thesis. This Master Thesis has not been submitted elsewhere for examination purpose.

Ich erkläre hiermit Eides statt, die vorliegende Arbeit eigenhändig, lediglich unter Verwendung der zitierten Literatur angefertigt zu haben. Diese Diplomarbeit wurde nirgends sonst zur Beurteilung eingereicht.

Leoben, November 8, 2011

(Christian Allerstorfer)

Acknowledgment

First, I would like to thank my advisor at OMV, Dipl. Ing. Hermann F. Spörker, Head of Well Engineering OMV Austria, for giving me the chance to write this thesis on Leak-Off Tests and for providing me the opportunity to include my thought and ideas in this work. I want to thank him for his guidance and for his critical view on the problems challenged throughout this work. I really enjoyed working with him at the OMV Headoffice and I am very thankful for his support.

Furthermore, I would like to thank Univ.-Prof. Dipl. Ing. Dr. mont. Gerhard Thonhauser for being my advisor at the University of Leoben whose help, advice and supervision was invaluable. I also want to thank all other staff members of the University of Leoben who have been involved in this thesis becoming a success, especially Univ.-Prof. Dipl.-Geol. PhD. Stephan Matthäi for his expertise.

Special thanks go to all my colleagues at OMV who supported me, especially Günther Fuhry, Team Leader of Pumping Service, OMV Gänserndorf, Dipl. Ing. Markus Mostegel and Dipl.Geol. Michael König.

Last but not least, I want to thank my family and friends who have always been a great support, not only during my academic studies but throughout my whole live.

Abstract

Aim of this master thesis was to investigate Leak-Off Tests (LOT) in more detail. Throughout the industry different explanations for the actual shape of the pressure vs. time and pressure vs. volume curve exist. The part of the curve where the first deviation from a straight line is observed should be investigated in more detail.

A literature research has been conducted, studying literature published throughout the industry as well as publications of different universities and scientific literature.

First, all factors affecting a Leak-Off Test as well as the Leak-Off Test procedure have been reviewed in detail. Data available at OMV was studied in detail and reevaluated. Aim was to identify the impact of the single effects on such a test. Focus of investigation was the linear region in the first place. Reason was to narrow down the possible effects responsible for the first deviation. These effects, termed cased hole effects, include casing expansion and mud compressibility as well as gas trapped in the drilling fluid. Furthermore, operational influences, like the way of measurement are discussed, to finally closer investigate effects that might be a possible reason for the observed behavior. These effects, termed open-hole effects, are induced fracturing, filtration but also preexisting fractures.

Moreover, theories explaining what happens at the Leak-Off Point are discussed. Leak-Off Test data is analyzed in more detail and conclusions on permanent formation damage and what causes the slope of the pressure vs. volume chart to decline after the Leak-Off Point has been exceeded and therefore what the physical meaning of this point is made.

Kurzfassung

Ziel dieser Arbeit ist es Leak-Off Tests genauer zu untersuchen. Da verschiedene Erklärungen des resultierenden Druck – Volumen und Druck – Zeit – Graphen aus solchen Tests existieren, sollen diese, insbesondere aber der Punkt der ersten Abweichung vom linearen Teil der Kurven, genauer untersucht werden.

Eine umfassende Literaturrecherche, welche sowohl einschlägige Fachliteratur als auch Publikation an verschiedenen Universitäten und Wissenschaftliche Abhandlungen umfasst, wurde durchgeführt.

Zuerst werden sämtliche Faktoren welche einen solchen Test, als auch die Test Prozedur selbst, detailliert behandelt. Verfügbare Test Daten wurden ausgewertet und Beispiele berechnet. Der Fokus der Untersuchung und Berechnungen liegt in den ersten Kapiteln auf dem linearem Bereich der Kurve. Ziel ist es die möglichen Gründe der ersten Abweichung vom linearen Verhalten einzuschränken. Die behandelten Effekte beinhalten Expansion der Verrohrung, Kompressibilität der Bohrspühlung und Gaseinschlüsse in der Bohrspühlung.

Des Weiteren, werden Einflüsse welche auf die Durchführung des Tests selbst zurückzuführen sind, wie Pump rate und Messanordnung, behandelt um letztendlich jene Effekte welche als mögliche Gründe für die erste Abweichung übrig bleiben genauer zu untersuchen. Dies beinhaltet, Spaltenbildung im Gestein, bereits vorhanden Spalten und Klüfte sowie Filtration an permeablen Gesteinsschichten.

Verschiedene publizierte Theorien welche erklären was am Lek-Off Punkt passiert werden mit den zuvor gewonnenen Erkenntnissen genauer untersucht und auf Plausibilität hin überprüft. Leak-Off Test Daten werden genauer analysiert um Schlüsse hinsichtlich permanenter Schädigung der Formation, Gründe für die Abweichung vom linearem Verhalten und der physikalischen Bedeutung der Leak-Off Punktes ziehen zu können.

Table of Contents

1 Introduction

As the Oil and Gas industry is forced to move into more and more difficult environments, understanding geomechanics becomes increasingly important. Knowledge of the downhole stress field is of major importance when combating wellbore stability issues or planning shale gas development wells which will be subject to extensive fracturing treatments.

During drilling, information on the principal stresses can only be obtained by performing Formation Strength Tests (FST). These Formation Strength Tests, in particular Leak-Off Tests (LOT) and Extended Leak-Off Tests (xLOT) have been performed throughout the industry for decades. The data obtained, is used to evaluate the strength of the formation, to verify the quality of cement jobs as well as to estimate the main principal stress magnitudes. The interpretation provides the basis for critical decisions such as casing setting depth, maximum allowable mud weight, well-control response and cement integrity verification. Wrong estimations can not only result in increasing costs but may also cause potentially dangerous situations like lost circulation, problems during well control and wellbore stability problems. Hence, proper identification of downhole stresses will ultimately result in a reduction of non-productive time and thereby reduce drilling cost and improved safety, especially in regions of small pressure margins.

Even though Formation Strength Test are widely considered as well established and routine operation, with straightforward execution and interpretation, they provide a series of challenges, which are rarely accounted for in daily operation (van Oort & Vargo, 2007).

Up to now, slightly different explanations, nomenclature and interpretations of the pressure vs. volume and pressure vs. time plot as it is obtained from Formation Strength Tests exist, what raises the need for further investigation of these interpretations.

Especially, the part of the plot where the first deviation from a straight line is observed is interpreted differently. The mentioned behavior is often referred to as "plastic behavior" in analogy to the plastic behavior of steel under stress. The point of the first deviation is usually called "Leak-Off Point" (LOP) or "Fracture Initiation Pressure" (FIP). The reason for this deviation however is explained by different physical phenomena. Oort and Vargo 2007 explain the behavior by change in system stiffness due to the initiation of a near wellbore fracture. Zoback 2007 sees the additional volume created, as a fracture which is initiated, as sufficient for the deviation. Aadnoy 2009 introduces an approach suggesting a stress bridge to form allowing the pressure to increase beyond the fracture initiation pressure. Other explanations explain the behavior by fluid leaking off into the formation. In the later, a fracture is assumed to be initiated at the point where no further increase in pressure can be achieved, which is commonly termed "Formation Breakdown Pressure" (FBP).

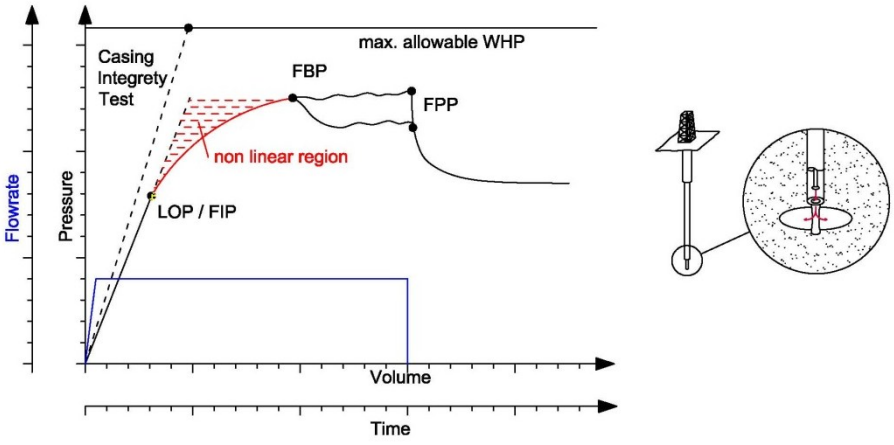

Figure 1 – Formation Strength Test

Obviously, the behavior has to come with a very specific, significant change in the system. In order to evaluate different explanations. The factors influencing Formation Strength Tests data will be investigated, to identify their impacts. Leak-Off Test volumetrics will be analyzed in order to be able to evaluate different explanations. Furthermore, the observed behavior raises the question if Leak-Off Tests damage the formation or have impact on the post-test formation strength. The near wellbore stress field, as well as fracture mechanics, will be used to challenge the question of what happens during the deviation from the straight line.

2 Formation Strength Tests

Formation Strength Test are performed routinely after one section has been drilled, the casing has been run and cemented into place. The casing shoe and about 3-5m of new formation is drilled after the cement has set before the test is performed. Depending on the maximum test pressure and the impact of the pressure on the formation, Formation Strength Tests can be separated into three general types of tests. These are Formation Integrity Tests (FIT), Leak-Off Test (LOT) and Extended Leak-Off Test (xLOT). A variety of procedures, test nomenclature and test interpretation methodologies exist, as there is no standard procedure throughout the industry. The procedures and nomenclatures introduced in this chapter are a recommendation.

Aim of performing Formation Strength Tests is:

- Verify the integrity of the cement at the casing shoe
- Verify the integrity of the formation up to the maximum pressure (required mud weight including kick tolerance) expected during drilling the next section
- Identifying the limits of the formation
- Get information on minimum insitu stress magnitude
- Estimate other formation properties like permeability

2.1 General Definitions and Nomenclature

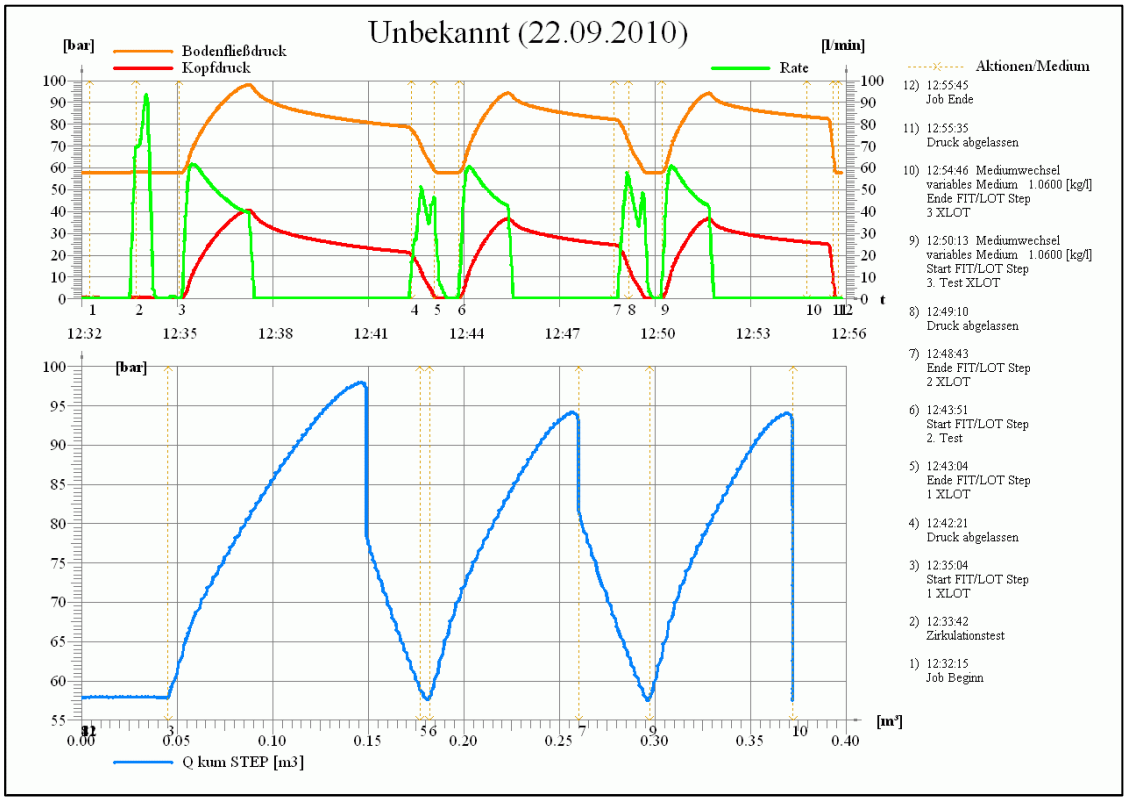

Figure 2 – Typical Test Chart (LOT)

During a Leak-Off Test, pressure is nowadays recorded against time by a computer. To make any value from this data, flow rate has to be constant or if not, flow rate has to be recorded vs. time as well. The data is usually presented in X-Y-plots showing pressure vs. time and flow rate vs. time or just pressure vs. volume as shown in Figure 2. Pressure vs. time plots provide the possibility to interpret the whole test from a single chart under the limitation flow rate has to be constant throughout the test. As this is usually not the case both, pressure vs. time and pressure vs. volume charts are needed to properly interpret the test. The reason is that if the flow rate changes, this will result in a nonlinearity in the pressure vs. time plot making it hard to identify the Leak-Off Point (LOP). A plot showing pressure plotted vs. volume is better suitable to identify the Leak-Off Point. On the other hand, a pressure vs. volume plot will not enable one to evaluate the shut-in phase. During the shut-in phase, the volume is constant as the flow rate is equal to zero. Therefore, the pressure decline during the shut-in phase will appear as straight, vertical line in a pressure vs. volume plot. The pressure vs. time plot provides the possibility to evaluate the shut-in phase and helps to decide if a stable pressure has been reached or not. This can be seen very clearly on real life examples recorded in the field such as the plot shown in Figure 2. As one can see on this picture,

identifying the Leak-Off Point from the upper graph alone is hardly possible. On the other hand, when looking on the lower, blue curve, one can very well identify a deviation from the linear behavior. It has to be noted that this graph is recorded as the test is performed and one has to decide rather quickly if the Leak-Off Point has been exceeded and the test has to be stopped.

2.2 Formation Strength Test Methodologies

2.2.1 Casing Integrity Test

Casing Integrity Tests are performed prior to drilling out of the casing shoe after the casing string has been run and cemented into place. Although a Casing Integrity Test is not an Formation Strength Test it is important to understand as it allows one to evaluated the behavior of the system excluding open-hole effects. It is therefore a yardstick for any follow up Formation Strength Test. The test is used to verify the integrity of the casing sting. It usually shows a straight-line unless gas is trapped in the drilling fluid. The dominant factors during these tests are drilling fluid compression and casing expansion. Maximum test pressure is limited by the burst pressure of the casing/tubing string or the pressure rating of the surface equipment.

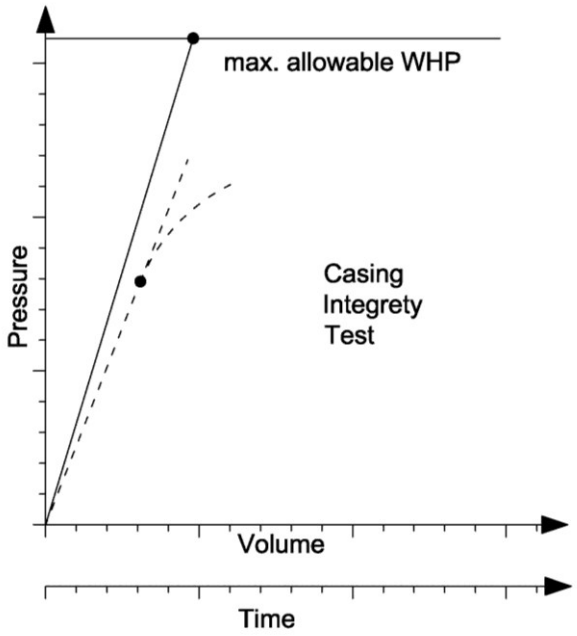

Figure 3 – Casing Integrity Test

2.2.2 Formation Integrity Test (FIT)

Formation Integrity Tests or Limit Tests are used to verify the integrity of the formation as well as the cement job, up to the maximum pressure expected during drilling this section. The test's result does not give any information about the strength of the formation as the maximum test pressure is in the linear region of the pressure vs. volume plot if the test was successful. It is a quick and therefore cheap test performed on a regular basis during drilling operations. Purpose is to gather just enough information to safely drill ahead. Due to the shorter test time, and therefore reduced cost, this test is often preferred against other Formation Strength Test. Another reason why Formation Integrity Tests are preferred is the fear of weakening the formation due to fracturing during Leak-Off Test or extended Leak-Off Tests. The downside is not getting any information about the actual strength of the formation and therefore no information about the limit during drilling.

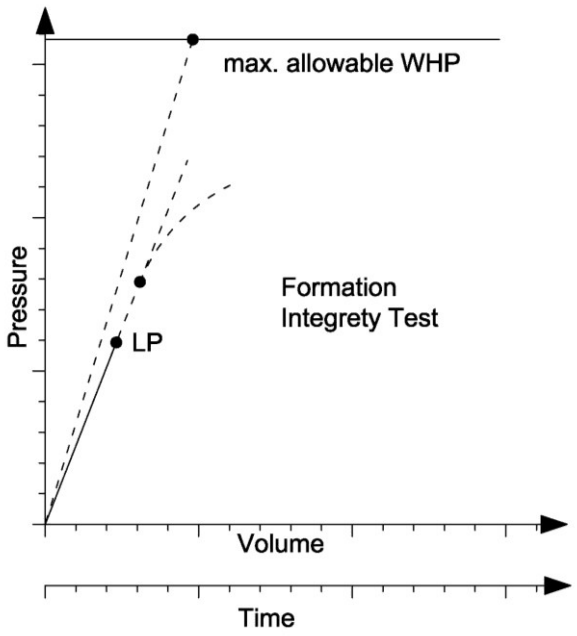

Figure 4 – Formation Integrity Test

2.2.3 Leak-Off Test (LOT)

In a Leak-Off Test, the wellbore is pressured up until a deviation from the straight line is observed. As soon as this point is identified, the well is shut-in for pressure observation. Finally, the pressure is bled off the well and drilling is continued. As the pump is stopped, an instantaneous pressure drop can be observed which reflects the friction pressure losses in the system. Depending on the depth of the well and the equipment used, this pressure drop is more or less pronounced. Proper identification of the Leak-Off Point takes a certain time and volume to be pumped beyond this point. Hence, the maximum test pressure is above the Leak-Off Point. As indicated in Figure 5, a difference in the slope of Casing Integrity Tests and Formation Integrity Tests exists. This behavior can be related to the fact that in Casing Integrity Tests no open-hole section influences the behavior whereas in all kinds of Formation Integrity Tests, open-hole effects, mainly filtration and borehole expansion have to be considered. Furthermore, the pressure after the well is shut-in is monitored for some time before the pressure is bled off. This shut-in period can give information on filtration properties.

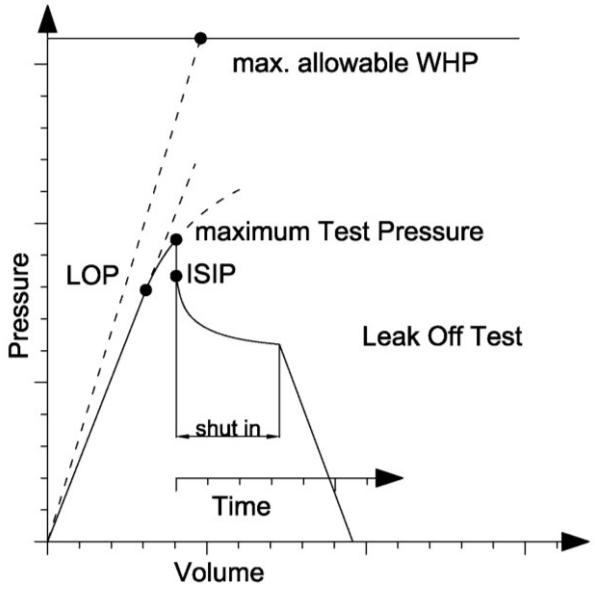

Figure 5 – Leak-Off Test

2.2.4 Extended Leak-Off Test (xLOT)

Extended Leak-Off Tests (xLOT) are defined by pumping beyond the Leak-Off Point until a stable pressure is reached. Aim of Extended Leak-Off Tests is to get information about the in-situ stress magnitudes unaffected by near wellbore effects. Therefore, the pressure in the wellbore is increased until no further pressure increase can be achieved and a stable Fracture Propagation Pressure is reached. Extended Leak-Off Tests are usually performed in several cycles in order to observe fracture reopening without working against the tensile strength of the formation and to verify the results. Flow back period analysis is often included in the interpretation of the results. Extended Leak-Off Tests are usually not considered being a standard test but are performed if special interest into the downhole stress conditions exist for example prior to a fracturing treatment.

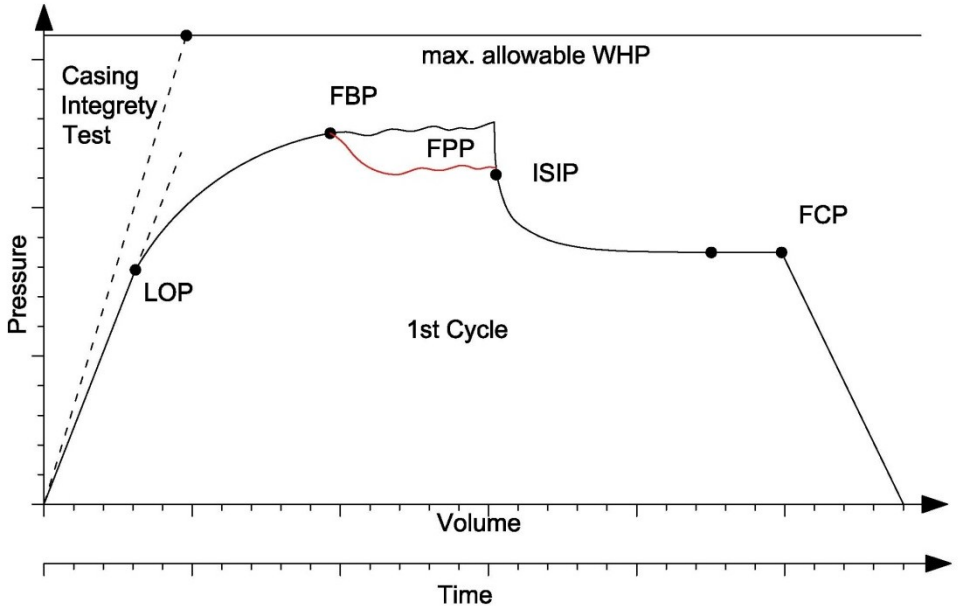

Figure 6 – Extended Leak-Off Test

2.3 Detailed Test Description

In general, these plots show significant points and sections as indicated in Figure 7 for a Leak-Off Test:

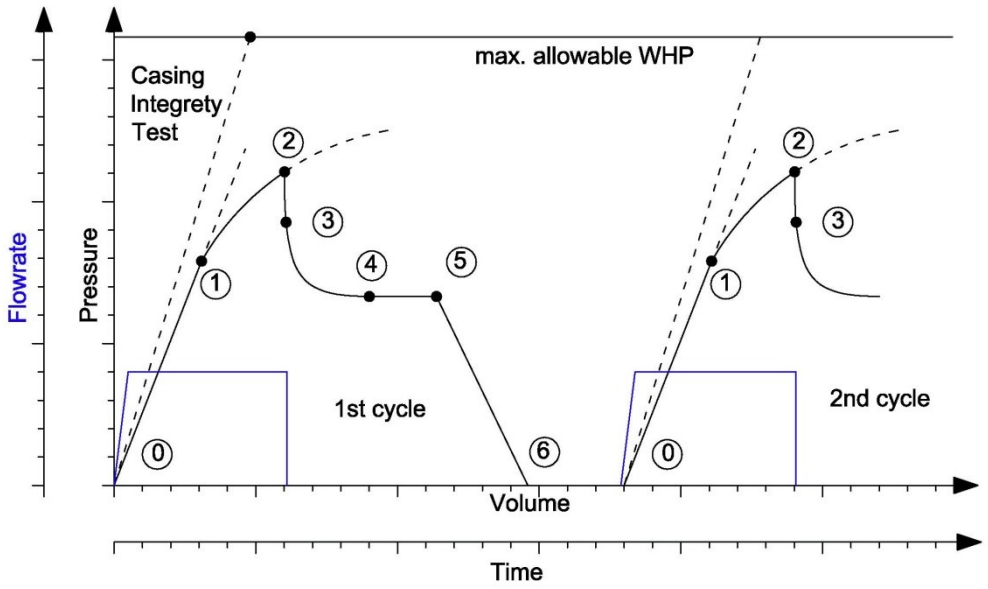

Figure 7 – Significant Points during an Leak-Off Test

0 Test starts at atmospheric pressure on surface, resulting in hydrostatic pressure of the mud column downhole. After conditioning the drilling fluid by the well is assumed to be filled with drilling fluid of uniform properties free of any gas. In case the plot shows downhole pressure either measured or calculated, the initial pressure will be the hydrostatic bottom hole pressure.

0-1 Drilling fluid is pumped into the well at a slow pump rate resulting in a linear pressure increase dominated by fluid compression, casing expansion, borehole expansion and fluid leak off. During a Formation Integrity Test or Limit Test, the maximum test pressure is within this interval.

1 The first deviation from the straight line is observed. This point is referred to as the "Leak-Off Pressure" (LOP) or "Fracture Initiation Pressure" (FIP). In this paper Leak-Off Pressure will be the terminology used.

1 - 2 In Leak-Off Tests (LOT), the pump is stopped as soon as the LOP has been clearly identified. Hence, the maximum test pressure in a Leak-Off Test is within this interval.

2 In Leak-Off Tests, this will be the final test pressure at which the pump has been shut-in.

2 - 3 After the pump is stopped an instantaneous pressure drop can be observed reflecting the friction pressure losses of the system. In most tests, this pressure drop can be hardly seen. This is due to the fact that the pumps cannot be stopped instantaneously, in reality. Furthermore, frictional pressure losses are small due to the slow pump rate. Hence, this pressure drop can only be seen if the frictional pressure loss due to drill collars, mud motor, downhole tools and bit nozzles is large even at low rates.

3 - 4 After the pump has been shut-in, the pressure will stabilize governed by filtration on the fracture faces. The fracture created during the test is expected to close on the fluid.

4 - 5 As soon as a stable shut-in pressure has been reached, the test is completed.

5 - 6 The pressure is bled off the well what marks the end of the test cycle. The process of pressurizing the well is repeated in some more cycles. If possible, the return volume should be recorded the same way as the pumped volume has been measured. If this is not possible due to limitations of the equipment used, the return volume can also be measured by bleeding off into a small tank or a bucket.

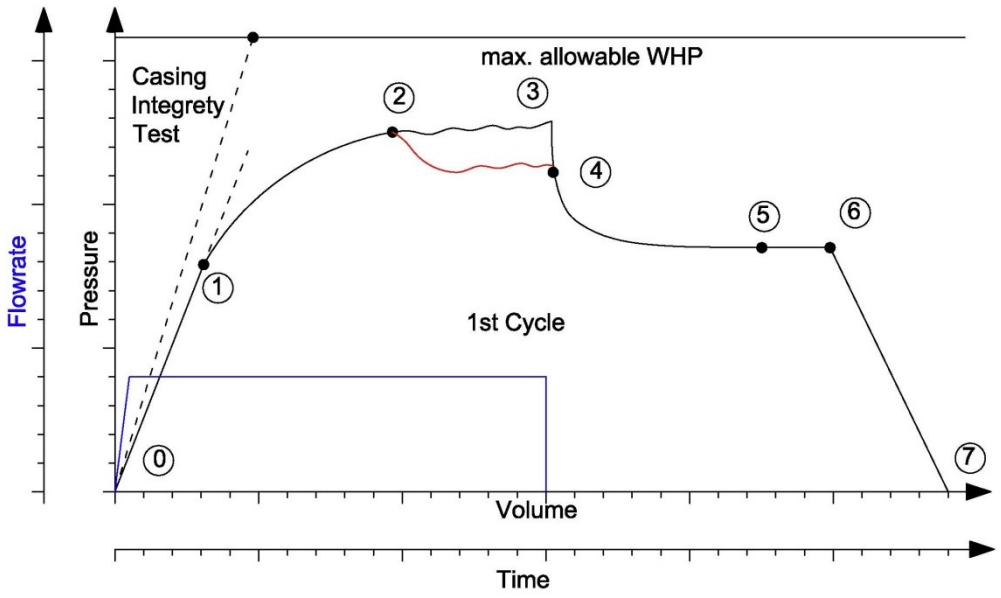

Figure 8 - Significant Points during an extended Leak-Off Test

In contrast to Leak-Off Test, an extended Leak-Off Test is shown in Figure 8. The difference to an Leak-Off Test is that it is not stopped after the Leak-Off Point has been identified. More fluid is pumped into the well and the fracture is thereby extended further into the formation.

0 - 2 The pressure in the well is increased, even after the first deviation has been observed.

2 In some tests, a distinctive pressure drop can be observed at this point. The maximum pressure is usually termed Formation Breakdown Pressure. It is believed that at this point the fracture leaves the area of disturbed stress around the wellbore. In other cases, however, the pressure stays more or less constant as pumping is continued. Examples of both variations are presented in Appendix F.

2 -3 The fracture is extended further into the formation.

3 As a stable pressure is reached, this pressure is referred to as the Fracture Propagation Pressure (FPP). The fracture is now believed to open against the far field stress only.

3 – 4 At this point the pump is shut-in and as already discussed previously, a pressure drop as the frictional pressure loss disappears might be observed.

4 - 7 After the pressure stabilized the pressure is bled off the well and another test cycle may be performed. Controlled bleeding off the pressure and measuring the return volume is often used to further analyze extended Leak-Off Test. Typically the Fracture Closure Pressure is taken for the minimum horizontal stress. It is typically associated with a change in slope during bleeding off the pressure as the fracture closes.

2.4 Equipment and arrangement

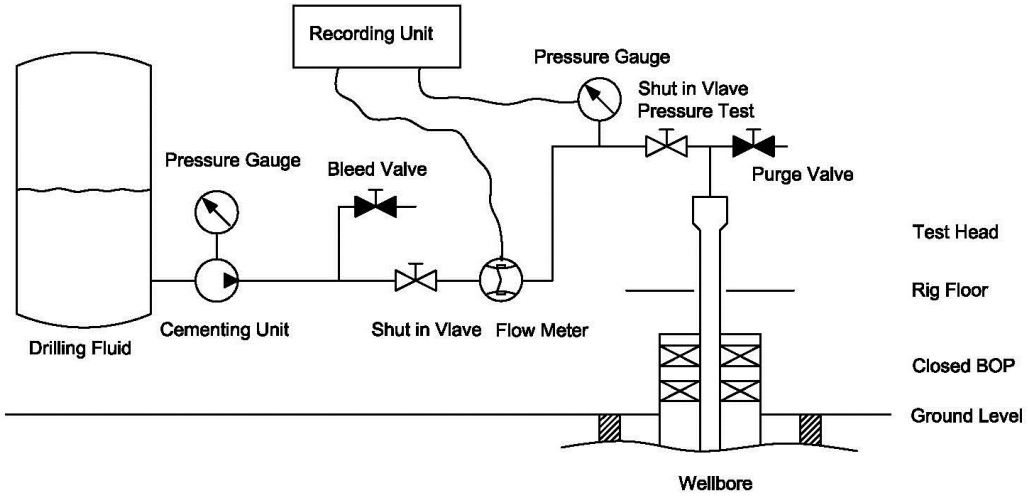

Figure 9 – Formation Strength Test Surface Equipment

Figure 9 shows a recommendation of the arrangement of surface equipment for performing Formation Strength Tests. As shown in the configuration, pressure is measured on surface, as it is the case in most tests. Still there is the possibility to record the pressure downhole via a pressure while drilling tool (PWD). This has the obvious advantage of more accurate measurement and the pressure has not to be corrected according to the weight of the mud column. This will be discussed in more detail in a later section of this thesis.

As shown in Figure 9, a cementing unit is recommended for pumping drilling fluid into the well as it usually can provide more accurate pressure measurement but above all other it is capable of more controlled pumping at a low flow rate at high pressures in contrast to the rig pumps.

The purge valve, mounted on the test head is used to purge any air from the surface equipment. The shut-in valve is used to shut-in the well, as one should not rely on the pump preventing any flow back from the well (Postler, 1997). The bleed valve is used to check if the shut-in valve is leaking during shut-in. Therefore, it is opened as soon as the well is shut-in and the pump is stopped and monitored for flow. The valve for shut-in during the pressure test is used during the pressure test of the surface lines prior to the Leak-Off Test.

Proper measurement of volume and pressure data is the key to a successful Leak-Off Test. For pressure measurement, a good quality cementing unit pressure gauge can be used in case no equipped for digital data acquisition is available. A 4”, liquid-filled pressure gauge with a range of 125-150% of the maximum expected test pressure and a resolution as low as 50-25psi

should be used. Sufficient pressure range and resolution are obvious requirements on the gauge. For volume measurement, a flow meter as shown in Figure 9 provides the most accurate measurement. If no flow meter is available, pump strokes should be the preferred way of measurement rather than tank volume increments as long as the pump is calibrated (Postler, 1997).

Digital data recording is highly recommended and should be preferred against manual data recording. Digital recorded data avoids errors in gauge reading, time shifts between pressure and volume measurement and provides the capability of recording data at much higher frequencies. A certain minimum data recording frequency is crucial to precisely identify the Leak-Off Pressure. State of the art digital data acquisition systems record pressure and volume at one second intervals or even faster. This is more than sufficient to clearly identify the Leak-Off Pressure but provides the capability to take a closer look at the test after it has been performed.

Figure 10 – OMV Cementing Unit during an Extended Leak-Off Test

In the following, Figure 11 and Figure 12, show the arrangement of the sensors in two formation strength tests performed by OMV. During the test shown in Figure 11, the backflow volume had been measured by bleeding off into a bucket. Therefore, it is important that the backflow hose is filled with fluid before the test is started to avoid errors in volume measurement.

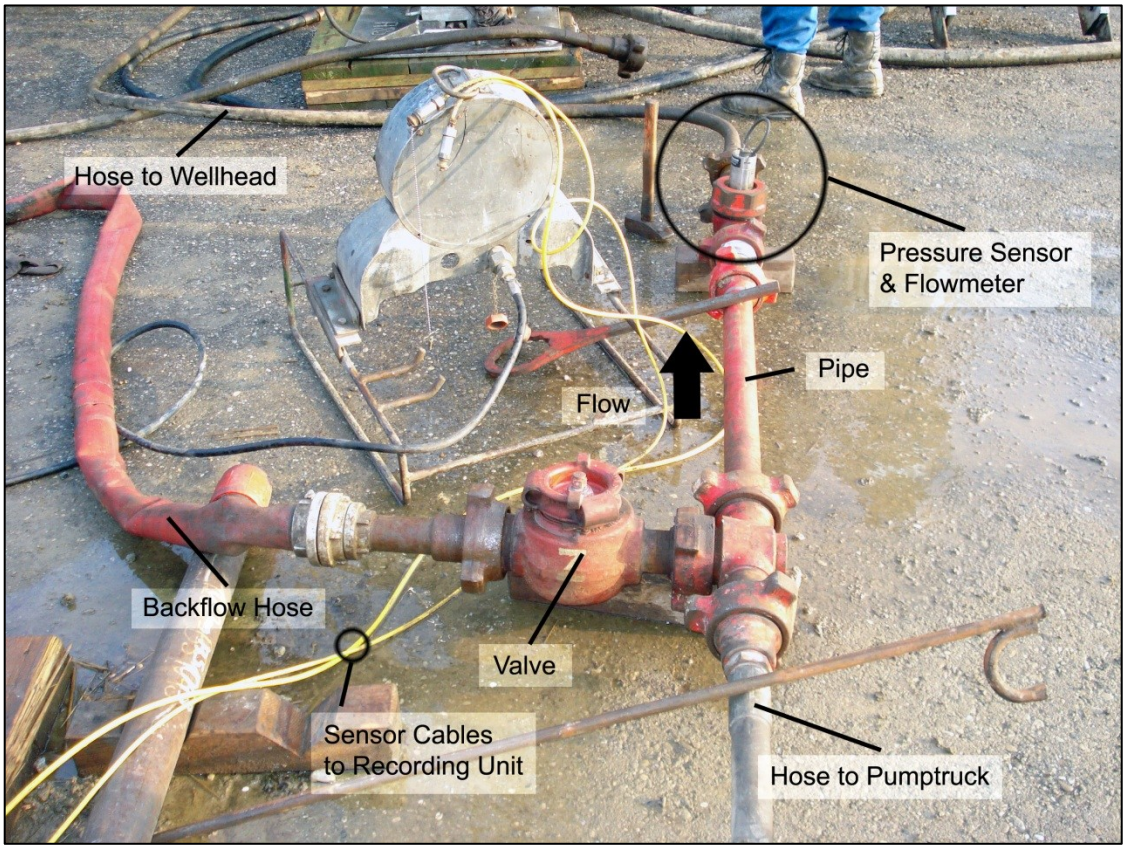

Figure 11 – Formation Strength test Arrangement including Backflow Volume Measurement

Figure 12 shows a close up of the sensors used for pressure and flow measurement. One can see that a pipe is used instead of a hose directly in front of the flow meter to reduce turbulences and thereby ensure a more accurate measurement. Figure 13 shows the recording bus used for data acquisition. During the test, all parameters can be permanently monitored in real time on two screens. The system provides an online view of the Pressure vs. Time as well as the Pressure vs. Volume plot what is important to clearly identify the Leak-Off Point. Furthermore, a graphic of the borehole and all important parameters is displayed.

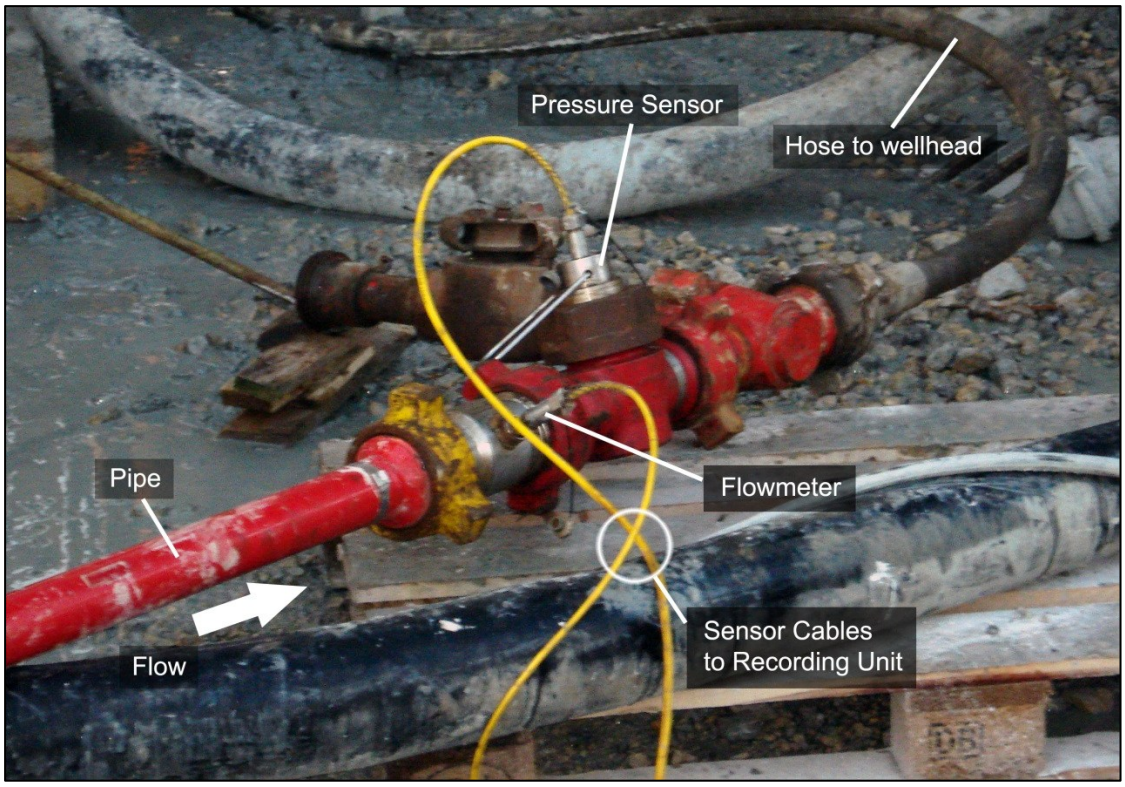

Figure 12 – Sensor Arrangement

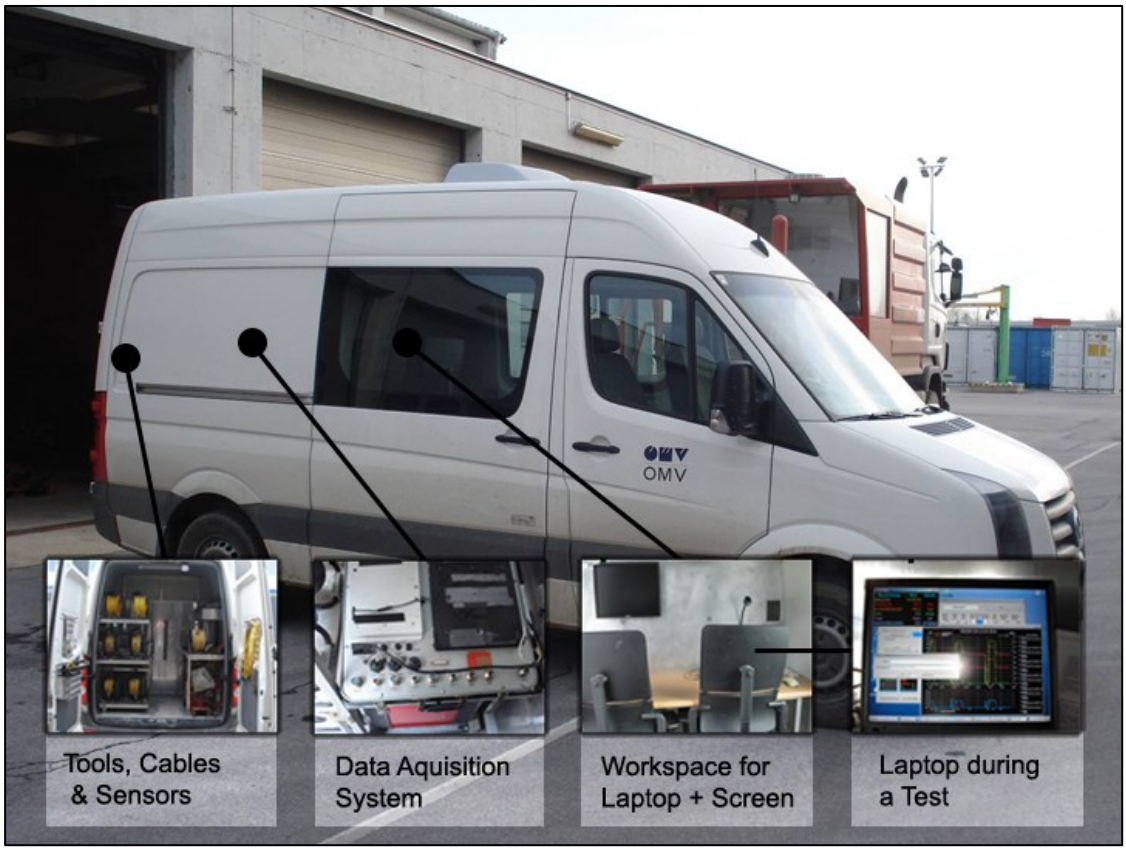

Figure 13 – OMV Data Acquisition Bus

2.5 Leak-Off Test Procedure

The drillstring is pulled back into the last casing to perform the test after 3-5m of new formation has been drilled.

The surface equipment is rigged up as described in the previous chapter. Before performing the test, the drilling fluid should be conditioned to confirm mud of even density, free of solids and gas throughout the wellbore. One "bottom ups" usually obtains these objectives (Postler, 1997). Any gas that might be trapped in the system has to be removed using the purge valve. The surface equipment is pressure tested as shown in Figure 15a.

Before the Leak-Off Test is performed, a graph should be prepared according to Figure 14, suggested by Postler, 1997 in case data is recorded manually.

- 100psi lines and ¼bbl increments should be drawn on the pressure and volume axis to simplify recording the data.

- The expected Leak-Off Pressure represented by a horizontal line estimated based on offset wells and/or local overburden and pore pressure gradient will act as a guideline, if leak off has occurred.

- A line of the expected Leak-Off Pressure reduced by ½ppg EMW will act in the same manner as the Leak-Off Pressure line. Leak-off below this line may indicate inaccurate Leak-Off Pressure estimation, cement channels, mud gelletation effects or measurement errors.

- The maximum allowable wellhead pressure line marks the maximum pressure the surface equipment can withstand which must not be exceeded.

- The casing pressure test line acts as guideline as it indicated the minimum volume that has to be pumped during the test.

- The maximum volume line acts as a lower flow rate reference as if the observed data drops below this line, the flow rate might not be sufficient to overcome leak off due to permeability. In such a case, the flow rate should be slightly increased (¼bbl) for repeating the test.

After the pump is shut-in, the pressure is recorded vs. time instead of volume as the flow rate is zero at this point.

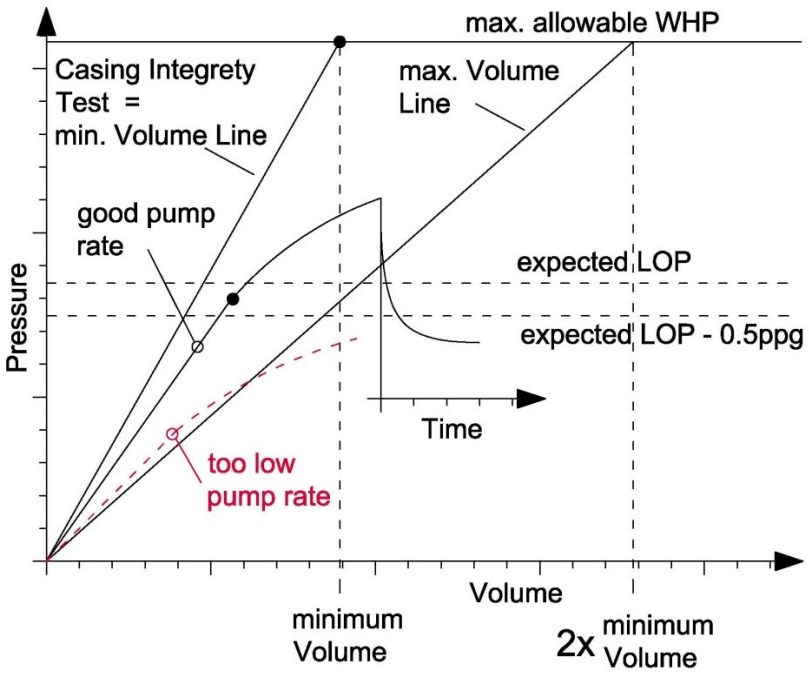

Figure 14 - Leak-Off Test Guide Lines as suggested by Postler 1997

A cementing unit is used to pressure up the system by pumping in small volumes of drilling fluid through the closed BOP. Valve positions are shown in Figure 15b. Keeping the flow rate low and constant is crucial to obtain good quality test data. Flow rate is recommended to keep as low as possible. A rate as low as 0.25bbl/min – 0.5bbl/min (40l/min – 80l/min) is recommended (van Oort & Vargo, 2007) depending on the capabilities of the surface equipment and the permeability of the formations. Permeable formations might require slightly higher rates up t 1bbl/min (160l/min) in order to overcome filtration losses. High flow rates will influence the test data, as discussed in a later chapter. Furthermore, pumping too fast will make it hard to identify the Leak-Off Point. Not keeping the flow rate constant might cause confusion during test interpretation and should therefore be avoided as far as possible (Postler, 1997).

Once the final test pressure is reached, indicated by a deviation from the straight, the pump is stopped and the well is shut-in by the shut-in valve as shown in Figure 15c. At this point, the instantaneous shut-in pressure is recorded. The bleed off valve is opened to verify the shut-in valve is not leaking. It is recommended to monitor the pressure while the well is shut-in for as long as 10 -15 minutes to check for fluid leaking off (Postler, 1997).

Finally, the pressure is released from the well by opening the shut-in valve. In case the test is accepted as it indicates sufficient formation strength to safely drill the next section, drilling is continued. When there is doubt about the validity of the test, the test should be repeated. If

the pump rate was good according to the guidelines, it should not be changed to make the test better comparable.

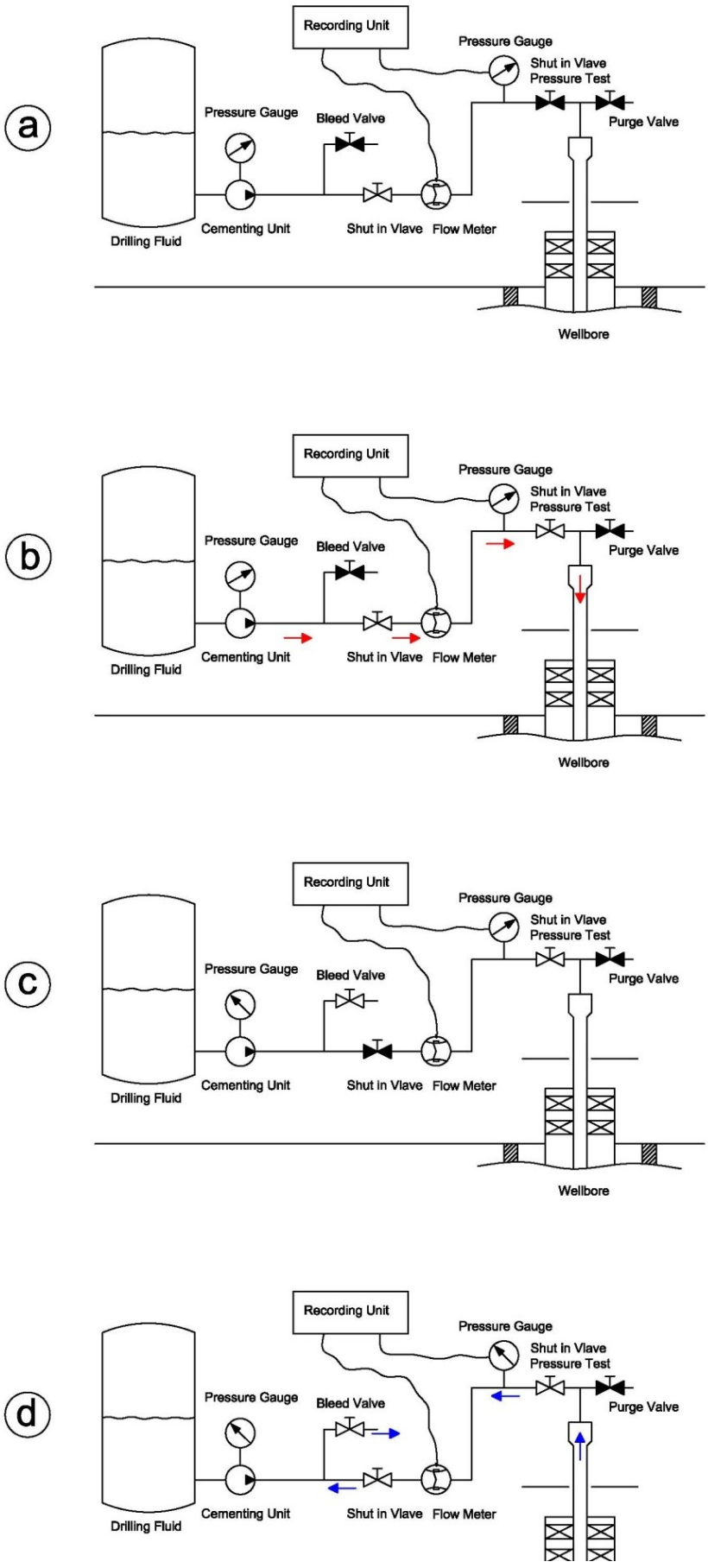

Figure 15 – Leak-Off Test Procedure

3 Factors affecting Leak-Off Tests

In this chapter, the whole system involved in a Leak-Off Test will be investigated in more detail and effects influencing Leak-Off Test results are discussed. A typical arrangement of surface equipment as well as the wellbore and the effects, which are subject to further investigation, are shown in Figure 16. As drilling fluid is pumped through the closed BOP into the well, the pressure increases governed the by the compressibility of the drilling fluid. The increased pressure increases the stresses induced in the casing, drill pipe and the wellbore. These stresses cause casing, drill pipe and wellbore to expand until the system is in equilibrium. This is true as long as pressure lines on surface equipment and the casing are not leaking and the formation has not been fractured.

The effects governing the behavior of Formation Strength Test can be separated into three basic groups. These are cased hole effects, open-hole effects and operational effects.

Cased hole effects are effects related to the system not accounting for an open-hole section as it is the case in Casing Integrity Tests. These are casing expansion, drilling fluid compression as well as gas trapped in the system, which will also heavily influence the system.

Open-hole effects are filtration governed by permeability, preexisting fractures and possible cement channels and initiated fractures. These are effects which are related to the open-hole section and are observed in addition to cased hole effects in Formation Strength Tests.

Furthermore, **operational effects** being non-newtonian fluid effects, gel strength, fluid viscosity and the ability of the fluid to penetrate the formation as well as flow rate, injection path and measurement methods will be discussed.

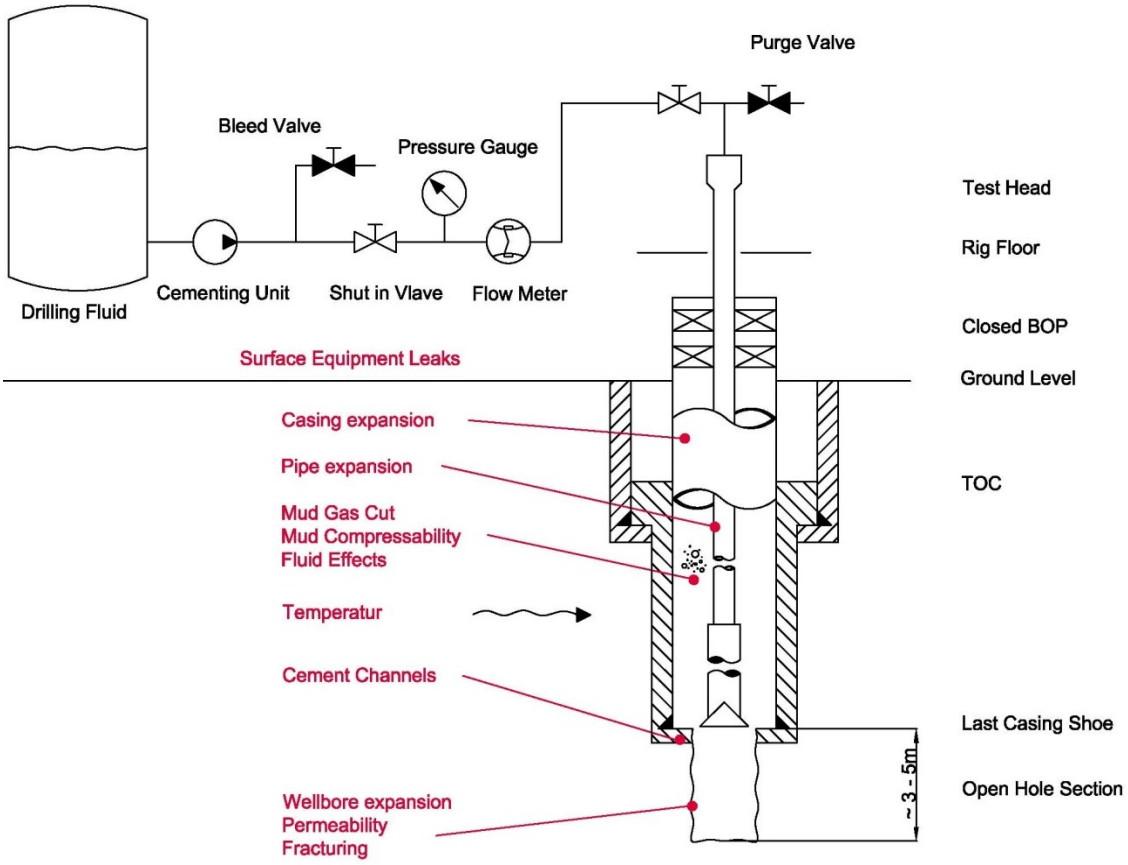

Figure 16 – Leak-Off Test Scheme (Valve Positions for Pumping)

3.1 Cased Hole Effects

Cased-hole effects are effects that can be observed without having an open-hole section. These are casing expansion, drilling fluid compression as well as gas trapped in the system. As these effects are observed independent of an additional open-hole section these govern the behavior of Casing Integrity Tests. It is important to understand these effects as deviations from the behavior expected based on observations during a Casing Integrity Test performed prior to the Formation Strength Test, are evidence for open-hole effects.

3.1.1 Casing expansion

When considering casing expansion, cemented and not cemented casing have to be evaluated separately. A casing not cemented in place will expand under internal pressure whereas a cemented casing's expansion will be negligible. Still, even if the casing is cemented the cement bond can be inadequate and therefore allow for at least some expansion. The different scenarios are shown in Figure 17. It is important to know that the top of cement (TOC) which defined to border of expandable casing and non-deformable casing is not always easy to clearly identify due to transition zone of cement and spacer during the cement job.

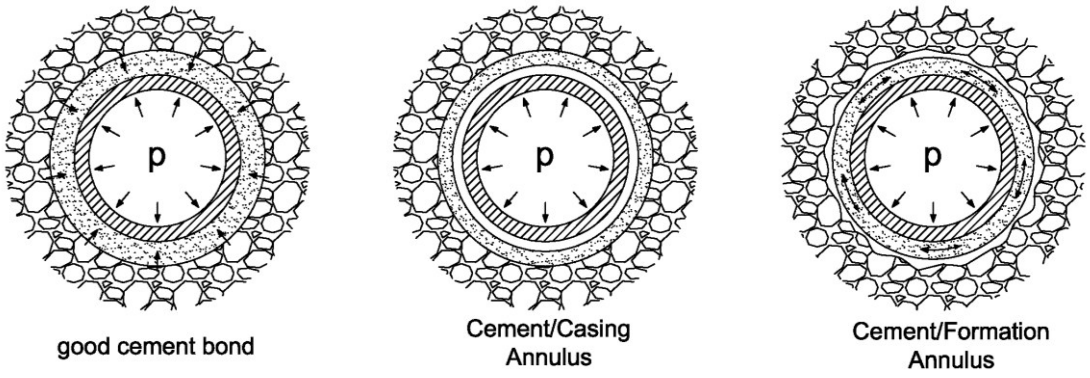

Figure 17 – Casing Cementing Scenarios as presented by de Aguiar Almeidar 1986

- **Casing - not cemented**

In most cases, the casing is not cemented up to surface, for cost reasons. Therefore, a certain section of the casing is not supported by cement and the formation. Hence, it will be easier to deform than the part of the casing, which is connected to the formation by means of cement.

For this consideration, the casing is assumed being a cylinder of ideal shape. The pressure behind the casing is assumed being constant. Even if communication through the cement exists, the pressure increase would be very slow and can be neglected for the short period during a Leak-Off Test. Furthermore, the length of the connections is short in comparison to the overall length of the casing string. The couplings will therefore be neglected.

Under the above assumptions the casing string can be treated like a smooth, continuous pipe which is suspect to a differential pressure loading with the inside pressure being larger than the outside pressure. The pipe made from steel will deform uniformly according to the stress-strain diagram for steel. It will deform elastically according to Hooks' law until the

stress exceeds the yield strength of the material, followed by plastic deformation and finally failure. The principal stresses acting on the material are σ_r in radial direction, σ_ϕ in tangential direction and the longitudinal stress σ_z as shown in Figure 18. During Leak-Off Test, the stresses within the casing usually do not exceed the yield strength, hence linear elastic behavior can be assumed. Furthermore, the casing is assumed to be ideally anchored by the cemented section below and therefore the longitudinal strain is zero. All this assumptions lead to a linear behavior of expansion of a non-cemented casing during a Leak-Off Test.

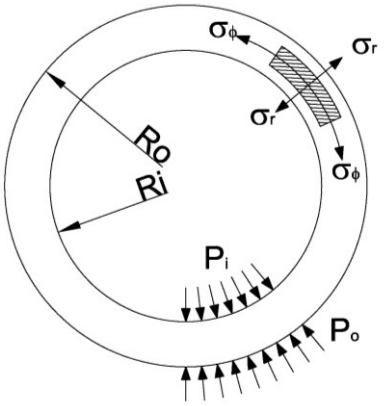

Figure 18 – Casing expansion

The expansion of the casing depends on material properties, casing dimensions and increases linear with the differential pressure until the yield strength is exceeded. It can be described by Equation 1, which is derived in Appendix A .

$$\Delta V_{csg} = 2 \cdot \pi \cdot L_c \cdot \frac{\Delta P_i}{E} \cdot \left(\frac{R_i^2 + R_o^2}{R_o^2 - R_i^2} \cdot (1 - \nu^2) + (\nu + \nu^2) \right) \qquad \text{Eq. 1}$$

Figure 19 shows the capacity of a 9 5/8" casing to expand under internal pressure. The lines represent the elastic deformation of a 9 5/8" casing of different nominal weights. It can be seen that the heavier the casing and respectively the stronger the casing wall, the harder it is to deform, as one would expect. Furthermore, the limits of elastic deformation are shown by markers on the different lines. The markers and associated values represent the maximum internal yield pressure of different casing steel qualities. The higher the casing steel quality, the more deformation will be allowed until the maximum internal pipe yield is reached and plastic deformation will occur. The material properties used with Equation 1 are held constant throughout different steel qualities. Even though different steel qualities would result in slightly different Young's moduli and different poison ratios, differences are small and not dominant in the calculation. For the calculation an average Young's modulus for steel E=210GPa, and a Poisson's ratio of ν=0.3 has been used leading to differential volumes of

below 0.5% for common steel qualities and below 0.7% for O125 casing quality as shown in Figure 19.

The expansion volume in Figure 19 is presented as a percentage of the initial volume making the plot independent of the casing length, which is subject to deformation. In order to present an example using the real volume, the same calculation has been made for the same 9 5/8 casing string assuming an arbitrary, non-cemented casing length of 400m. From Figure 20 it can be seen that the mentioned expansions correspond to differential volumes of below 150liters.

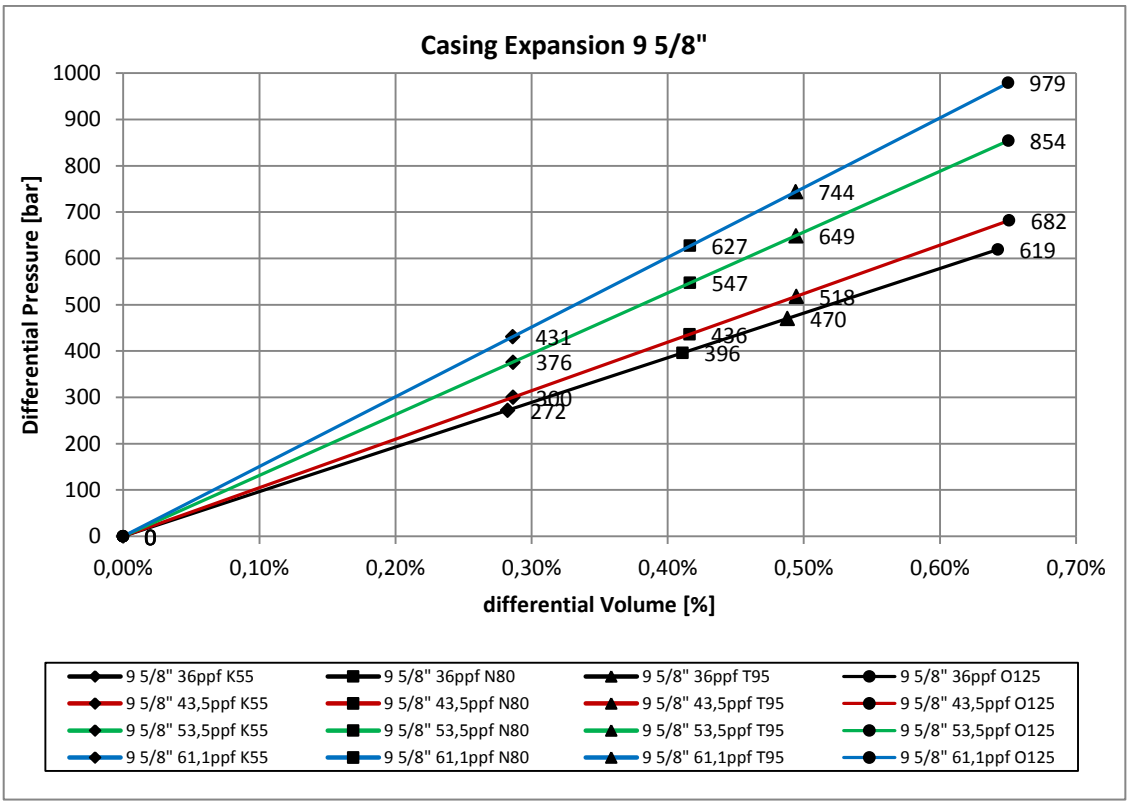

Figure 19 – Casing expansion capability of a 9 5/8" Casing

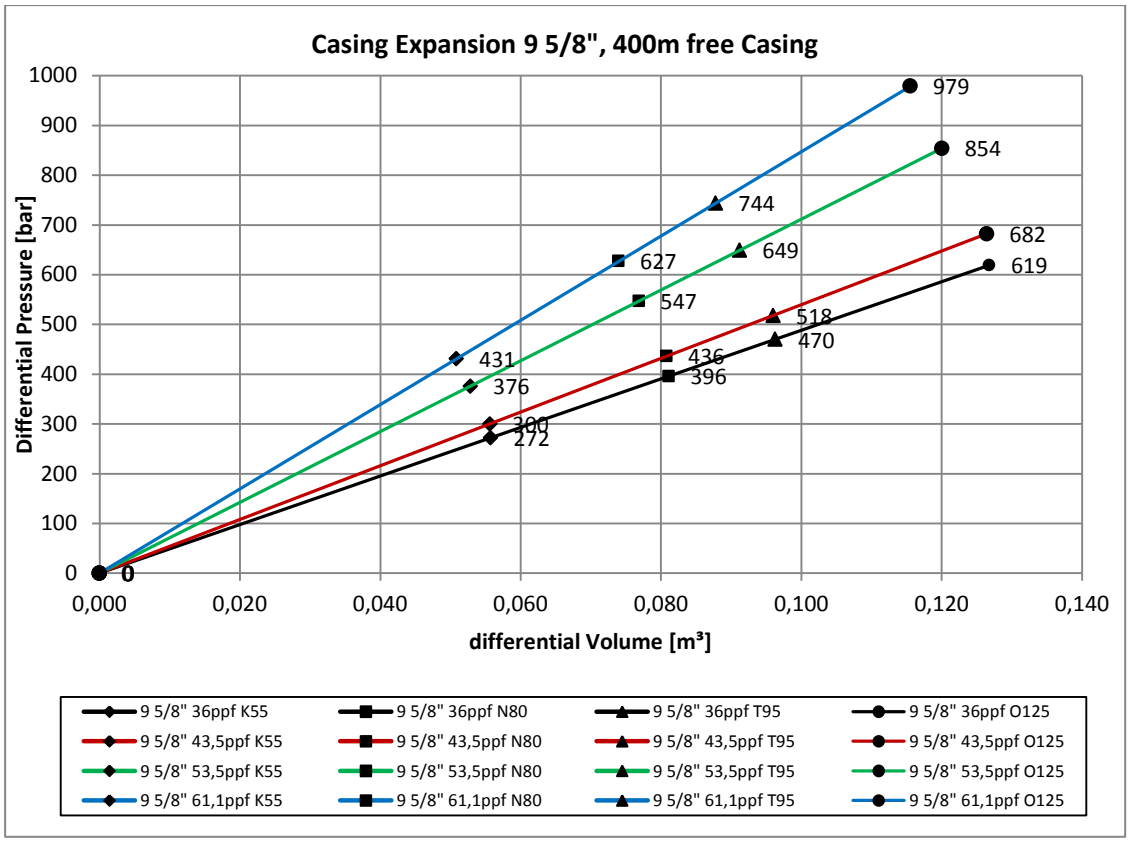

Figure 20 – Casing expansion of 400m of 9 5/8" Casing

▪ Cemented Casing – good cement bond

A casing cemented in place, showing good cement bond, will show hardly any expansion due to the restriction of the cement and the formation beneath the cement. Therefore the expansion of a well-cemented casing is negligible (de Aguiar Almeidar, 1986).

▪ Cemented Casing – Casing / Cement Annulus

In case of a bad cement bond between the casing and the cement, better known as micro annuli, the casing will be able to expand under internal pressure until expansion is restricted by the cement. Micro-annuli are formed during or after cementation by variations in pressure and temperature. These variations cause small movements of the casing, breaking the cement bond. A cement bond log (CBL) can be used to evaluate the bonding of the cement. Even though the behavior is non-linear, as the casing is able to expand elastically, it is restricted in expansion, as the gap to the cement is closed. Expansions are usually marginal as the annular space caused by a micro-annulus is usually smaller 0.2mm. Furthermore, expanding the casing after closing the gap would need much more incremental pressure for the same volume expansion and would therefore increase the inclination of the leak-off curve causing a dip to

the left. The effect of casing expansion in presence of a micro annulus will be small compared to other effects (de Aguiar Almeidar, 1986).

- **Cemented Casing – Cement / Formation Annulus**

In case of bad cement bond between the cement and the formation but good cement bond between casing and cement, the expanding casing will initiate tensile loading on the cement. As cement cannot withstand high tensile loads, it will possibly break (de Aguiar Almeidar, 1986).

3.1.2 Drilling Fluid Compressibility and thermal Expansion

The pressure on the formation is transmitted from surface via the drilling fluid in the wellbore. First, the drilling fluid's density has to be estimated with respect to compressibility and thermal expansion. This is important to reliably correlate surface pressure measurement and downhole pressure acting on the formation. Which effect is dominant mainly depends on depth and downhole temperature regime. In deep cool offshore wells, compressibility is generally the dominant effect. In high pressure, high temperature wells on the other hand, thermal expansion may play a more pronounced role. Furthermore, fluid compressibility is a function of mud type. Water-based muds are significantly less compressible than oil-based and synthetic-based muds. The magnitude of increase in density is hard to estimate, as the compressibility of the drilling fluid c_{mud}, itself is a function of pressure and temperature. The same is true for the thermal expansion coefficient α_{mud}, which also depends on pressure and temperature as shown in Equation 2 & 3. Hence, density change with depth and pressure is a non-linear function (van Oort & Vargo, 2007).

$$c_{mud} = \left(-\frac{1}{V}\frac{\partial V}{\partial P}\right)_{P,T} \qquad \text{Eq. 2}$$

$$\alpha_{mud} = \left(\frac{1}{V}\frac{\partial V}{\partial T}\right)_{P,T} \qquad \text{Eq. 3}$$

The correction of the density is of importance as Leak-Off Tests are interpreted from surface pressure measurements in most cases. The effects of compressibility of the fluid and thermal expansion can be avoided by using a pressure while drilling tool for downhole pressure measurement. Unfortunately, these tools are rarely available and their application still provides some challenges.

The mud temperature during a Leak-Off Test is assumed being constant with time and therefore does not have an impact on the elasticity of the system. For simplicity reasons, compressibility is assumed being independent on pressure. This assumption is valid as any

non-linearity of compressibility would affect the pressure vs. volume plot in a Leak-Off Test from the very beginning on and therefore cannot be responsible for the "plastic" behavior. Furthermore, the investigated Leak-Off Tests have been performed in shallow depths under normal conditions regarding temperature. Hence, the subscripts T and P can be dropped from Equation 2 & 3. Moreover, the minus sign can be dropped as the volume decrease due to compression is compensated by the volume, which is pumped into the well. The approximate solution of the compressibility equation relating differential volume, pressure and compressibility is shown in Equations 4 and is derived in Appendix B .

$$\Delta V_{mud} = c_{mud} \cdot \Delta P \cdot V_0 \qquad \text{Eq. 4}$$

The compressibility factor in Equation 4 represents the compressibility of the complete fluid system, accounting for solids as well as for other liquids like oil present in the mud but it does not account for gas. Calculating the compressibility of fluids, especially the compressibility of complex mixtures in relation to different temperature and pressure regimes is complicated, especially when multiple phases are present. For simplicity reasons, Equation 5 will be used to compute an average compressibility of the drilling fluid without taking temperature and pressure effects on the compressibility into account.

$$c_{mud} = (c_{water} \cdot S_{water} + c_{oil} \cdot S_{Oil} + c_{solids} \cdot S_{solids}) \qquad \text{Eq. 5}$$

Equation 5 relates the compressibility of the water fraction, oil fraction and solids contributing according to their fractional volumes of the drilling fluid to its compressibility. This leads to Equation 6 describing the differential volume increase due to compression of the drilling fluid.

$$\Delta V_{mud} = \Delta P \cdot V_0 \cdot (c_{water} \cdot S_{water} + c_{oil} \cdot S_{Oil} + c_{solids} \cdot S_{solids}) \qquad \text{Eq. 6}$$

For compressibility of the single fraction, the values presented in Table 1 have been used to calculate the behavior of the different fluid compositions as shown in Figure 21.

Compress abilities (c)		
Water	5,10E-05	1/bar
Oil	7,25E-05	1/bar
Solids	2,90E-06	1/bar

Table 1 – Fluid Compressibility

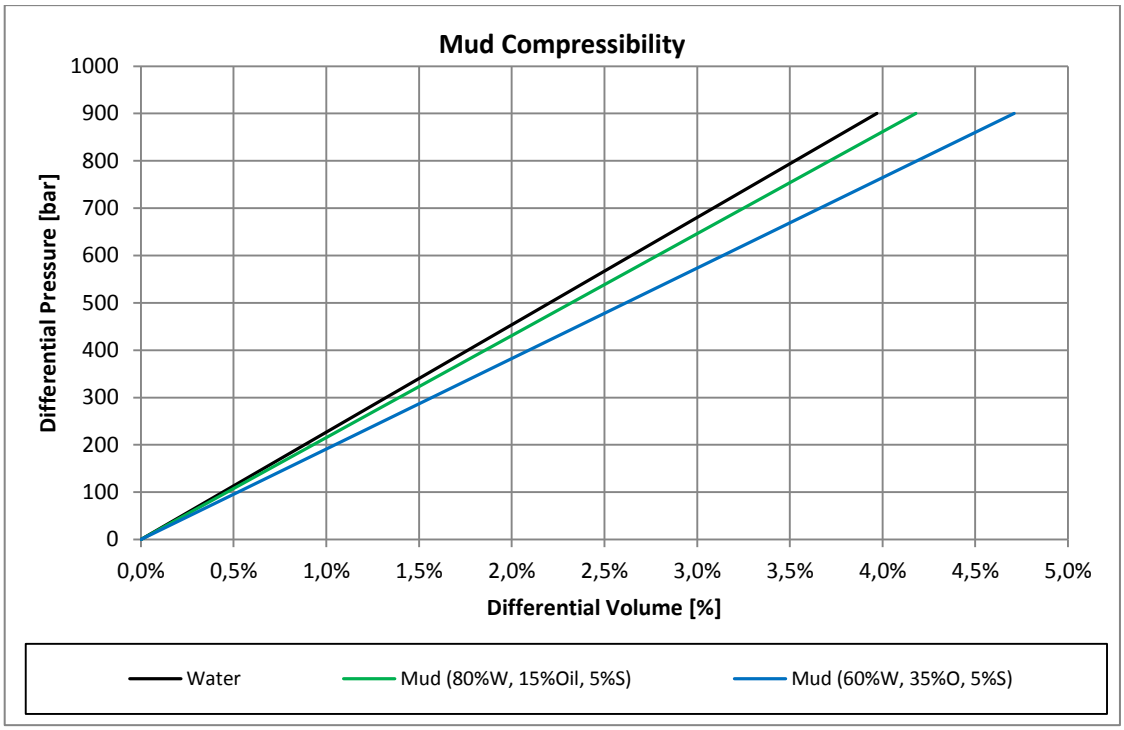

Figure 21 – Compressibility of different fluid systems

As shown in Figure 21, increased oil fraction will increase the compressibility of the fluid system as one would expect, as oil based fluid are more compressible than water. Furthermore, it can be seen that the differential volume gained by fluid compression is much higher than form casing expansion as discussed in the previous chapter.

The following example will more clearly point out the difference in volume gained by casing expansion and fluid compression.

Well Data		
Free Casing length (above TOC)	400	m
Total Casing Length (MD)	1600	m
Young's Modulus	2,10E+11	[N/m²]
Poisson Ratio	0,3	
OD	9 5/8	in
Weight	43,5	ppf
Casing Quality	T95	
Max Internal Yield Pressure	51,8	MPa
Mud Weight	10.5	ppg
Well Volume	62,14	m³

Mud compressibility	3,16E-06	1/psi
Water	80,00%	
Oil	15,00%	
Solids	5,00%	

Table 2 – Example Well Data

For this calculation, uniform expansion of the not cemented casing section is assumed, resulting from the average pressure within this section. Drilling fluid of the same density as within the borehole is assumed behind the casing above the cement. The differential pressure is thereby constant over the not cemented casing section being equal to the applied surface pressure.

For drilling fluid compression and the compressibilities presented in Table 1 are considered with the associated fractional volumes presented in Table 2. Integrating Equation 4 over depth, neglecting the change in fluid density with depth, leads to the following expression for the compression of the fluid column.

$$\Delta V_{\text{mud}} = \frac{1}{2} \cdot c_{mud} \cdot V_0 \cdot P(\text{TVD}) \qquad \text{Eq. 7}$$

The static pressure regime within the wellbore is shown in Figure 22. Compression of the fluid used to fill the volume gained by casing expansion and fluid compression is not considered as the volume is small compared to the overall volume of the wellbore.

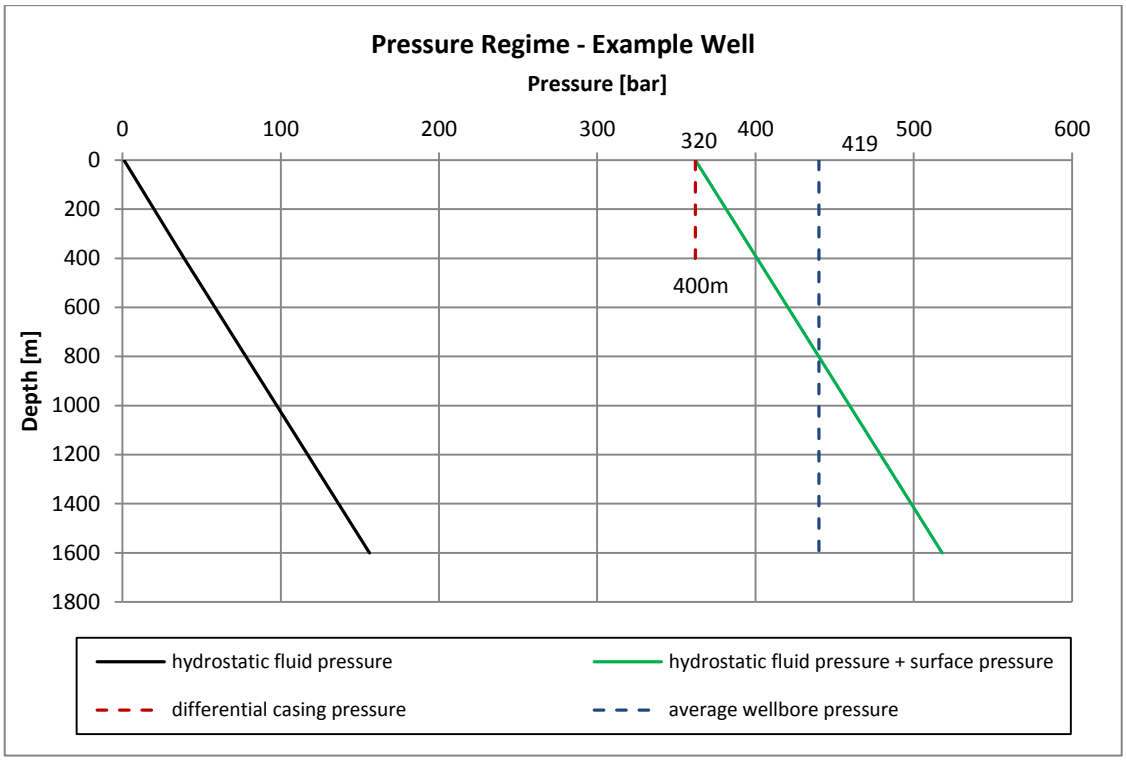

Figure 22 – Pressure Regime – Example Well

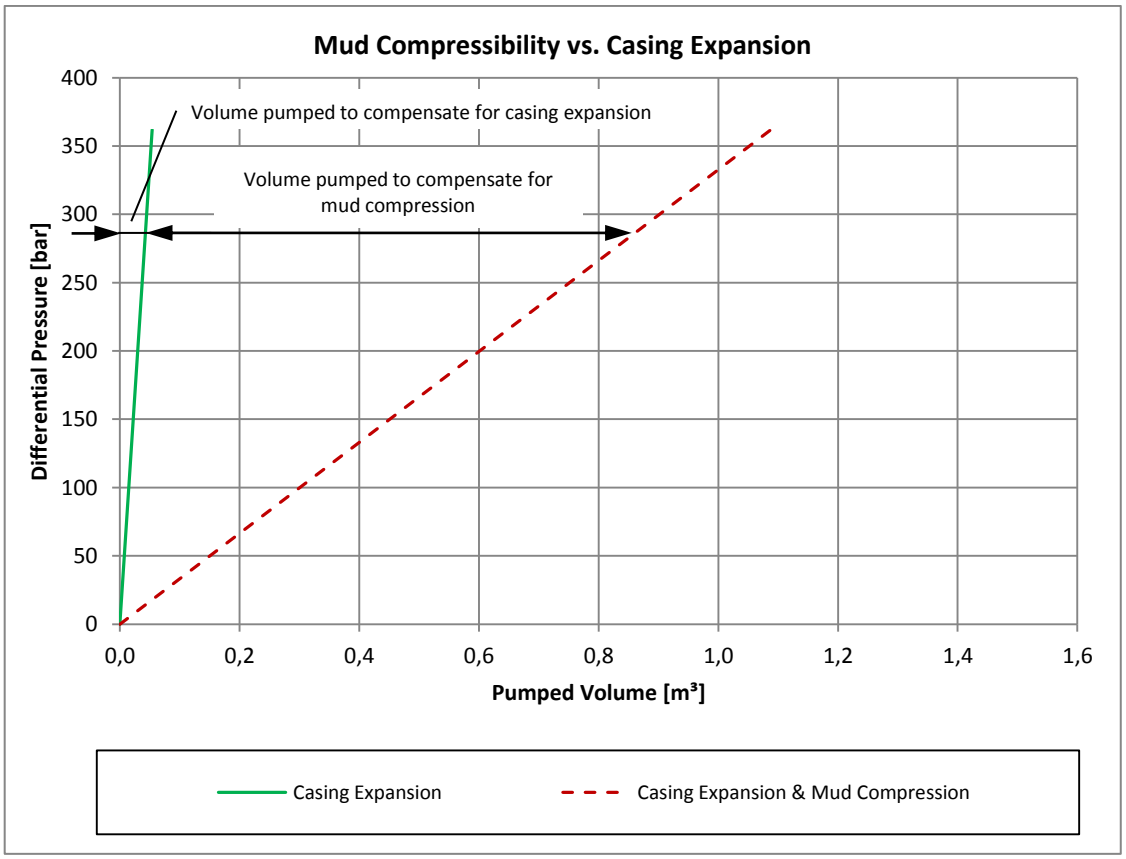

Figure 23 – Mud Compressibility vs. Casing Expansion

The resulting volume increase is shown in Figure 23 as a percentage of the total, initial wellbore volume. It can be seen that mud compressibility is the by far more important factor. The effect of casing expansion increases with decreasing casing weight and increasing free casing length. In this case, mud compression is responsible for more than 95% of the volume. Even if the whole casing would be free and subject to expansion and water would be used as a drilling fluid, mud compression would still account for 82% of the volume pumped.

3.1.3 Mud Gas Cut

The drilling fluid, used during a Leak-Off Test should be conditioned before performing the test to confirm mud of even density, free of solids and gas throughout the wellbore. One "bottom up" usually obtains these objectives (Postler, 1997). In case of any gas or air is captured in the system as a Leak-Off Test is performed, this will influence the test especially in the early pumping phase and during bleeding off the pressure. Hence, non-linear behavior in the beginning of the test as well as an extended "tail" at the end when bleeding off the pressure can be observed as shown in Figure 24. In any case, mud gas cut is a possible source of error, but it will not govern a sudden change in elasticity of the system causing the deviation from the straight line. The purge valve on the test head as shown in Figure 16 is used to purge air from the surface lines avoiding the effects mentioned above. If the test equipment is properly rigged up and prepared, errors due to trapped air can be avoided. Furthermore, it is important to store sufficient drilling fluid free of air and of the same properties as the fluid in the wellbore for performing the test on surface. It might be necessary to use de-foamers if the fluid seems to be aerated. In general, twice the amount of the fluid pumped in the Casing Integrity Test is sufficient (van Oort & Vargo, 2007).

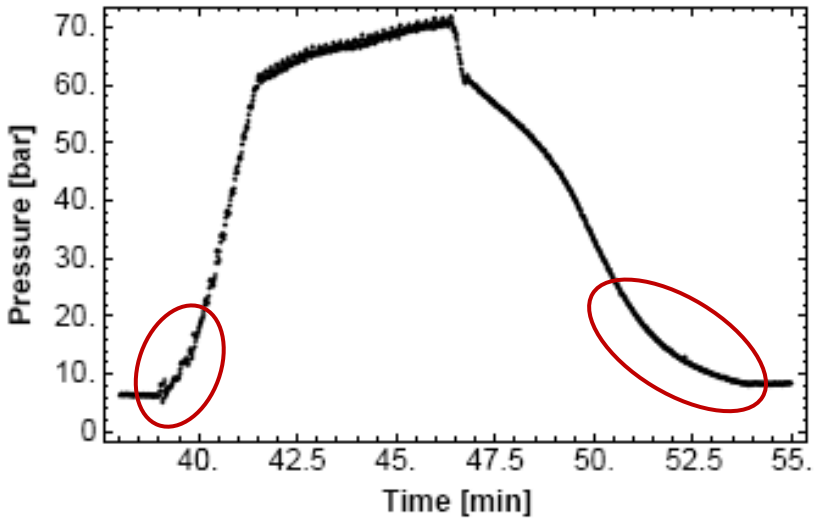

Figure 24 – Leak-Off Test with air trapped in the system (Brudy & Raaen, 2001)

3.2 Open-hole Effects

Open-hole effects are of major importance during Formation Integrity Tests. These effects are responsible for the different behavior of Formation Integrity Tests and Casing Integrity Tests. Conclusions regarding formation properties and downhole stresses are drawn back from the behavior in the tests governed by these effects.

3.2.1 Wellbore expansion

The behavior of the borehole will mostly depend on the geology and the type of formation. Even on the relatively small open-hole section, layers of different properties are likely to be present. In general, the open-hole section will be subject to elastic deformation, whereas the behavior will depend on the properties of the formations. In the simplest case, assuming a uniform formation type with constant properties, the deformation of the borehole will mostly depend on the young's modulus of the formation. Elastic rock expansion of the wellbore can be described by Equation 8, which is derived in Appendix C . The equation treats the wellbore as a tube of infinite outer radius that is subject to internal pressure and restricted in longitudinal expansion. The borehole is assumed to deform evenly over its length meaning the effects of the bottom hole and the casing interface are neglected. This means that this equation can only give an estimate on the volume gained by borehole expansion.

$$\Delta V = 2 \cdot \pi \cdot L_c \cdot R_i^2 \cdot \frac{\Delta P}{E_f} \cdot (1 + \nu) \qquad \text{Eq. 8}$$

As borehole deformation is related by a linear function of the pressure increase inside the borehole this adds additional elasticity to the system from the very beginning of the test. If leak off due to filtration is neglected, borehole expansion is responsible for the decrease in slope of the linear region. The significance of elastic borehole deformation however can be estimated by comparing the slopes of a Casing Integrity Test and the Leak-Off Test itself.

Again, the example presented in the previous chapter is used to indicate the influence of borehole expansion. The example well is assumed to be drilled ahead for 10m at 8 ½" and a Leak-Off Test is performed afterwards. An estimated young's modulus of E_f=2GPa and Poisson's ratio ν=0,4 was used in the example as presented in Table 2. For the pressure, the average pressure in the borehole is considered.

Open-hole Properties		
Open-hole Length	10	m
Diameter	8 1/2	in
Formation young's modulus	2,00E+09	N/m²
Formation Poisson‘s Ratio	0,4	
open-hole Volume	0,18	m³

Table 3 – Example Well – Open-hole Section

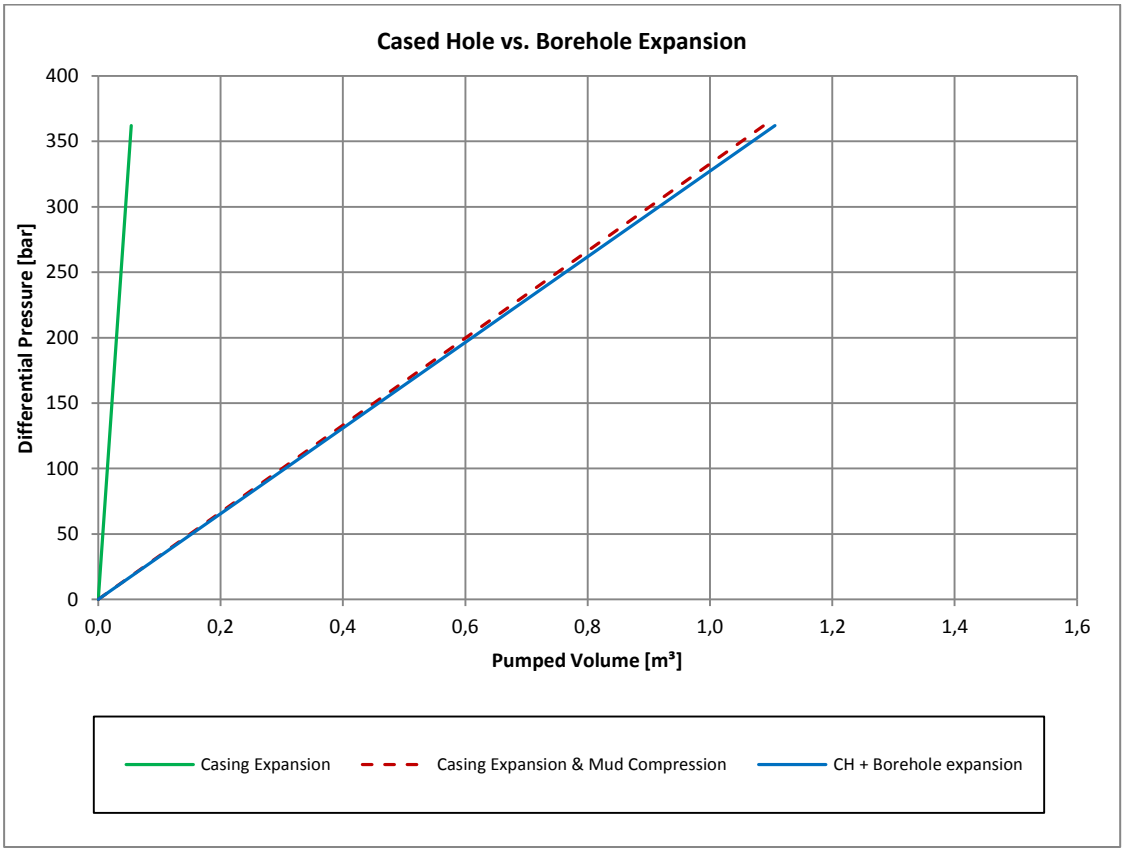

Figure 25 – Effect of Borehole expansion on pumped volume

It can be seen from Figure 25 that in this case, expansion of the borehole has an almost negligible contribution to the overall change in volume. This picture changes however if the length of the open-hole section increases or unconsolidated layers are present with associated low Young’s moduli. Due to the low Young’s modulus, the open borehole is relatively high deformable compared to the casing. However, the open-hole length is usually small and so is the associated increase in volume.

In some areas, a significant difference between the Casing Integrity Test and the Leak-Off Test can be observed, which may be related to deformation of unconsolidated shale (de Aguiar Almeidar, 1986).

3.2.2 Permeability and Filtration

Filtration will influence Formation Strength Tests especially in high permeability formations. However, also in formations, where the expected permeability is low, thin layers of high permeable sands may be present and thereby lead to unexpected results.

Drilling fluids are designed in a way to avoid losing large amounts of fluid to the formation as this might result in a well control situation as the hydrostatic pressure decreases due to the reduced height of the fluid column. During drilling out of the casing shoe and circulating for drilling fluid conditioning, a filter cake will build up and reduce fluid loss to the formation. Equation 9 (Bourgoyne, Millheim, Chenevert, & Young, 1986) shows that under dynamic filtration conditions, assuming constant filter cake height, the fluid loss rate through the filter cake increases linear with pressure but also depends on time and therefore on flow rate. Hence, flow rate has to be sufficient to overcome any filtration losses.

$$\Delta V = \frac{k \cdot A \cdot \Delta P \cdot t}{\mu \cdot h_{mc}} \qquad \text{Eq. 9}$$

In case a Formation Strength Test is performed in a permeable formation or if the open-hole section includes some permeable layers, leak off can significantly influence the test. It is observed that the test shows a non-linear behavior from the very beginning on. This makes it hard to evaluate if a fracture has been formed or not. As presented in the Leak-Off Test procedure in Chapter 2.5 the minimum volume line can be used to determine if leak-off is a dominating factor during the test. If this is the case, it is recommended to repeat the test at a higher flow rate.

In this paper, it is assumed that the casing shoe has been set in a competent clay formation with low permeability. This is supported by the test data reviewed as none of them shows significant non-linear behavior during pressuring up the well. Furthermore, if analyzing the shut-in phase, more evidence for low permeability can be seen as the pressure drops and stabilizes after the well has been shut-in. In case no permeability is present, the pressure should stay constant during the shut-in phase. This can be explained by spurt loss via the additional surface area as the wellbore is fractured after the Leak-Off Point is exceeded.

In the following example, a Leak-Off Test has been analyzed in terms of permeability using Equation 9. First, the non-linear region has been analyzed under the assumption that no fracture has been created but the whole Leak-Off Volume was lost due to filtration. The properties of the drilling fluid are known, whereas the filter cake height had been estimated. Secondly, the shut-in phase had been analyzed for two different scenarios, with and without the additional surface generated by a fracture.

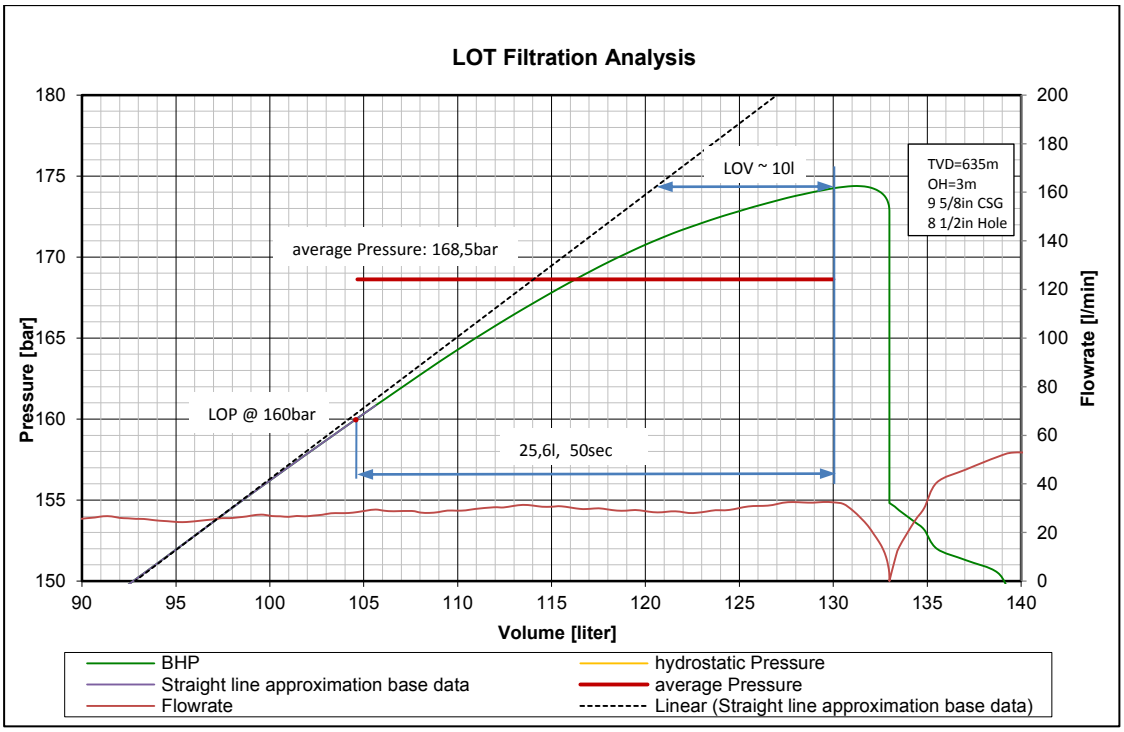

Figure 26 – Leak-Off Test Filtration Analysis

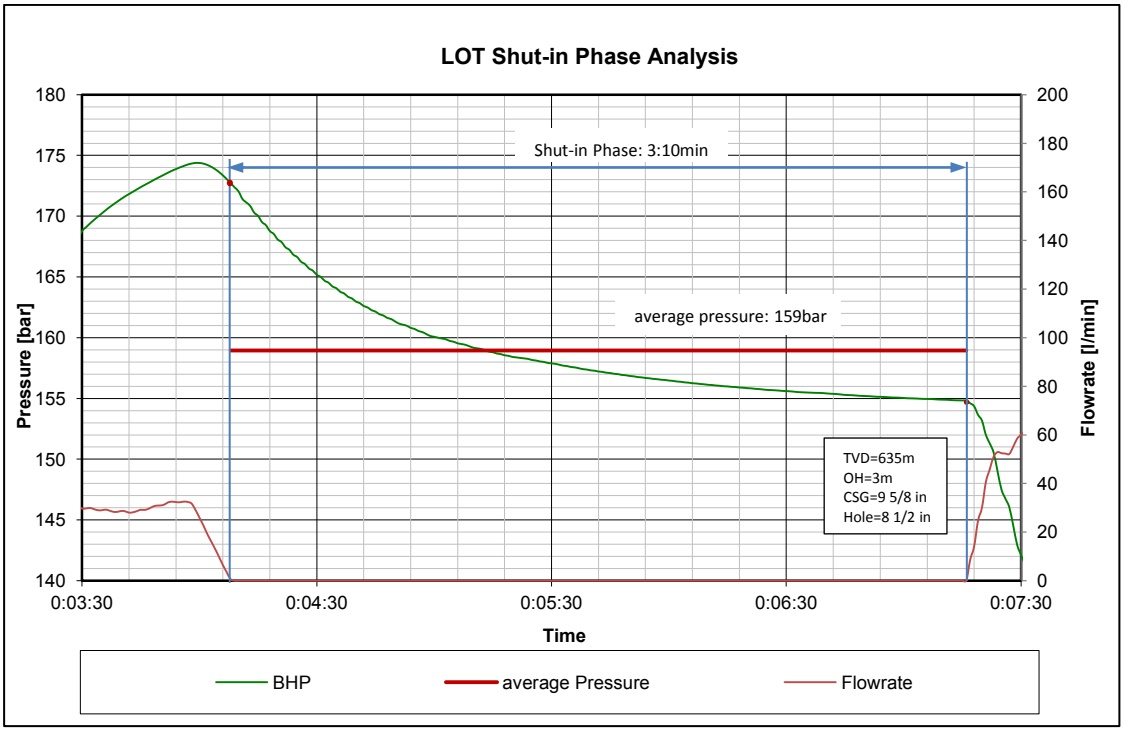

Figure 27 – Leak-Off Test – Shut-in Period Analysis

The fluid and wellbore properties shown in Table 4 and the average pressures according to Figure 26 and Figure 27 have been used to estimate the required permeability.

Properties		
Open hole length (formation only)	3	m
Wellbore diameter	8 ½	in
Leak-Off Volume	0,01	m^3
Viscosity	10	cp
Depth	635	m
Filter Cake Thickness	0,3	cm
Pressure Regime	hydrostatic	

Table 4 – Well, Fluid and Formation Properties for the permeability estimation

As the wellbore is fractured, the fracture faces are considered not being covered by a filter cake. Only the wellbore surface permeability is reduced by a filter cake.

Results								
LOT – no Fracture			**Shut-in – no Fracture**			**Shut-in - Fracture**		
Time	50	s	Time	190	s	Time	190	s
avg. Pressure	168,5	bar	avg. Pressure	159	bar	avg. Pressure	159	bar
Frac. length	0	m	Frac. Length	0	m	Frac. Length	2	m
Permeability	**35**	**mD**	**Permeability**	**10**	**mD**	**Permeability**	**200**	**µD**

Table 5 – Required Permeability estimation Results

The results presented in Table 5 show that without creating a fracture, the permeability of the formation being tested would have to be substantial to generate curves such as shown in Figure 26 and Figure 27. On the other hand, when considering a fracture, the permeability required to explain the behavior as it can be observed during the shut-in phase, is dramatically lower and by far more realistic.

3.2.3 Casing Shoe: Casing - Cement - Rock Interface (Cement Channels)

Cement channels are a possible source of uncommon curve shapes obtained during Formation Strength Tests. Cement channels provide communication through or around the cement at the casing shoe. Differentiation between bad cementation of the casing shoe and therefore communication to a possibly weaker zone and a weaker layer within the open-hole section might not be possible.

In the literature, (Postler, 1997) cement channels are divided into three groups: large open cement channels, small open cement channels and plugged channels as shown in Figure 28. However, a single test cannot confirm a cement channel but it is stated that these channels lead to a certain behavior of the test result. A second test has to be run after remedial cementation to differentiate between cement channel and formation effects as sometimes formation related effects cause the test result to resemble that of a cement channel.

The problem with this approach is that differentiation of the test result from an expected Leak-Off Pressure, or expected test behavior, is considered for the interpretation. This raises the question if it is possible to expect a certain behavior from the test. It might only be plausible in very well known geology. In case of wildcat drilling, no experience at all might be available. The second problem is that confirmation of a bad cementing job is only possible after a remedial cementation has been made and a second test was run. It seems to be very hard to decide for a costly cement squeeze job, which are often of not much of a success, based on a deviation from an expected Leak-Off Test behavior that may be more likely caused by geology. From this point of view, it seems not to be possible to find clear indication of bad cementing during a Leak-Off Test. It can only be said that cement as well as formation behave as needed or not to continue drilling operation as planned. Without further investigation, one cannot say if formation or cement is the weakest point of the open-hole section. A small layer of unconsolidated sand might not be recognized during drilling and misinterpreted as a bad cementing job.

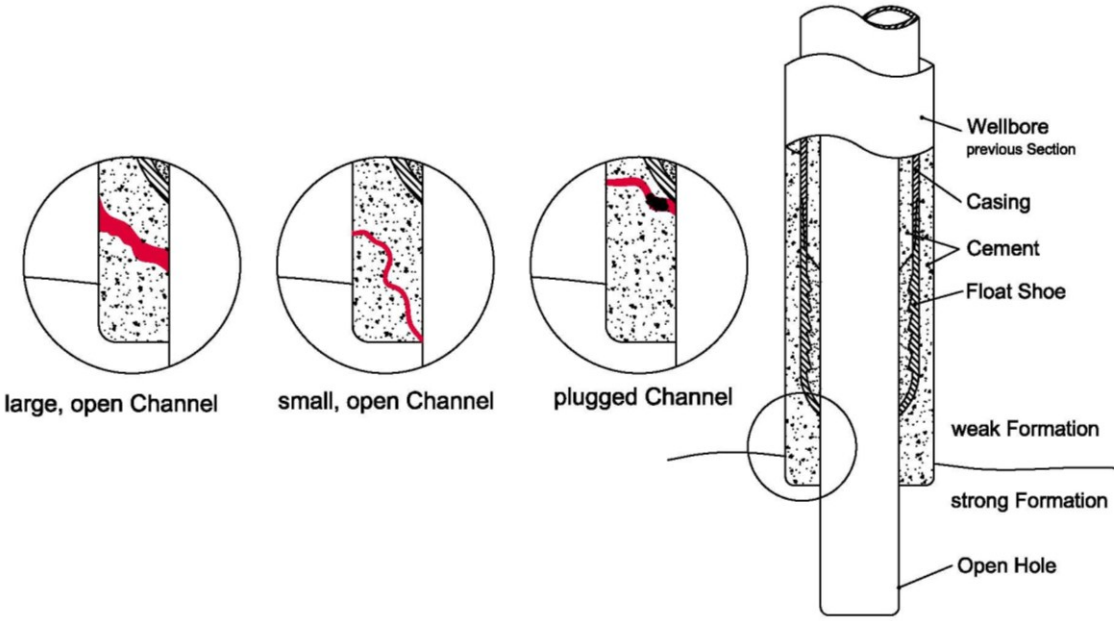

Figure 28 – Cement Channel Scenarios as suggested by Postler 1997

▪ Large open Cement Channel

A large, open cement channel or over-displaced cement and therefore no sufficient zonal isolation at the casing shoe will allows immediate communication to a possibly weaker zone. Therefore, the Leak-Off Tests results will be governed by the weaker formation. Whereas the shape of the obtained graph is in general not affected, the fracture initiation occurs at a pressure lower than expected. This is illustrated in Figure 29b where leak off occurs at a significantly lower pressure than expected as shown in Figure 29a. Due to errors in the estimation of expected Leak-Off Pressure, the result is never expected to perfectly match the expectations. Therefore, cement channel should not be suspected to be present unless the deviation from the expected Leak-Off Pressure is large. Furthermore, the estimation of the Leak-Off Pressure should be subject to reevaluation before it is decided to go for a cement squeeze job to repair the faulty cements (Postler, 1997).

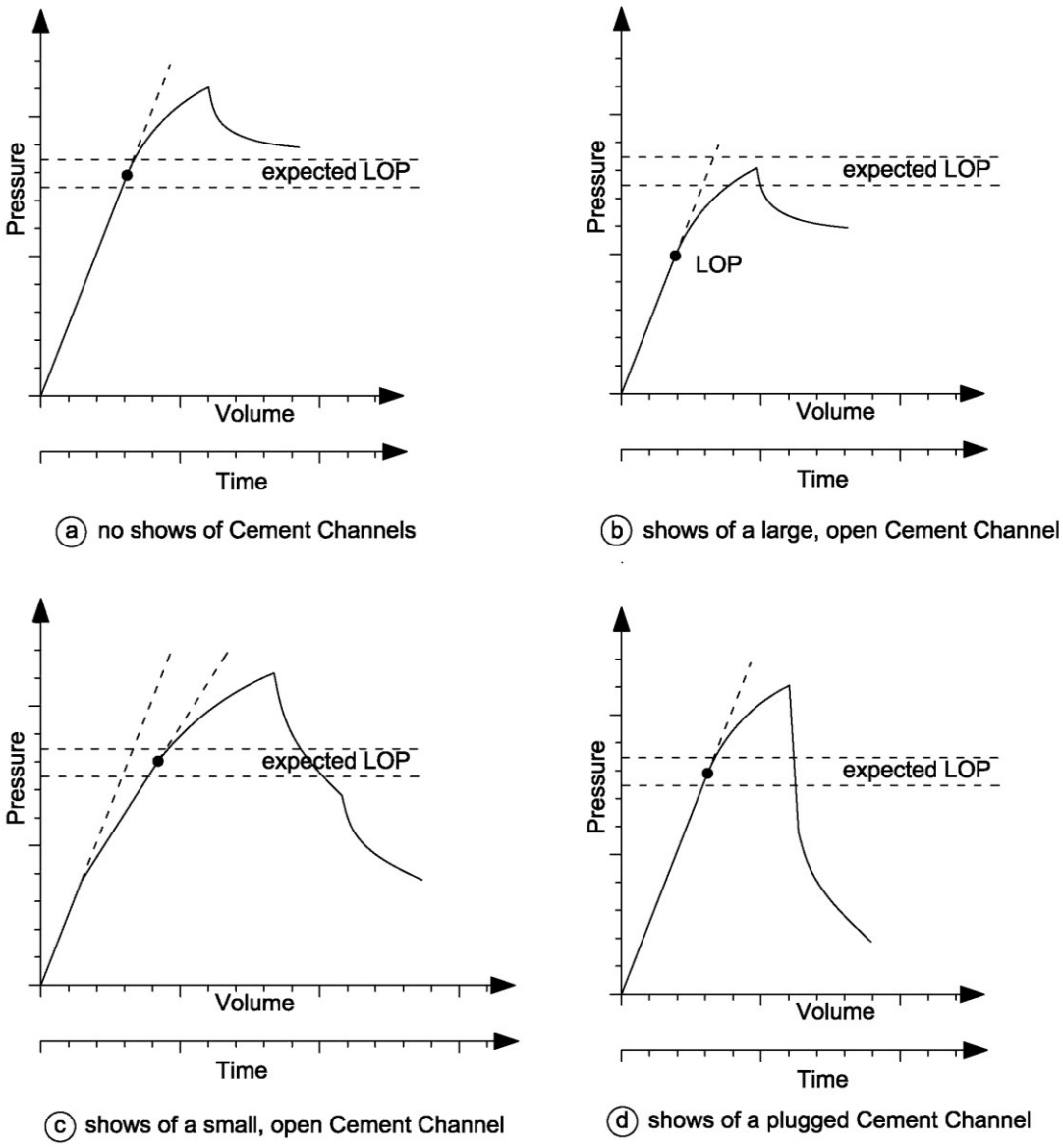

Figure 29 – Shows of different types of Cement Channels on pressure vs. Volume Plots

- **Small open Cement Channel**

A small cement channel, in contrast to a large one, does not allow direct communication but acts as a choke allowing only a portion of the pumped fluid to divert to the weaker zone. The diverted fluid acting against the weaker zone will initiate a fracture there. As only a portion of the fluid is acting against the weaker zone, pressure is still able to build up in the borehole. This pressure acting on the stronger formation is building up, but on a lower rate, until the Leak-Off Pressure of the stronger formation is reached. Hence, the pressure vs. volume plot will show a two-slope shape as shown in Figure 29c. A normal slope until a fracture within the weaker zone is initiated and a reduced slope due to losses to the weaker zone, until a second fracture in the stronger formation is initiated. In some cases, also a second

inflection in shut-in pressure can be observed below the Leak-Off Pressure of the weaker zone due to a different minimum horizontal stress in this zone (Postler, 1997).

This analysis seem to be very hard to verify in actual field data. Sometimes it is already difficult to identify a single change in slope and thereby the Leak-Off Point. Differentiating between different changes in slope and referring this to cement channels seems to be even harder. The availability of precise downhole pressure measurement might give a better results and might enable one the see indications of bad cementation in the recorded data. But still, any suspected cementing problem can only be verified after remedial cementation.

- **Plugged Cement Channel**

The third category of cement channels are channels that are plugged and unplugged during the Leak-Off Test. It is believed that gelled mud entered the channel, plugging it off. Hence, pressure communication cannot be established until the channel is unplugged. This can occur suddenly or slowly as the fluid starts passing by the plugging material and is removing it. Once the channel is unplugged, the weaker zone may break as the pressure removing the plugging material might be quite high resulting in a pressure drop. The shut-in pressure usually drops significantly due to the large pressure difference between pumping pressure and the breakdown pressure of the weaker zone as shown in Figure 29d. The shut-in pressure might even reduce to zero indicating that the minimum stress within the weaker formation is lower than the hydrostatic of the drilling fluid used in the test. In case the test is repeated, it will show the behavior of a small or large cement channel as described above, as the plugging material is already being removed (Postler, 1997).

Identifying cement channels based on Leak-Off Test shapes might be possible in some cases but it is believed that this approach can not be used in day to day operation. Furthermore, the drilling fluid is expected to plug small cement channels rather than unplugging the same. There is no doubt that cement channels may lead to Leak-Off Test results lower than expected, but differentiating between cement channels and geology seems to be impossible in many cases.

3.2.4 Pre-existing Fractures and Bed Boundaries

Pre-existing fractures are frequently observed especially in shale formations. As the fracture is assumed to open under tension, the work done by opening the fracture equals the stress acting perpendicular to the fracture plane times fracture width. As the state of least energy is the preferred configuration of any system, the fracture will propagate in direction perpendicular to the least principal stress.

Pre-existing fractures can have an impact on fracture propagation, the overall trajectory however is controlled by the direction of the least principal stress (Zoback, 2008). These preexisting fractures as well as bedding planes are natural planes of weakness in the formation. They might be just a weakness in rock strength or a high conductive shear zone. Under a normal faulting stress regime, which is the most common stress regime ($\sigma_v > \sigma_{max} > \sigma_{min}$), the largest stress will act on the horizontal plane, but even in this case interaction is possible. Furthermore, it has been observed in many projects that fractures do not propagate in a single plane but form complex geometries. As it will be discussed in a later chapter, the basic fracture mechanism is that in a porous material the fracture propagates with a process zone, at the fracture tip. As in this process zone, complex fracture mechanism like micro cracking and de-bonding take place, the fracture can offset if a pre-existing fracture within the process zone, but at a distance from the fracture plane, is opened. This has been observed in pavements and rock outcrops as well as during microseismic monitoring of stimulation treatments. Fluid cross flow, which is necessary to propagate the opened fracture within the process zone, may be established due to secondary fractures. Fracture propagation can be limited if a fracture hits a joint or the fluid opens orthogonal fractures, as if it is suggested to happen in the Barnett Shale. Both effects lead to increased complexity of fracture geometry. Complex near wellbore fracture geometry may be an explanation for different results in subsequent injections. (Meng & de Parter, 2011)

3.3 Operational Influences

In this chapter, the influence of the operation itself and the materials involved is discussed. These influences are flow rate, injection path, and fluid properties. Some parameters are easier to adjust, like flow rate, as others like mud properties. In addition, the influence of the method of pressure and flow rate measurement is discussed.

3.3.1 Fluid Viscosity

As known from hydraulic fracturing operations, fluid viscosity is an important parameter influencing the ability of the fluid to transfer pressure through the fracture to the crack tip and is therefore influencing crack stability. Higher viscous fluids are associated with a larger pressure drop within the fracture. Hence, the pressure at the crack tip might be below the breakdown pressure even though the pressure in the wellbore exceeds this pressure. As a result, no crack growth can be observed. In order to transmit sufficient pressure to the crack tip, an increased pressure at the crack entrance will be required. This ultimately leads to the observation of increasing Leak-Off Pressure with increasing fluid viscosity regardless of the

fracture opening pressure. For viscous drilling fluids, a significant delay exists between fracture initiation followed by crack growth. For low viscous fluids this difference is significantly lower, what makes identification of Leak-Off Pressure harder. (Postler, 1997).

3.3.2 Gel Strength Development of the Drilling Fluid and Non-Newtonian Fluid Effects

During a Leak-Off Test, drilling fluid, which usually behaves as a non-newtonian fluid, is pumped through the drillstring, annulus or through drillstring and annulus into the well. If the fluid in the well has not been recently circulated prior to the test the drilling fluid develop its gel strength what requires a certain pressure to restart circulation. The pressure loss due to frictional pressure losses is however small due to the low flow rate and independent from the pressure compared to the pressure that might be required to break the gel strength. After circulation is established, the pressure will fall to the constant frictional pressure losses as indicated in Figure 30.

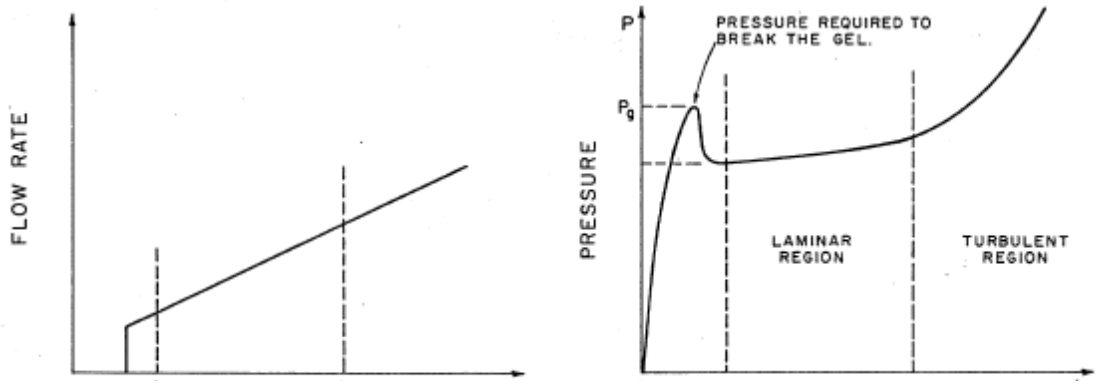

Figure 30 – Typical pressure – flow rate response of drilling fluids (de Aguiar Almeidar, 1986)

If a drilling fluid is used, which develops a high gel strength, it should be circulated prior to the test to minimize its effect on the test. If gel strength is still a problem modifying the fluid properties to lower gel strength will be beneficial. Also pumping through drill pipe alone might help to overcome the gel strength due to the reduced area compared to pumping through drill pipe and annulus (van Oort & Vargo, 2007).

In the tests reviewed during this theses, a drilling fluid with low viscosity developing a low gel strength or even water was used. Therefore the effect on this particular test is marginal.

3.3.3 Flow Rate

It is recommended to keep the flow rate low during the test as this makes identification of the Leak-Off Pressure and stopping the pump shortly after the Leak-Off Pressure has been observed easier. Field observations and experiments have shown that Leak-Off Pressures increase with increasing pump rate.

3.3.4 Injection Path

There are in general three optional pathways to pressurize the well either by pumping drilling fluid through the drill pipe alone, casing-drillpipe annulus or by pumping drilling fluid through drill pipe and annulus simultaneous. All options hold the danger of recording artifacts due to frictional pressure losses and the effect of gelletation. In case of using a drilling fluid that develops high gel strength, it is recommended to pump through drill-pipe alone. As a smaller volume is involved when pumping through drill pipe alone, it is easier to break the gel (van Oort & Vargo, 2007). The effect of gelletation of the drilling fluid can be seen in Figure 31. It also shows that this discussion becomes unnecessary when downhole pressure measurements are taken as discussed in the next chapter. It mainly depends on the equipment available and what option is the most convenient to connect the Pump to the well. In OMV the cementing pump is usually connected to the Casing below the BOP. Drilling fluid is pumped through the casing-drillpipe annulus.

3.3.5 Downhole Pressure Measurement with PWD Tools vs. Surface Pressure Measurement

Pressure while drilling tools are used to measure the pressure downhole during drilling in order to evaluate ECD, detect kicks, evaluate surge and swap pressures during tripping and to provide an accurate measurement of the hydrostatic and thereby the effective mud weight. Pressure While Drilling tools (PWD) can also be used to determine accurate pressure measurements during Leak-Off Tests (Halliburton, 2010). The use of downhole pressure measurement eliminates the effects of mud compressibility, mud gas cut and casing expansion as well as the need of pressure correction from surface to downhole pressure what may not always be straight forward.

Figure 31 shows a pressure vs. time plot comparing surface vs. downhole pressure measurement. The example shows how the effect of gelletation of the drilling fluid effects the pressure measured on surface (van Oort & Vargo, 2007). Another advantage provided by downhole measurement is the reduction of measurement artifacts as the curve provided by the

downhole pressure measurement tool is by far smoother than the plot of the surface measurement. This makes identification of the Leak-Off Pressure much easier. The results of some tests interpreted from surface pressure measurement alone might be very uncertain (Lee, Birchwood, & Bratton, 2004).

As the BOP is closed during the test, data from downhole tools cannot be transmitted to surface via mud pulses during this time. PWD Tools are capable of recording the pressure and storing the pressure data in downhole memory. As soon as circulation has been reestablished after the test, the tool can transmit the data to surface. The data has to be synchronized with the data being recorded on surface to correlate the pressure data with the volume data, which is only recorded on surface. Still, also if using a pressure while drilling tool, during the test itself, data acquired by surface measurement is necessary to evaluate the test as it is performed to decide when the final test pressure has been reached. The downhole data can then be used to further investigate the test and to more precisely evaluate the Leak-Off Pressure.

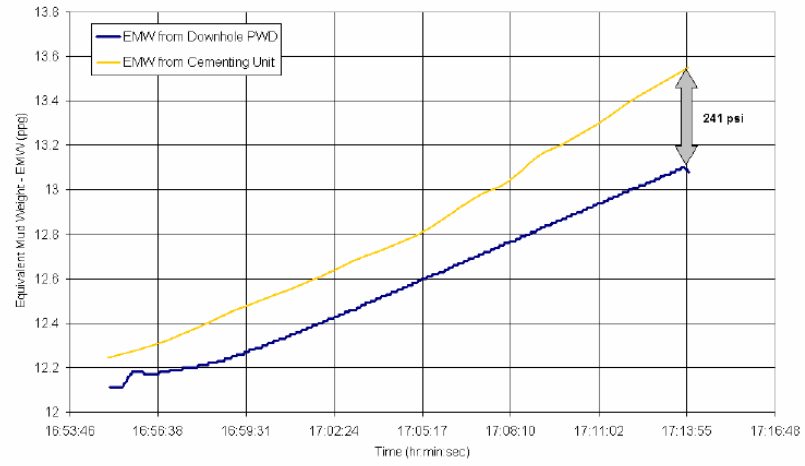

Figure 31 – Surface Pressure vs. Downhole Pressure Measurement during a LOT in the Gulf of Mexico (van Oort & Vargo, 2007)

Besides pulsing the pressure data to surface for reevaluation of the test, also real time monitoring is possible. Therefore, a different method for data transmission has to be used instead of mud pulse. A wire-line connection between the downhole tool and surface can solve this issue making real time evaluation of the downhole pressure possible, also with the BOP being closed.

Such a real-time Formation Integrity Test was performed on the Shell Auger in the Gulf of Mexico, combining wire-line and pressure while drilling services. During the test, an annular pressure while drilling sensor was included in the bottom hole assembly used to drill out the casing shoe. The downhole pressure was monitored in real-time by means of a wire-line-

operated logging while drilling inductive coupling tool sitting inside the collar containing the annular pressure sensor. This enabled the downhole pressure data to be transmitted to the surface. This tool is usually used to retrieve nuclear sources, or data from logging while drilling tools that got stuck downhole, but it had never been used for a Formation Strength Test. The LWD inductive coupler allows the recorded data in the tools to be downloaded without having to pull the tool to the surface. The coupler assembly is pumped down on a wire so as to latch onto a special bullnose on the top of the uppermost tool in the bottom hole assembly. Once secured it provides bi-directional communication: data can be downloaded, tool-recording parameters can be reprogrammed.

One advantage of having a real time measurement of the pressure during a Formation Strength Test is an instantaneous signal to stop the test once the slope of the pressure build-up curve changes. Therefore, it helps avoiding unnecessary over pressuring of the formation. It also removes the uncertainties in the compressibility and expansion of the drilling fluid due to pressure and temperature. This is especially important for synthetic muds in offshore wells where the mud is subject to cold seawater in the riser and the hot environment downhole. Furthermore, it increases the accuracy of the Formation Strength Test, allowing casing points to be more precisely determined, improving drilling safety, and potentially reducing the number of casing strings (Rezmer-Cooper, Rambow, Arasteh, Hashem, Swanson, & Gzara, 2000).

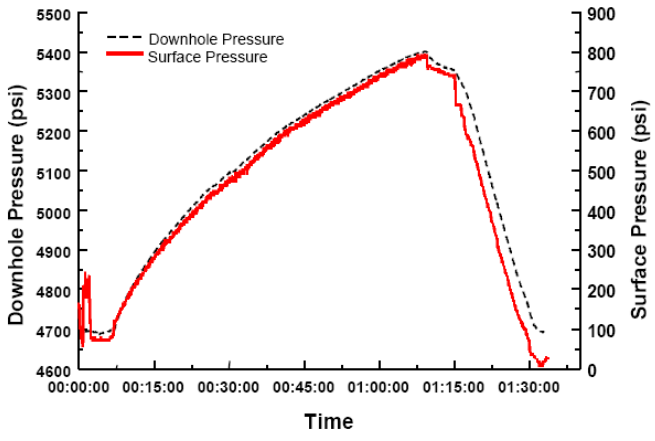

Figure 32 - Time development of Auger FIT, indicating the maximum pressure for both downhole and surface sensors. The downhole annular pressure measurement is less noisy.

4 Review of Leak-Off Test data

In this chapter, Leak-Off Test data acquired within OMV will be reviewed. Leak-Off Tests performed in OMV are recorded digital and stored in a database. These tests have been used as the basis of further assumptions.

4.1 Leak-Off Test Data Set

During this thesis Leak-Off Tests performed at eight wells drilled in the Vienna Basin in the north-east of Austria have been evaluated.

Well	Test TD [m, TVD]	Nr. Of Cycles
Dobermannsdorf 2	561	1
Dobermannsdorf 2	1225	2
Ebenthal 20	995	2
Erdpress 9	513	2
Erdpress 10	548	2
Erdpress 12	510	1
Hausleiten 86	555	3
Poysbrunn 3	635	2
Roseldorf 22	491	1

Table 6 – Leak-Off Data Set - Wells

The locations of the wells are shown in Figure 33, the well data is shown in Table 6. The complete Data used for the evaluation is presented in Appendix E

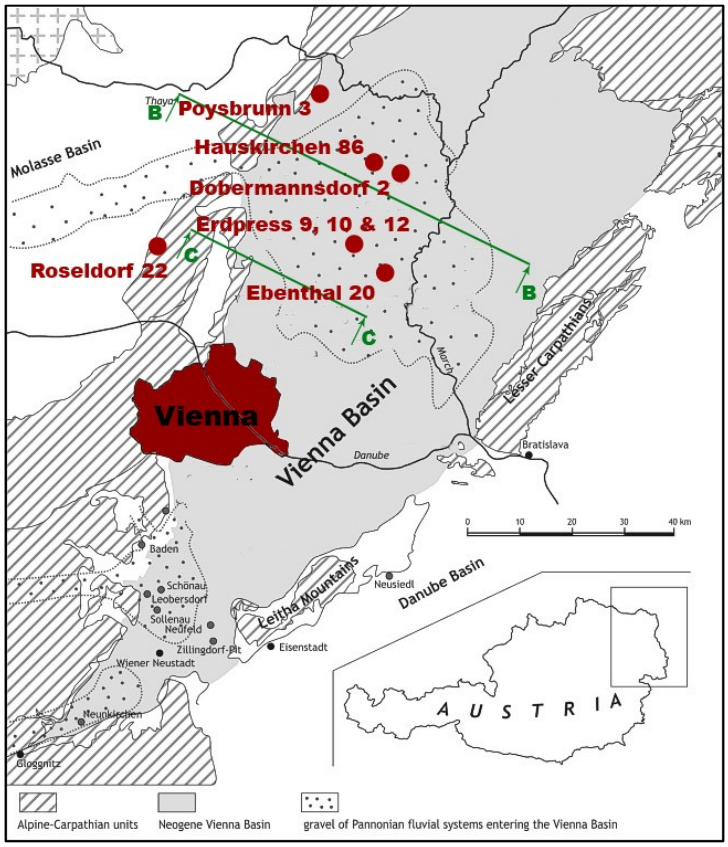

Figure 33 – Well Locations (Harzhauser, Daxner-Höck, & Piller, 2004)

4.1.1 Leak-Off Point & Leak-Off Volume Estimation

Estimation of the Leak-Off Point is not always easy. Reason is that due to filtration the initial phase of the test must no longer be a straight line. This leaves room for interpretation. In general, the mid two quarters of the test up to the final test pressure provide a good base for interpolation by a linear function. The decision what data points are used for the interpolation has to be made for each test individually.

The Leak-Off Volume (LOV) was determined by extrapolating the straight line used for the determination of the Leak-Off Point up to the maximum test pressure. The difference between the extrapolated straight line and the recorded test result has been measured as Leak-Off Volume as shown in Figure 34.

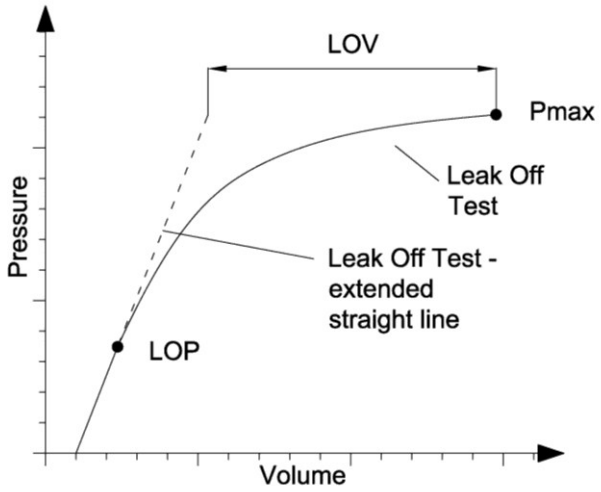

Figure 34 – Leak-Off Volume Estimation

The obtained volume was within a range of 4 to 16 liters with 9.5 liters in average. In general the pump has been stopped within one minute after the LOP has been observed. At this time, flow rate already dropped to about 30 l/min whereas a part of this volume was still used to compress drilling fluid, expand casing and open-hole and some portion of the fluid is forced into the formation. An example of showing the estimation of the Leak-Off Pressure and Leak-Off Volume is presented in Figure 35 and Figure 36. It can be clearly seen that from the pressure vs. time chart alone the Leak-Off Point cannot be correctly measured due to the unstable flow rate whereas the pressure vs. volume plot overcomes this problem. To analyze the shut-in period, the pressure vs. time plot has to be used.

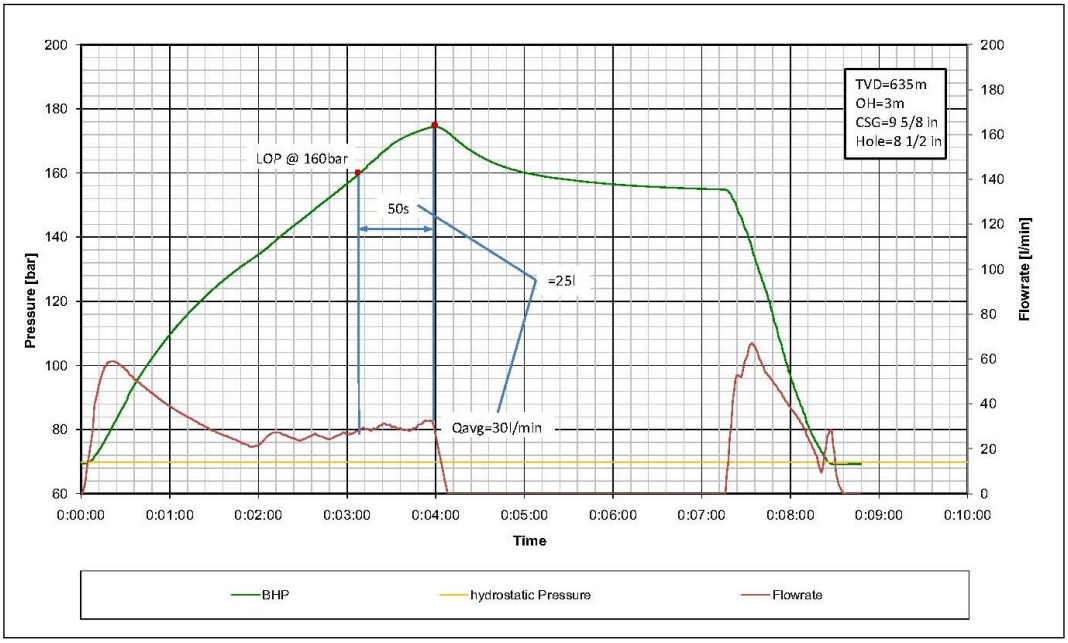

Figure 35 – LOT Pressure vs. Time Chart

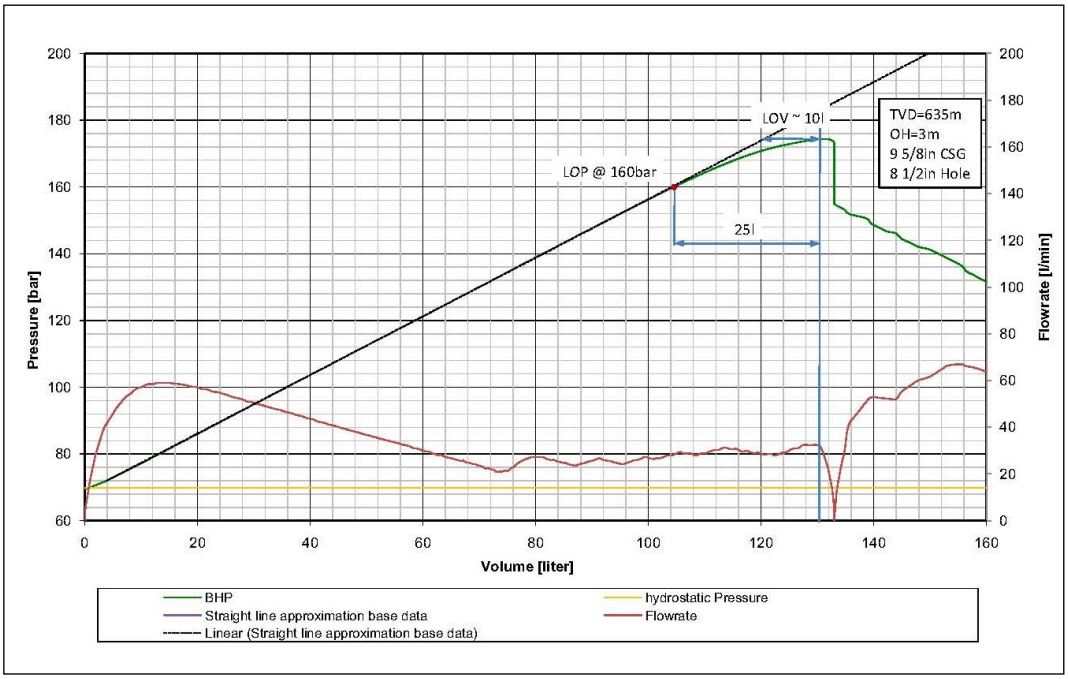

Figure 36 - LOT Pressure vs. Volume Chart

4.1.2 Well Configuration

For this evaluation, 15 Leak-Off Tests recently performed by OMV in the Vienna Basin have been reviewed. A detailed sketch of the well configuration during a Leak-Off Test is shown in Figure 37. Table 7 contains some more detailed information on the typical well configuration of the wells that have been reviewed. Most of the tests reviewed, have been performed at a similar depth and configuration but still, some have been performed at greater depth and/or a different configuration.

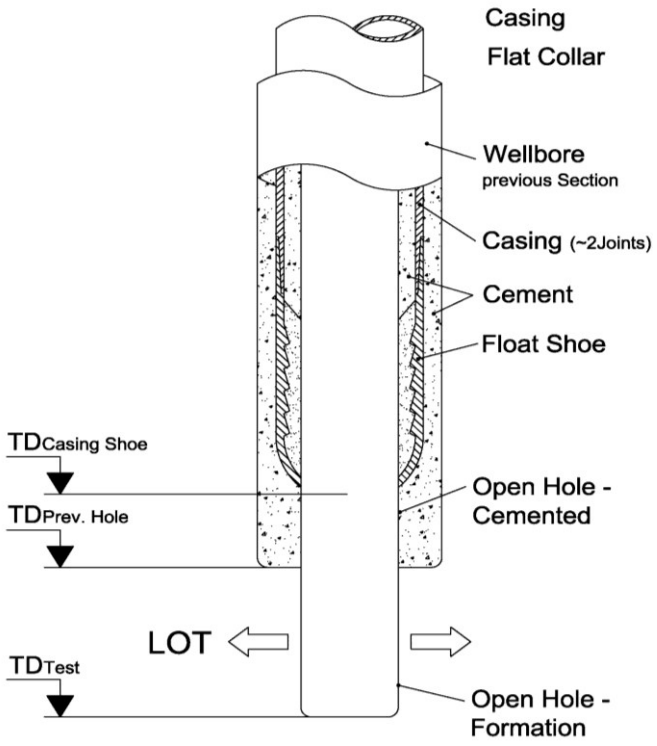

Figure 37 - Well Configuration during a Formation Strength Test

Casing Setting Depth (TVD)		450-600m
Casing	Diameter	9 5/8 in
	Weight	36ppf
	Quality	J55
Open-hole	Diameter	8 ½ in
	Length – Cement	2m
	Length – Formation	3m

Table 7 – Typical Well Configuration

4.1.3 Geology

All wells which have been review have been drilled in the Vienna Basin during the last years. The formation of interest for the investigation is the formation just below the first casing. Typically the first casing is set at about 450m to 600m TVD. According to the Drilling Program the Casing has to be set in a competent clay formation to ensure integrity at the casing shoe, as this is a potential weak point during drilling the next section. Prior to setting the casing, the final casing setting depth is defined by the well-site geologist who's decision is based on spot samples taken from the borehole. Aim is to keep the casing shoe as well as the rat-hole below free of any sand layers. Reason is to avoid problems during cementation of the casing.

The first casing is set at about 500m in the Lower Pannonian Formations. The Lower Pannonian contains up to 500m of sediments from basinal settings of mainly marl and compromises a 12-20m thick layer of sand and gravel in the north known as transitional beds (Harzhauser, Daxner-Höck, & Piller, 2004). The layers are very shallow and therefore young section within the Vienna Basin. It is typically very soft, of low permeability and of negligible stress anisotropy.

A more detailed view of the Geology, as it is encountered in the Vienna Basin, is shown by the Lithology Log shown in Figure 39. The logging equipment has been run during drilling of the 8 ½" section of the Erdpress 9 well. As the log was run as a logging while drilling the log start just below the depth in which the leak off test has been performed. Hence, it does not give any information about the geology which affected the results of the Leak-Off Test but it gives a general idea of what the geology looks like.

Figure 38 shows the cross section through the Vienna Basin as indicated in Figure 33. It can be seen that all tests have been performed in the same formation.

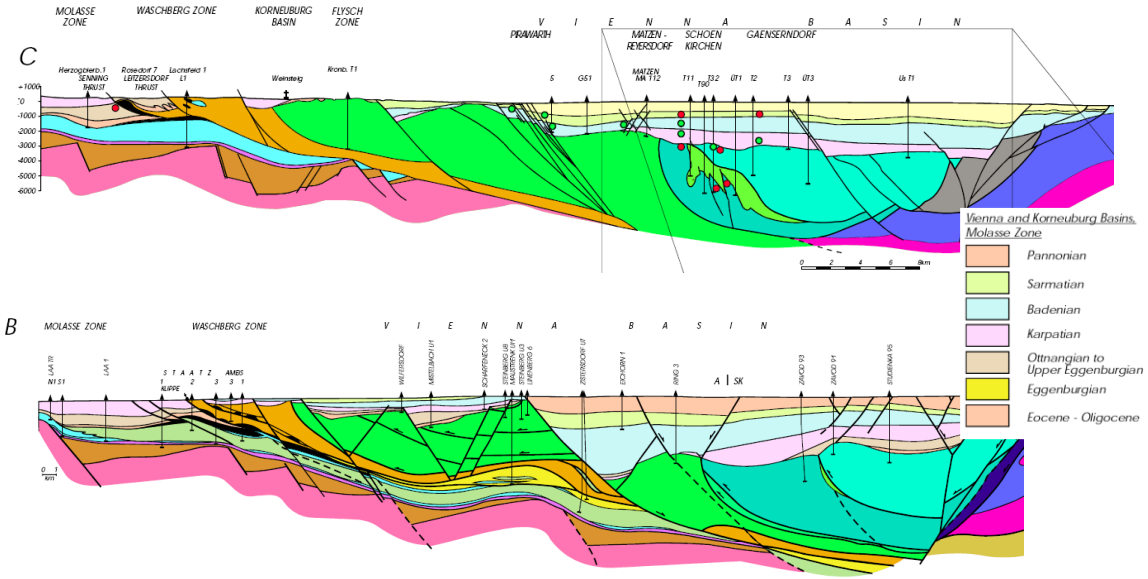

Figure 38 – Cross Section through the Vienna Basin (Arzmüller, Buchta, Ralbovský, & Wessely, 2006)

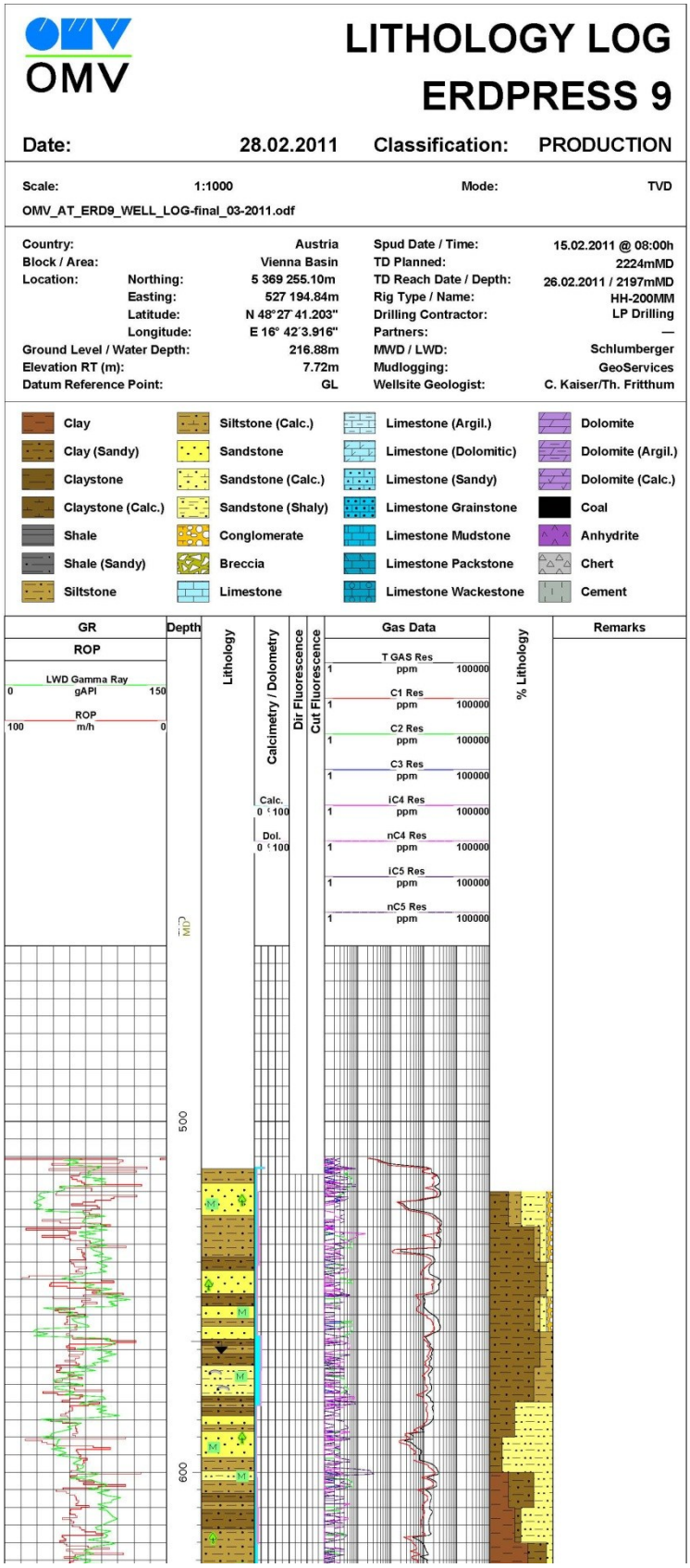

Figure 39 – Lithology Log – Erdpress 9

Figure 40 shows a Standard Log run after drilling of the 8 ½" section of the Erdpress 10 borehole. The section of the Leak-Off Test is marked in red. It seems like it has been conducted in a layer of shale just above a layer of higher sand content.

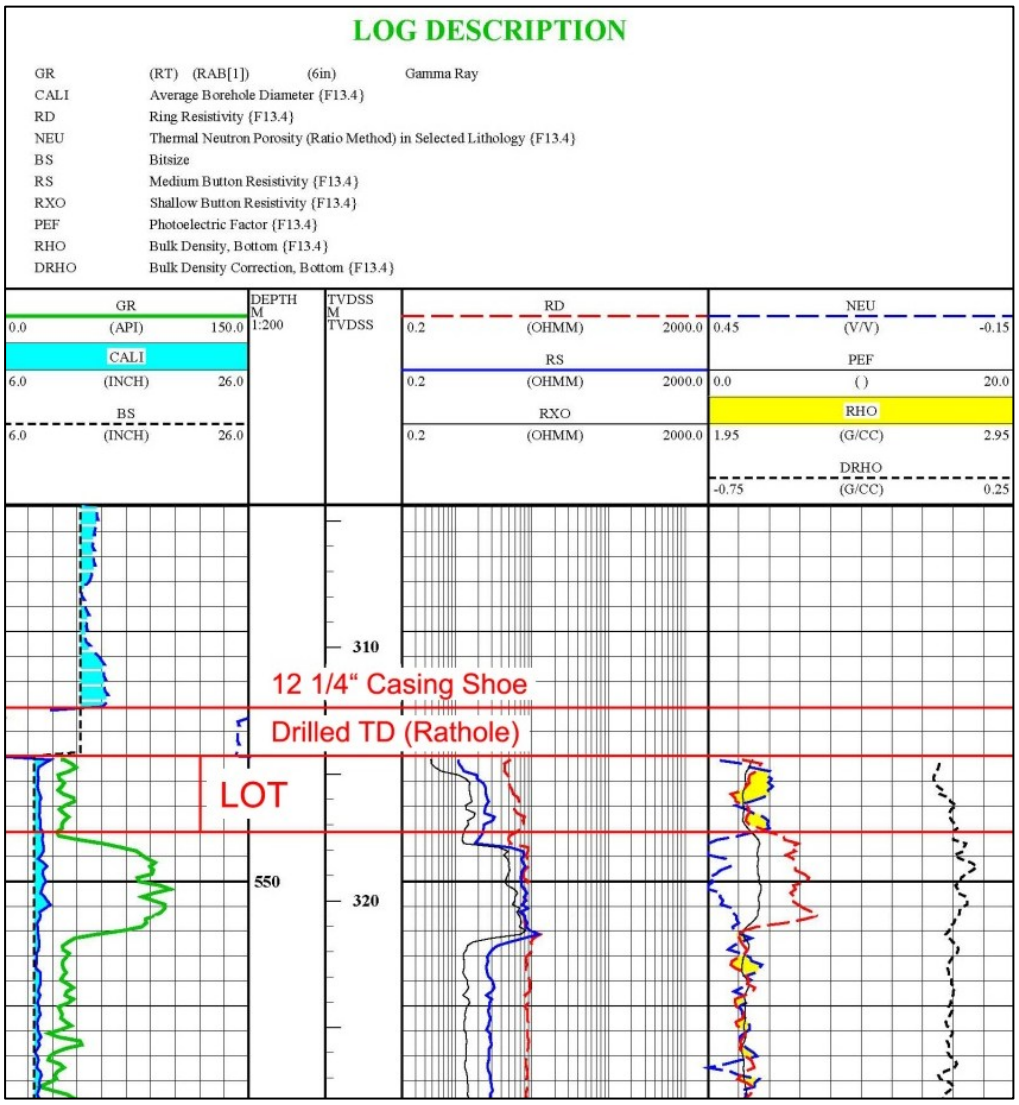

Figure 40 – Standard LOGs Erdpress 10, 8 ½" Section

Geology is always different and hard to predict. In terms of Leak-Off Test, it has a huge impact on the results. It is always necessary to evaluate the results of a Leak-Off Test with keeping the geology in mind. A good idea about permeability or the presence of high permeable layers of fractures can give an analysis of the shut-in phase of a Leak-Off Test. As one can already see from the lithology log, geological properties can change significantly over a short interval of the well. Therefore it is always hard to make assumptions on the properties further down the well from a single test.

4.2 Stress distribution around the wellbore

The insitu stress distribution in the subsurface is governed by the three principal stresses. These are, vertical stress σ_v, minimum horizontal stress σ_h and maximum horizontal stress σ_H, all being perpendicular to each other.

After a well has been drilled, the stress field is disturbed by the hole as the load that has previously been taken by the material that has been drilled has now to be supported by the rock surrounding the wellbore resulting in an increase of insitu stress. The pressure within the wellbore helps to support the load and therefore reduces the stresses around the wellbore. It is often believed that this disturbed stress field around the wellbore leads to an increased resistance of the formation against failure and is therefore responsible for the pressure to be further increased after a fracture has been initiated. Furthermore, many explanation of Leak-Off Tests describe the fracture created in such a test as being a "near wellbore fracture" which does not leave the area of disturbed stress.

If the pressure inside the wellbore is increased as it is done during a Leak-Off Test, at some point, the area of the wellbore in maximum horizontal stress azimuth will see tensional stress. If this tensional stress exceeds the tensional limit of the rock, a fracture is initiated.

4.2.1 Tensile failure of rock

During a Leak-Off Test, at some point tensile failure occurs at the borehole wall, typically at maximum horizontal stress azimuth. The tensile strength of rock is generally low. There are multiple reasons for this. First, tensile strength of rock is generally as low as a few MPa only and if preexisting cracks are present, tensile strength is expected to be near zero. At depth, usually all stresses are of compressional nature. However, if the fluid pressure is large, tensional failure can occur naturally resulting in joints. These are usually closed by any means of compressive stress. Hence, one can conclude that as soon as the tensional stress at the wellbore wall occurs – tensional failure of the rock can be expected (Zoback, 2008).

4.2.2 Linear-elastic approach – Kirsch Equations

The insitu stress distribution around the wellbore is described by equations derived by E. G. Kirsch in 1898 and are therefore known as Kirsch Equations. The Kirsch Equation describing tangential effective insitu stress and its relation to the LOP is shown in Appendix D . The Fracture Initiation Pressure is thereby given by Equation 10. This model is based on linear elasticity and is assumed to underestimate the Fracture Initiation Pressure.

$$P_{FI} = 3\sigma_h - \sigma_H - P_o + \sigma_T \qquad \text{Eq. 10}$$

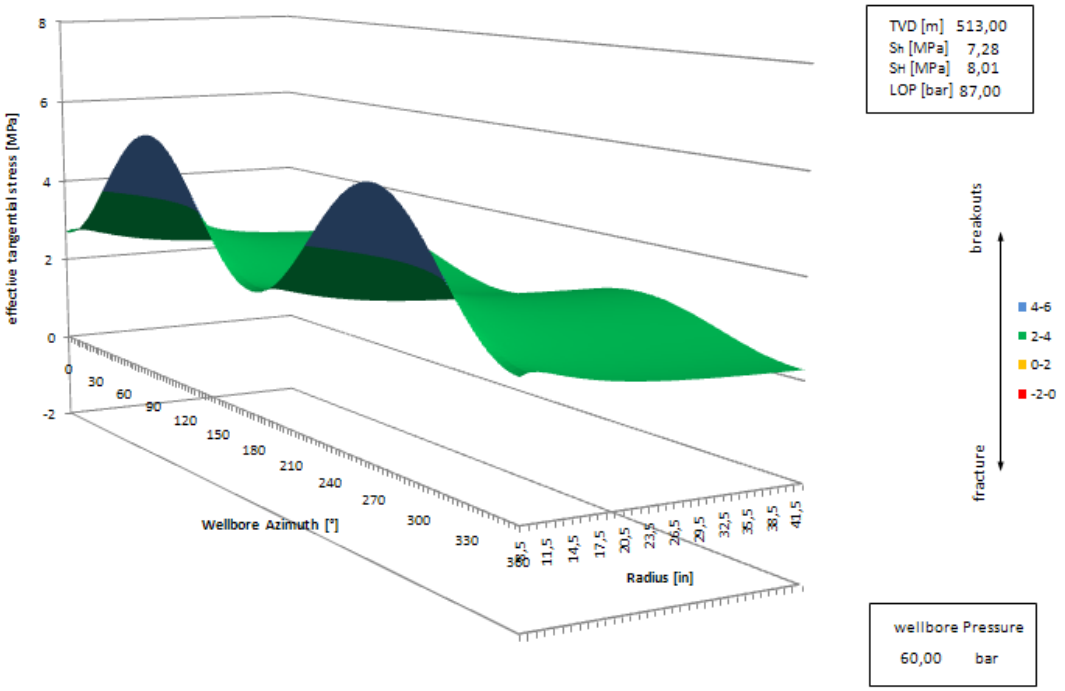

Figure 41 – Stress Distribution around the wellbore with wellbore pressure slightly over hydrostatic

Figure 41 shows the stress distribution around the wellbore for the wellbore pressure being slightly over hydrostatic. The minimum and maximum horizontal stress value has being calculated based on an arbitrary, low stress contrast β of 1,10. In case the wellbore pressure is lowered, stresses at 90° and 270° azimuth increase what will at some point cause breakouts. The other way round, in case the wellbore pressure is increased, 0° and 180° azimuth stress will decrease exceeding the tensional limit at some pressure causing the wellbore to fracture.

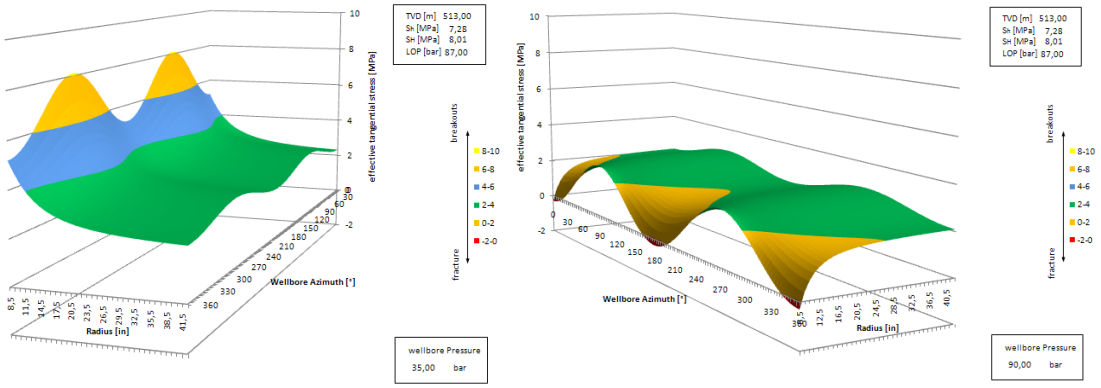

Figure 42 – Stress distribution around the wellbore for lower wellbore pressure (left) indicating breakouts and higher wellbore pressure (right) indicating fractures

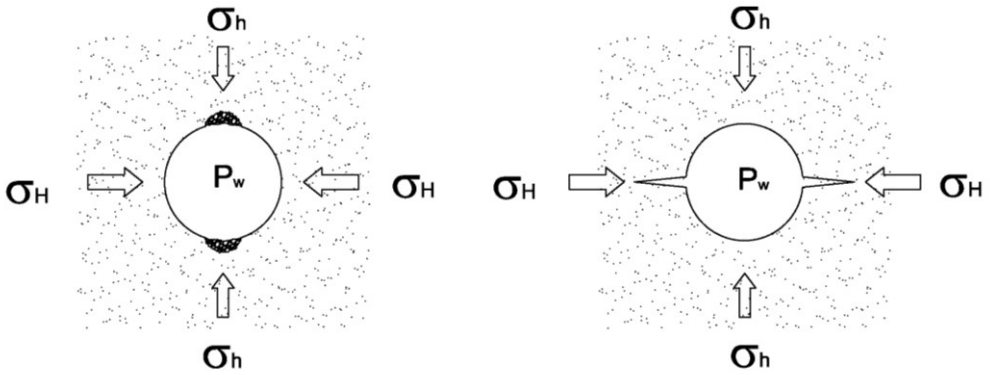

Figure 43 - Compressional (left) and Tensional (right) wellbore failure – Breakouts and Fracture

In the following example, the horizontal stresses had been estimated from the Leak-Off Pressure assuming a low stress contrast β of 1,02. The assumption on the stress contrast is usually not easy. As shown in Figure 44, small errors in stress contrast can lead to a large error in the estimated stresses, especially if stress contrast gets larger. In this example, the Leak-Off Test was performed in a relatively shallow, young formation assuming low stresses and a low stress contrast.

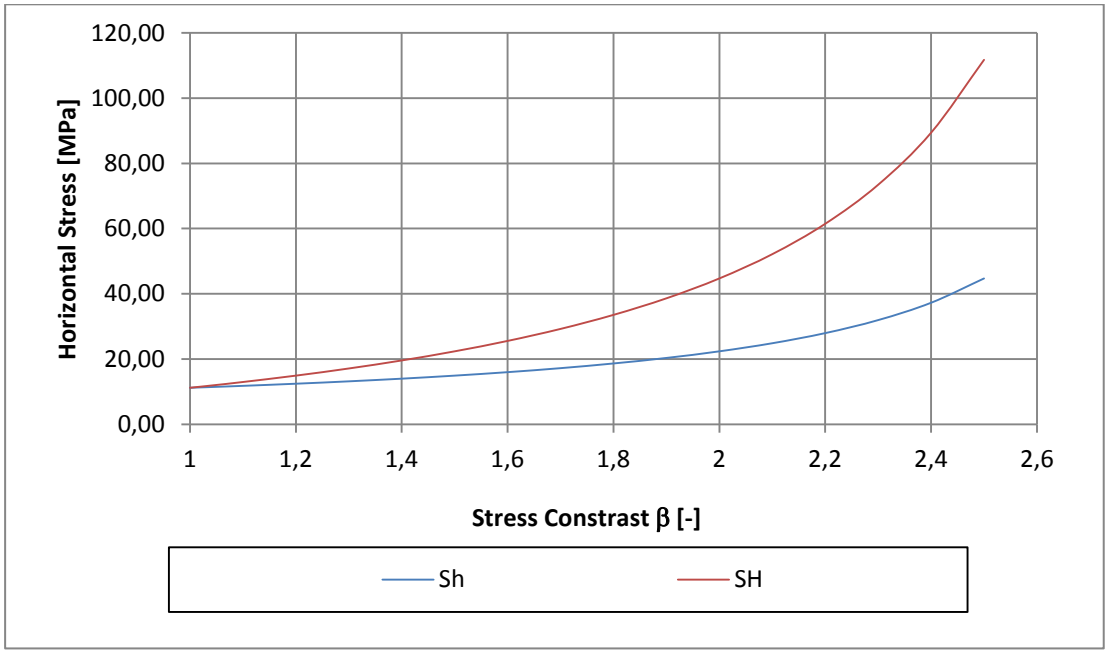

Figure 44 – Stress contrast

The Kirsch Equations were used to calculate the tangential stress distribution around the wellbore. Figure 45 shows the effective tangential stress distribution around the wellbore at the Leak-Off Pressure. It can be seen that tension will be seen first at 0° and 180° azimuth, which represents maximum horizontal stress direction. It can also be seen that the zone of

stress distortion by the wellbore reaches about two times the wellbore diameter into the formation in this particular case.

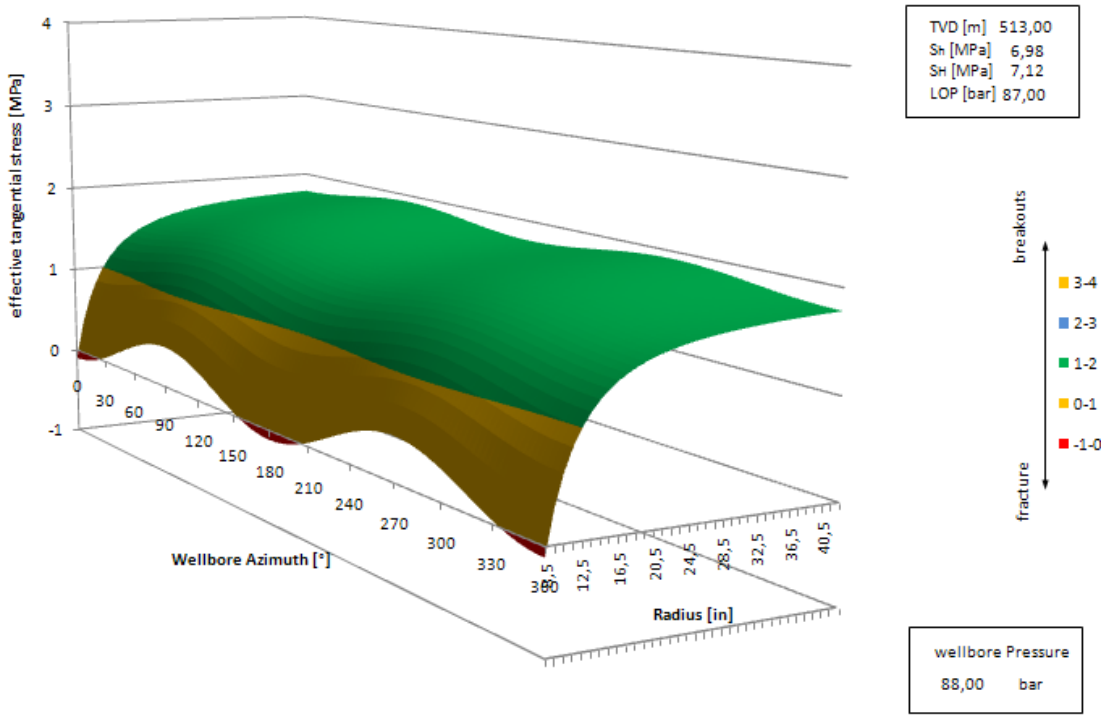

Figure 45 – effective tangential stress at maximum test pressure

In the later, "near-wellbore" area will be defined as the zone around the wellbore in which the stress deviation as defined in Equation 11 exceeds ±10%. In case the stress deviation is below this value the zone is defined as undisturbed area.

$$\text{stress deviation} = 1 - \frac{\sigma_{\tan,\text{eff}}(\theta=0;r)}{\sigma_{h\,\min}} \qquad \text{Eq. 11}$$

Figure 46 shows the stress deviation between absolute tangential stress and minimum horizontal stress at zero degree wellbore azimuth, for different stress contrasts, β, over a dimensionless distance from the wellbore, r/r_w. It shows that at a distance more than three times the wellbore diameter from the wellbore wall (r/r_w=4), the absolute tangential stress is getting as close as ±10% to minimum horizontal stress. Already from Figure 45 it can be seen that this assumption is valid.

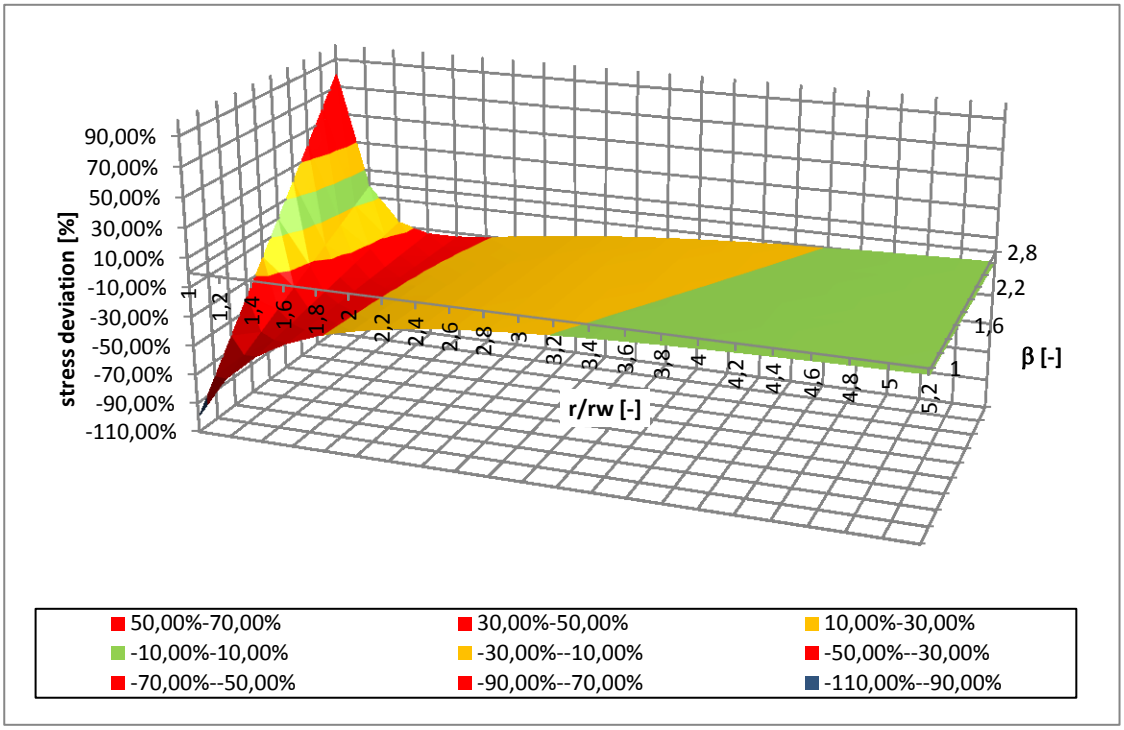

Figure 46 – Definition of "near-wellbore" area

The definition of the near wellbore area is of importance, as in this area the stress field deviates from the insitu stresses. Reason is that the surrounding rock has to support the load of the rock, which has been drilled. Many explanations of Leak-Off Tests refer to fractures which are opened but do not propagate further into the formation than this zone reaches. Furthermore, in extended Leak-Off Test, aim of the test is often to create a fracture reaching the undisturbed stress field to get measurements of the undisturbed insitu stresses.

4.2.3 Elasto-plastic borehole model (Aadnoy & Mesfin, 2004)

Experiments presented by Aadnoy 2004 suggest that the Kirsch Equations underestimate fracture initiation pressure. An elasto-plastic borehole model is presented to combat the deviations between Kirsch equations and the experiments.

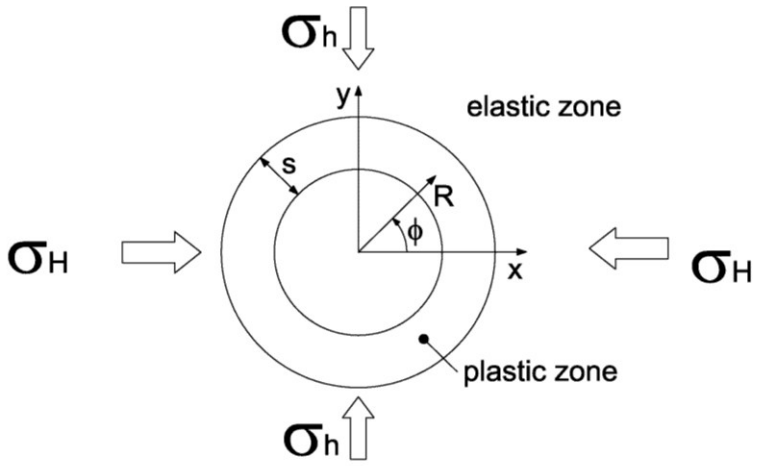

Figure 47 – Elasto-Plastic borehole model

The model considers a plastic zone at the inner wall of the wellbore whereas the surrounding rock behaves linearly elastic. The model has been derived assuming borehole pressure as the inner boundary condition for the plastic zone, a pressure match at the plastic/elastic zone interface and in situ stress as external boundary at infinity. The derivation of the model is shown in Aadnoy & Mesfin, 2004, Appendix A. Equation 12 shows the fracture initation pressure suggested by the elasto plastic model.

$$P_{FI} = 3\sigma_h - \sigma_H - P_o + \sigma_T + \frac{2\,Y}{\sqrt{3}} \cdot \ln\left(1 + \frac{s}{R_i}\right) \qquad \text{Eq. 12}$$

Equation 12 defers from the fracture imitation pressure given by the Kirsch Equation presented in Equation 11 by the last therm. Aadnoy & Mesfin, 2004 suggest deriving the plasticity parameters, s and Y, using least mean square error analysis of fracturing data. The parameter s represents the thickness of the plastic zone, whereas Y represents the yield stress for initial borehole failure.

4.3 Fracture Geometry and Volumetric

Fractures created during a Leak-Off Test are often believed of not leaving the zone of stress influenced by the borehole. As discussed in the previous chapter, this zone extends about four wellbore diameters into the formation. For the estimation of the fracture volume a fracture of constant cross section with fracture height is assumed as this would give a conservative estimation of fracture length at a given volume. Furthermore, the model considers the fracture being equal-sided and its cross-section being calculated by a semi-analytical solution for fracture opening under tension and shear due to an applied far field stress and ambient fluid pressure presented by Pollard and Segall in 1987, given by Equation 12.

$$W = (2\sigma_{h\,min} + P_i)\,\frac{(1-\nu)^2}{E}\,\sqrt{a^2 + x^2} \qquad \text{Eq. 13}$$

The fracture face is approximated being a straight line, neglecting the arched shape of the borehole/fracture volume interface. This assumption is valid as the influence on the volume is small in case fracture face width is small compared to borehole diameter, fracture height and penetration depth. Fracture height has been assumed being equal to the formation height which is exposed to the fluid pressure. Fracture face width and fracture penetration length results from the pumped volume and Equation 13. Not considered is complex fracture growth. The fracture is assumed to grow, following a straight-line path, parallel to the borehole, into the formation. Furthermore, the fracture is assumed to grow symmetrically against maximum horizontal stress direction.

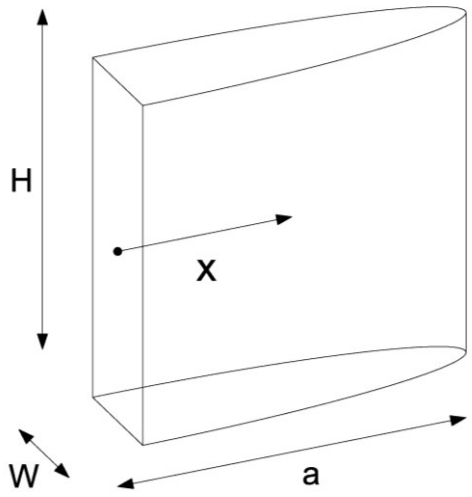

Figure 48 – Fracture Geometry

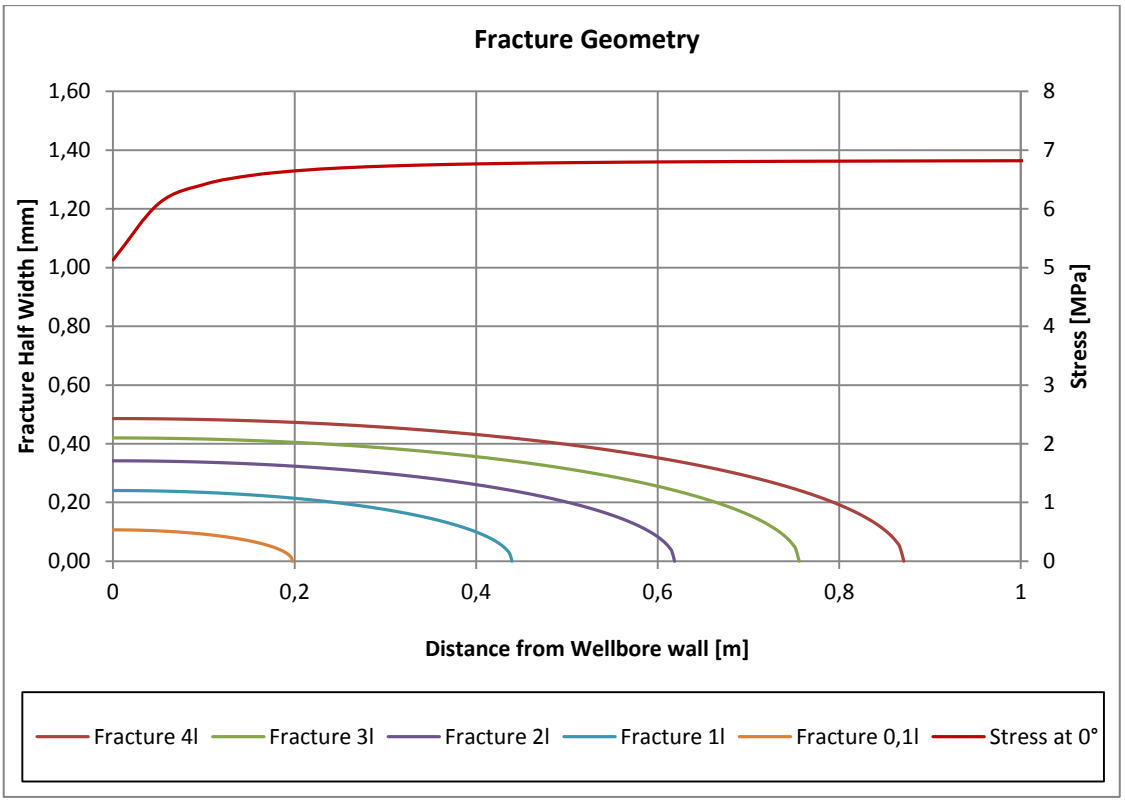

Figure 49 – Fracture Geometry and Stress distribution at zero degree wellbore azimuth

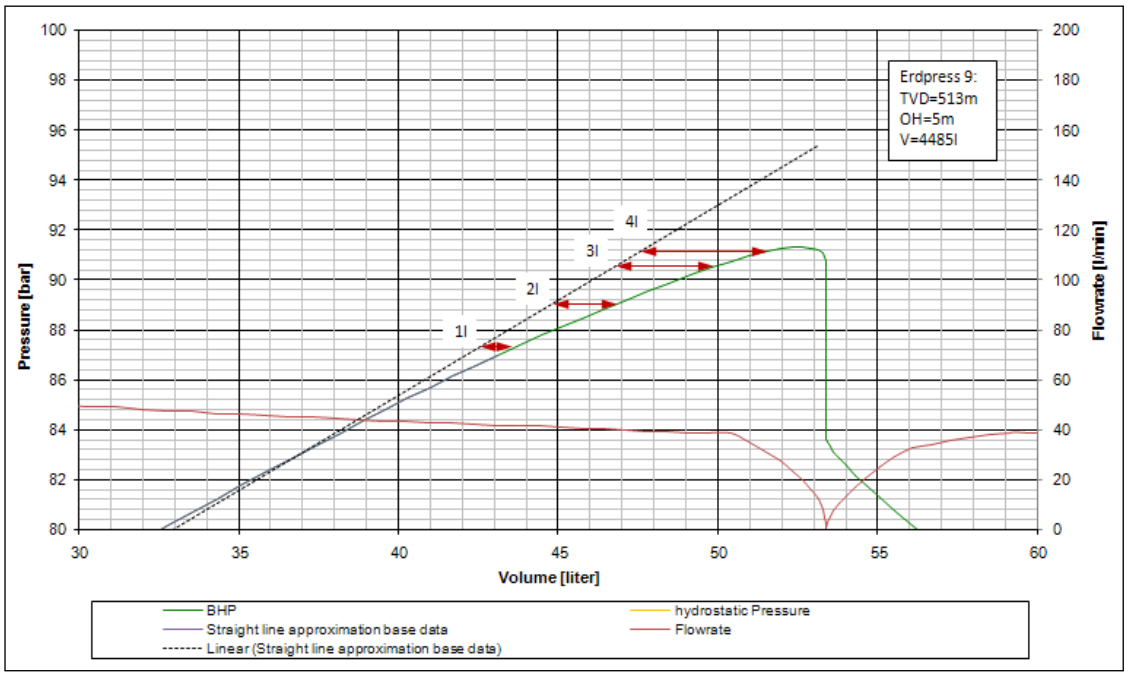

Figure 50 – Leak-Off Test – Leak-Off Volume for fracture volume estimation

From the example presented in Figure 49 and Figure 50, it can be seen that the zone of stress influenced by the wellbore has no significant impact on fracture growth. The near

wellbore stress regime defines tensile failure at the wellbore wall. Once a fracture is initiated, fracture growth is dominated by the far field stress and fracture mechanics. The fracture tip leaves the zone of stress influenced by the wellbore just shortly after the fracture has been initiated. At this point the fracture might not even be conductive to drilling fluid. Assuming the fracture is initiated at the Leak-Off Point, in Figure 49, it can be easily seen that a fracture of a volume of only 0,1 liter already extends already 0,2m from the wellbore wall. At this stage, just after the fracture has been opened, it already left near wellbore region. It has to be noted that the diagram presented in Figure 49 uses two different scales, millimeters on the ordinate and meters on the abscissa. Hence, the fractures created are of very small width compared to their length. Therefore, Leak-Off Volume sufficient to be noticed on a surface or even on downhole measurement can only be achieved by large fracture length as fracture height is more or less fixed and fracture width is small. Another factor influencing fracture growth may be fluid properties, as it might not allow full pressure transmission of the wellbore pressure to the fracture tip.

Figure 49 also suggests that a fracture already reaches a certain length before it can be invaded by the drilling fluid. The Leak-Off Point observed on the plots therefore does not correspond to the point of fracture initiation but does correspond to the point where the fracture becomes conductive to the drilling fluid. This provides an explanation why different Leak-Off Pressures can be observed with different drilling fluids. In general, Leak-Off Tests performed with oil-based muds show lower Leak-Off Pressures than Leak-Off Tests performed with water based or synthetic muds. The reason for this is that oil based fluids do penetrate fractures more easily than other fluids do.

5 Introduction to Fracture Mechanics

This chapter will give a short introduction to fracture mechanics. A fracture propagation criterion has to be fulfilled at the fracture tip to make the fracture propagate further from the wellbore into the formation. Different theories, introducing such criterion, are be discussed.

5.1 The Griffith Energy Theory

In Griffith' energy theory, generalized by Irwin 1957, the fracture energy required to produce a unit surface area of an open crack, what is the energy release rate G, is introduced. In this theory, the energy stored in the system has to exceed the fracture energy of the material. While the stress intensity factor describes the stress field near the fracture tip, the energy release rate represents the driving force to open a crack. Due to difficulties in experimental measurement of fracture energy, Griffith Energy Theory did not gain much attention until Irwin modified Griffith Energy Theory in 1957, using stress intensity rather than fracture energy. The relation between stress intensity factor and energy release rate is given by Equation 14 with E being the Young's modulus.

$$\mathrm{G_I} = \frac{\mathrm{K_I^2}}{\mathrm{E}} \qquad \text{Eq. 14}$$

$$U_m = -\frac{\pi\, a^2\, (\mathrm{P}_i - \sigma_{\mathrm{h\,min}})^2}{\mathrm{E}} \qquad \text{Eq. 15}$$

$$U_s = 4\, a\, \gamma_s \qquad \text{Eq. 16}$$

$$U = U_m + U_s = -\frac{\pi\, a^2\, (P_i - \sigma_{h\,min})^2}{E} + 4\, a\, \gamma_s \qquad \text{Eq. 17}$$

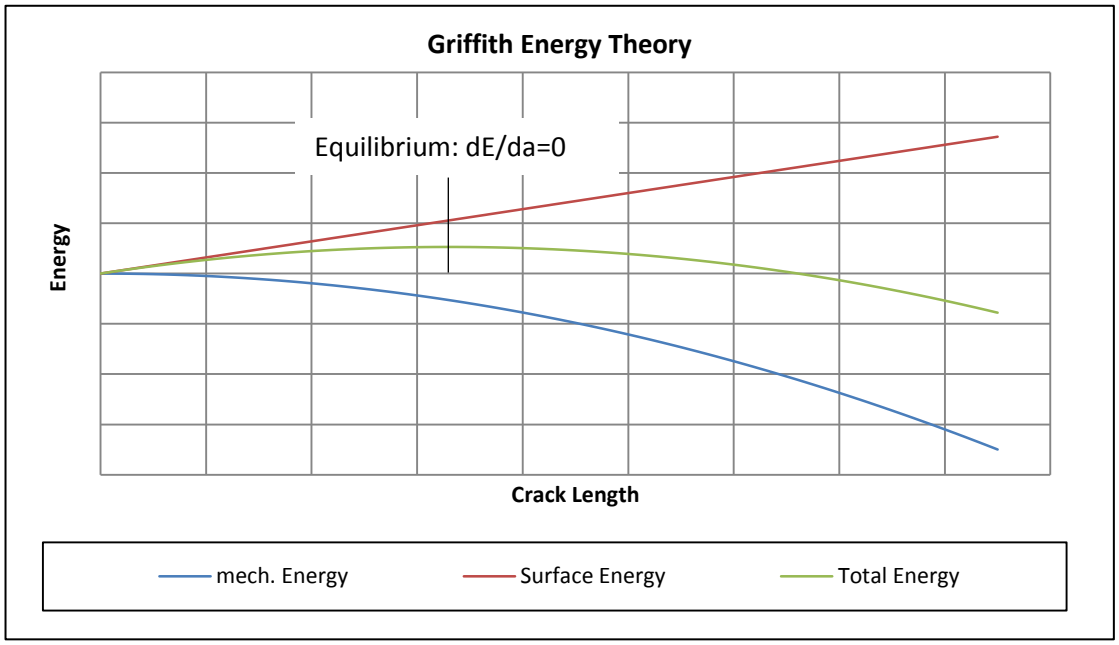

Figure 51 – Griffith Energy Theory – Mechanical vs. Surface Energy

Equation 15 to Equation 17 describe the mechanical energy which is needed to open a crack of a certain length, the surface energy which is released as the crack is opened and the sum of the above mentioned. From Figure 51, it can be seen that from a specific crack length on more energy is released as is needed to open the crack. This point represents the critical crack length from which the crack will propagate on its own as a system always tends towards the state of least energy causing ultimate failure.

5.2 Stress Intensity Factor

The stress intensity factor is a constant defining the amplitude of the stresses near the crack tip, with which the crack tip stress field is uniquely determined (Zihai, 2009). The criteria for fracture propagation is defined by the stress intensity factor K_I, exceeding the critical stress intensity factor also called fracture toughness K_{IC}. It describes the transition form stable to unstable crack growth or in terms of stress intensity factor the transition between subcritical and critical crack growth. A stable crack is defined by propagating comparably slow through a material and can be stopped at any stage. To continue the crack propagation an increase in stress is required. In contrast to stable crack growth, an unstable

crack is accelerated by excess energy. The terminal velocity of elastic waves of the material limits the crack propagation speed of an unstable crack as shown in Figure 52 (Backers, 2004).

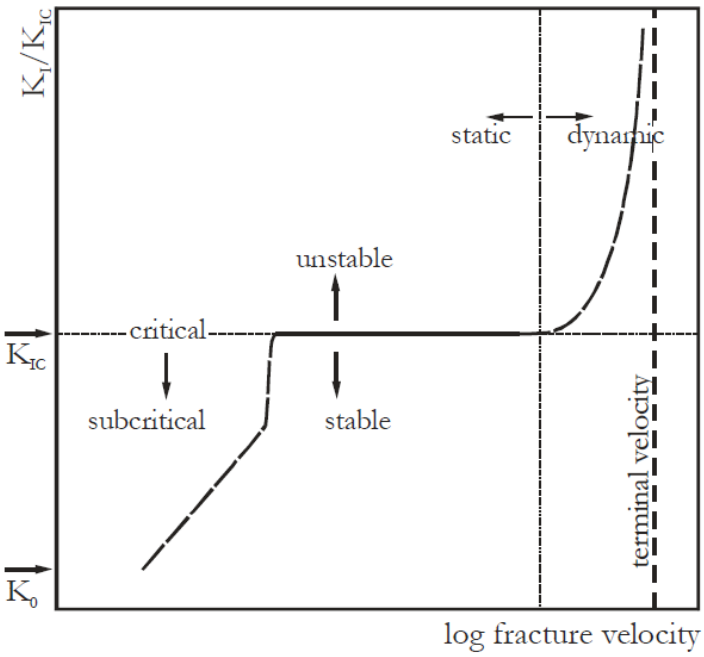

Figure 52 – Static - dynamic vs. stable (subcritical) – unstable (critical) crack growth schematic plot of K over crack propagation velocity for mode I opening (Backers, 2004)

The subscript 'I' defines the opening mode of the fracture. Opening mode 'I' refers to a fracture opening under tensional stress normal to the fracture plane as one would expect a fracture to open in a vertical borehole in a normal faulting stress regime. The different opening modes are shown in Figure 53. The stress intensity factor for a crack of length 2a, in an infinite plane, which is subject to a uniform stress field is defined by Equation 18. Whereas Y represents a geometry depended factor being one for an ideal sharp fracture and σ equals the far field stress. The effective stress acting on the fracture surface is defined by the pressure within the fracture, which tempts to open the same and the minimum horizontal stress, which is acting perpendicular to the fractures plane of propagation and tempts to close the fracture.

$$K_I = (P_i - \sigma_{h\,min}) \cdot Y_g \sqrt{\pi a} \qquad \text{Eq. 18}$$

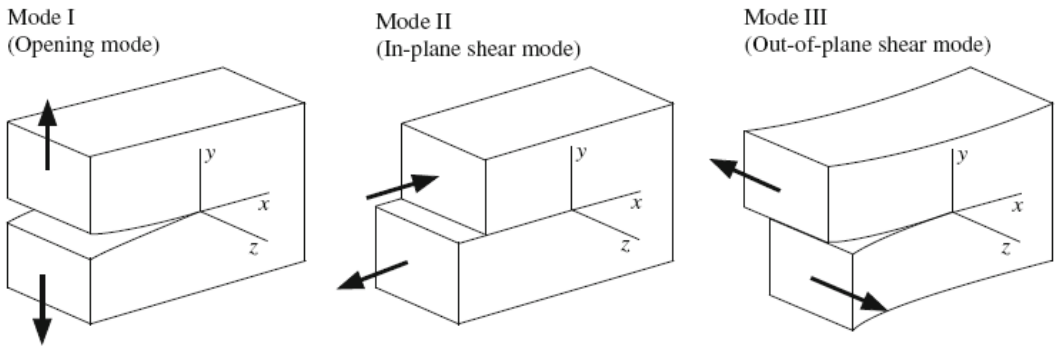

Figure 53 – Fracture opening modes (Zihai, 2009)

If considering a fracture initiated at the wellbore wall due to a pressure inside the wellbore, fracture opening would most likely follow mode 'I'. Bedding planes or preexisting fractures might cause a fracture opening in a mixed mode but this will not be subject of investigation.

Table 8 gives a summary of typical values of Fracture toughness under mode 'I' opening found in the literature presented by Bakers 2004. Usually a wide range of values is found as fracture toughness varies with environmental and loading conditions. Laboratory experiments have shown that fracture toughness increases with increasing confining pressure. For some samples a linear increase of fracture toughness with increasing confining pressure was found. Furthermore, temperature and loading rate are suggested to influence fracture toughness. As rocks are inhomogeneous materials, variations in physical properties like grain size, density, Young's modulus, tensile strength and Poisson's ratio cause experimental data to scatter.

Rock Type	K_{Ic} [MPa $m^{1/2}$]	Reference
Diorite (Äspö)	3,21	Staub et al. (2003)
Diorite	2,22 – 2,77	Bergman et al. (1989)
Dolostone	0,81 – 2,57	Gunsallus & Kulhawy. (1984)
Granite	~ 2,0 1,88 0,65 – 2,47	Ingraffea (1981) Rao et al. (2003) e.g. Müller & Rummel (1984), Ouchterlony (1988), Ouchterlony & Sun (1983)
Limestone P=0,1MPa P=28MPa	~0,8 0,82 – 2,21 0,42 1,57	Ingraffea (1981) e.g. Bergman et al. (1989), Guo (1990), Ouchterlony & Sun (1983) Al-Shayea et al. (2000)
Marble	2,21 0,46 – 2,25	Rao et al. (2003) e.g. Bergman (1990), Guo (1990); Müller & Rummel (1984), Ouchterlony (1988)
Sandstone P=0,1MPa P=40MPa P=80MPa	1,67 0,67 – 2,56 1,08 2,21 2,54	Roa et al. e.g. Guo (1990), Ouchterlony (1988), Meredith (1983) Müller (1984)

Table 8 – Fracture toughness data from various sources, confining Pressure P is given for confining pressure depended data (Backers, 2004)

5.3 Fracture Process Zone – Cohesive crack model

The model presented has originally been developed for concrete structures but most rock types are assumed to behave comparable. As concrete, also rock consists of particles bonded together at the interface. The material is therefore weak in tensional capacity and preexisting micro cracks are likely to exist. In the process zone at the fracture tip, complex fracture mechanisms including micro-cracking, de-bonding and crack deflection take place as it is shown in Figure 54.

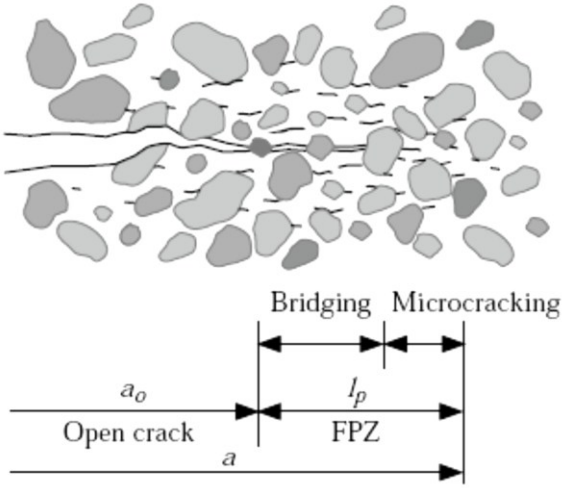

Figure 54 – Concept of fracture process zone and tension-softening in concrete: FPZ in front of an open crack, Bridging and Micro-cracking (Zihai, 2009)

As discussed in the previous section, the stress intensity factor describes the stresses in vicinity of the crack tip. As the assumption of the smallness of changes at the boundary conditions at the surface of an unstrained body is not satisfied in bodies with cracks, the equilibrium of a body with cracks is non-linear. Hence, linear elastic theory, more precisely, Hook's law is applied beyond its limits of validity. The strength of the formation is limited by it's yield strength. Therefore, a small zone directly in front of the crack tip, called fracture process zone, is expected to behave in-elastically (Backers, 2004).

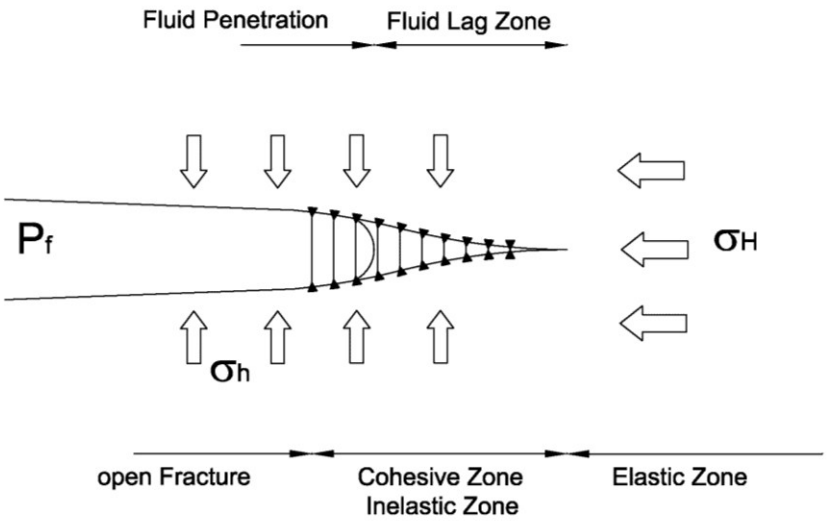

Figure 55 - Cohesive Crack Model

Figure 55, shows a crack including an extensively developed inelastic zone in front of the fracture tip. The crack is divided a free length and the fracture process zone, where cohesive stress tends to close the crack. The material in the fracture process zone is damaged but can still withstand a stress, which is transferred from one surface to the other. The material outside the fracture process zone is assumed to be linear elastic. The fracture process zone starts to develop when the minimum principal stress reaches the tensile strength and the corresponding true crack tip opening displacement is zero. With increasing crack tip opening the stress is reduced to zero while the corresponding crack tip displacement reaches a critical maximum value. The crack closing cohesive stress is assumed to be a constant having the value of the yield strength, the closing cohesive stress is a function of the true crack tip opening displacement.

5.4 Fracture Mechanics in Formation Strength Tests

To propagate a fracture through the formation a fracture propagation criteria has to be fulfilled. In terms of fracture propagation speed, it seems as a fracture in Formation Strength Tests is always propagating with its critical velocity. The fracture growth until its propagation criteria is no longer fulfilled, either due to a change in material property, a drop in pressure or as the fracture hits an obstacle like a joint of pre-existing fracture. The fracture is believed to grow step by step rather than continuously.

Subcritical fracture growth takes place at very low velocities. The velocity at which a fracture travels though the formation is given by the rate at which fluid is forced into it. This rate is typically too high for subcritical fracture growth to take place. A more realistic picture would be an increasing pressure inside the fracture until the fracture tip moves for a certain distance at critical velocity. At some point the pressure is not high enough and the fracture propagation criteria is no longer fulfilled. As the pressure now increases due to pumping more fluid into the wellbore, causing the pressure at the fracture tip to increase, the fracture propagation criteria is at some point fulfilled causing the fracture tip to move further through the formation.

The additional increase in pressure between Leak-Off Pressure and the maximum pressure which can be seen in Extended Leak-Off Test is believed to come from the drilling fluid not allowing for full pressure transmission to the fracture tip and thereby causing the fracture propagation criteria not to be fulfilled earlier. At some pressure however, every increase of volume will ultimately result in the fracture propagation criteria to be fulfilled and thereby

resulting in a stable fracture propagation pressure. This would explain different formation strength graph generated as a test is performed with different fluids.

6 Leak-Off Test interpretation and theories

6.1 Review of different theories explaining Leak-Off Tests

Aim of this thesis is to review and evaluate different explanations of the deviation in the pressure vs. volume plot obtained in Leak-Off Test. In this chapter, some theories found in the literature are presented and further investigated.

The main question is whether a fracture is created at the point of the first deviation from the straight line and if so, does this influence the formation strength during drilling of the next section.

Many papers published try to model the behavior of Leak-Off Tests. Common approach is modeling the elastic behavior in different levels of details. Effects such as drilling fluid compressibility, casing expansion as discussed in an earlier chapter are considered. But when it comes to the point of deviation assumptions like fracture initiation, increased filtration or arbitrary cement channels are made.

6.1.1 Fracture Initiation at the Leak-Off Pressure – System Volume Increase due to fracturing

(Zoback, 2008)

In Zoback 2008, the decrease in rate of wellbore pressurization is explained by sufficient additional system volume generated by a fracture propagating far enough into the formation. The fracture is assumed to propagate perpendicular to the least horizontal stress. Hence, the Leak-Off Pressure is therefore approximately equal to the least horizontal stress although the Leak-Off Point might reflect some near wellbore resistance. Leak-Off Pressures higher than the least horizontal stress are caused by pressure losses in perforations or by the use of highly viscous fluids. The Formation Breakdown Pressure is described as the pressure at which unstable fracture propagation occurs. Unstable fracture propagation occurs as fluid flows faster into the fracture as fluid is supplied by the pumps. Hence, the pressure drops after the Formation Breakdown Pressure is reached and pumping is continued to the so-called Fracture Propagation Pressure. This behavior is explained by propagating a fracture away from the wellbore under absence of near wellbore resistance.

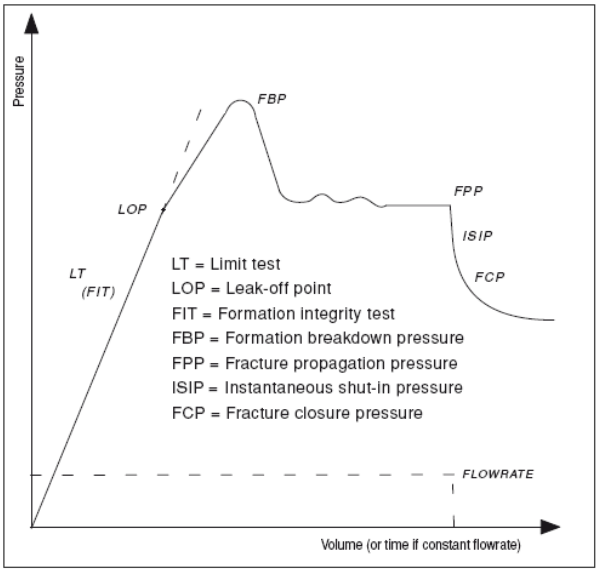

Figure 56 – Frequently used schematic of an Leak-Off Test

Questions left open by the explanation:

? The formation breakdown pressure is explained by the absence of near wellbore resistance. As shown in Chapter 4.3 and earlier Chapters, the near wellbore area is small compared to the fracture length created, even at early

stages of the test. It is questionable why at some point the near wellbore effects should suddenly disappear.

? The drop in pressure marking the transition between formation breakdown and fracture propagation is not present in many tests as shown in the examples presented in Appendix F .

6.1.2 Fracture Initiation at the Leak-Off Pressure – System Stiffness approach

(van Oort & Vargo, 2007)
(Raaen, Skomedal, Kjorholt, Markestad, & Økland, 2001)
(Brudy & Raaen, 2001)

The so-called system stiffness approach, introduced by van Oort & Vargo 2007 is usually applied to extended Leak-Off Test evaluation in order to define the Fracture Closure Pressure. It is assumed that a fracture closes in two stages resulting in a change in slope of the pressure vs. volume chart. Fracture closure is divided into mechanical and hydraulically closure.

Mechanical closure occurs when the "hinge-like" initial closing ends, and asperities of the fracture faces start to meet. The fracture is physically closed but still conductive to fluid.

Hydraulically closure occurs when the fracture faces are forced against each other and the fracture gets non-conductive to fluid. If this happens, the system stiffness reverts to the value corresponding to the stiffness of the well only.

When the fracture is open, this will give additional contribution, which will reduce the stiffness of the system meaning inverse stiffness is added. The fracture stiffness for a non-penetrating fracture as presented by Raaen & Brudy is independent of the fracture width. Hence, the fracture stiffness will be constant during flow-back and the inverse stiffness will increase with fracture length as it propagates. This can also be seen in the typical Leak-Off Test plots as the slope decreases during pumping within the plastic behavior region. It provides an explanation for the change in slope as well as for the increase in volume.

Reversing the theory of system stiffness and applying it to fracture opening, one could conclude that the Leak-Off Point might more probably reflect the point where the fracture becomes conductive to fluid rather than tensile failure occurs. This would be in accordance with observation as the Leak-Off Point, or the point at which tensile failure occurs is underestimated by the Kirsch Equations. It seems evident that tensile failure occurs according to Kirsch Equations but the fracture stays non-conductive until the pressure is high enough to

allow a non-penetrating fluid to enter. At this point the first deviation of the leak-off curve is observed.

Questions left open by the explanation:

- The theory does not provide an explanation for the formation breakdown as it is observed in some tests. If the fracture would increase further in length at some point the added inverse stiffness would tend towards zero and would result in a straight, horizontal line.

- It is not clear in how far one can deduct on fracture opening from the observations made during fracture closure.

6.1.3 Fracture Mechanics Interpretation of Leak-Off Tests

(Aadnoy, Vahid, & Hareland, 2009)

The Paper presented in 2009 presents a model applicable to Leak-Off Tests performed with a particle laden drilling fluid and small fracture volume compared to large annular volume. The observation that Kirsch Equation underestimated ultimate fracture pressure significantly for most drilling fluids triggered their search for an explanation. Experiments showed that only a measured and calculated fracture pressures are only identical for special drilling fluid with less particles.

The theory states that a fracture is initiated at the Leak-Off Pressure and some drilling fluid is invading it. However, near the fracture entrance the drilling fluids particles form a stress bridge preventing more fluid to enter the fracture and allowing the pressure to increase. The stress bridge will have to be of a curved shaped form for reasons of mechanical equilibrium as indicated in Figure 57. At the Formation Breakdown Pressure, this stress bridge fails, the pressure drops, fluid is forced into the fracture and propagates it further into the formation.

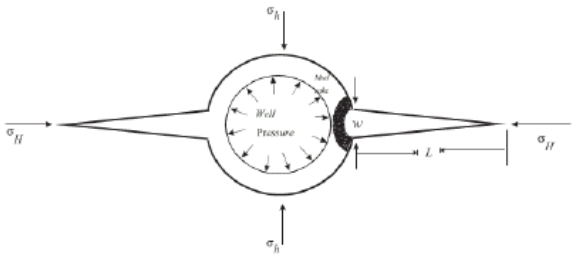

Figure 57 – Post failure establishment of a stress bridge (Aadnoy, Vahid, & Hareland, Fracture Mechanics Interpretation of Leak-Off Tests, 2009)

Questions left open by the explanation:

- ? After the stress bridge collapsed and the pressure drops, fluid is assumed to enter the fracture. What prevents the drilling fluid particles to build up another stress bridge, either at the same place or somewhere within the fracture?

- ? As the pressure further increases supported by the stress bridge, also Leak-Off Volume increases. The theory states that the stress bridge prevents fluid from entering the fracture so where do these volumes go?

6.1.4 Fracture initiation at the Formation Breakdown Pressure

(Lin, Yamamoto, Ito, Masago, & Kawamura, 2008)

In the progress report about setting up a procedure for the estimation of minimum horizontal stresses it is stated that at the Leak-Off Pressure drilling fluid starts to diffuse into the formation faster than fluid is supplied to the well by the pump. At the Formation Breakdown Pressure, a new fracture is created and several 100liters of fluid injection is necessary to ensure the fracture propagates beyond the disturbed stress regime.

Questions left open by the explanation:

- ? Only in porous rocks, sufficient fluid penetrating the formation without creating a fracture can be expected to cause a non-linearity in a Leak-Off Test. Furthermore, fluid diffusing into the formation would be expected to happen throughout the whole test and will not start dominating the test at a certain point. In competent formation it is not possible to gain sufficient additional system volume to cause the deviation from the linear behavior without taking a fracture into account.

6.1.5 Fracture Propagation can be explained by distribution of the near wellbore confining stress

(Heger & Spörker, 2011)

At the Leak-Off Pressure a fracture is initiated. Fracture growth is now dominated by the near-wellbore stress regime causing the fracture to grow in width mainly until formation breakdown is observed. Pressure increase causes the fracture to propagate until the fluid pressure inside the fracture equals the stress perpendicular to the fracture face. The pressure is further increased until the fracture leaves the near-wellbore area. Now far field stress

dominates fracture growth causing the fracture to propagate at a low pressure – formation breakdown is observed.

Questions left open by the explanation:

- Leak-Off Test Volumetric and fracture geometry suggests that a fracture leaves the near wellbore area just shortly after it has been initiated. Therefore, fracture propagation is controlled by the far field stress whereas only fracture initiation is governed by the stress state at the wellbore wall.

7 Permanent Formation Damage due to Formation Strength Tests

Extended Leak-Off Tests are often not performed due to the fear of permanently weakening the formation by creating a fracture reaching the undisturbed stress field. As discussed earlier, already the fracture created in a standard Leak-Off Test might reach further into the formation than one would expect. As a fracture is created, the formation strength is ultimately reduced by the tensile strength, which however is low in most cases. Furthermore, the wellbore pressure containment is influenced by the fracture as it might provide a pass way for flow and also might connect to other natural fractures present in the formation.

However, in most Leak-Off tests reviewed during this study, no evidence for a significant reduction in wellbore pressure containment could be found as repeated Leak-Off Test do show almost the same results. The same is true for Extended Leak-Off Test. An example is presented in Figure 58 where one can see that multiple injection and backflow periods allow for pressurization up to almost the same maximum test pressure. No evidence of reducing the ultimate pressure containment of the wellbore can be found in this example.

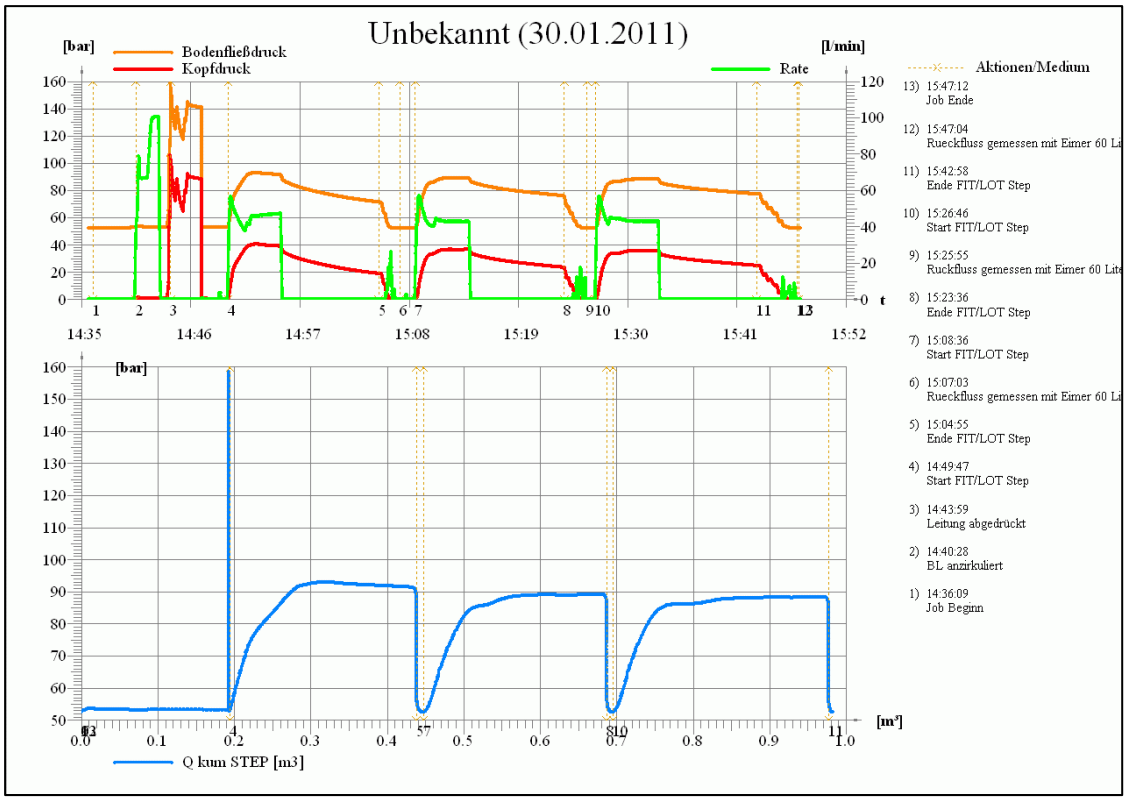

Figure 58 – Extended Leak-Off Test Rabensburg 12

However, a general answer to this question is not easy as it depends on many factors. The fact that in most Leak-Off Tests a fracture will be created ultimately leads to the assumption that the strength of the wellbore is reduced. The fracture can be reopened at the fracture initiation pressure reduced by the tensile strength of the formation. This additional volume can now be connected to the wellbore by reopening of the fracture whereas further fracture propagation will still require a pressure in the range of the fracture propagation pressure. The phenomena of reopening fractures, thereby increasing the wellbore volume and loosing drilling fluid to this fracture, which is recovered as the pressure is lowered again is known as wellbore breathing, ballooning or loss/gain. It has to be noted that a reopening a fracture is not the only source of loss/gain in daily drilling operations as also thermal effects on the drilling fluid and elastic wellbore deformation are believed to cause similar events.

As both, Leak-Off Tests and extended Leak-Off Test are assumed of not permanently influencing the strength of the wellbore, extended Leak-Off Test should be the preferred option. The results of extended Leak-Off Tests are more precise and give better information on formation strength and downhole stresses.

8 Conclusions

After investigation of factors affecting Formation Strength Test, research on stress state around the wellbore, fracture mechanics and the review of Leak-Off Test data the following conclusions are made and are subject to discussion and further investigation as most of them are based on theoretical work only:

The main conclusion that can be made is that what happened during a Leak-Off Test is not fully understood in many cases. Especially the picture of a near wellbore fracture, which does not leave the area of disturbed stress field around the wellbore could not be proven. Moreover, a fracture which is capable of accommodating the fluid volume which is associated with the deviation from the straight line in a Leak-Off Test, is of such significance that the fracture length has to be large. This conclusion is based on simple fracture volumetrics in combination with a fracture model.

The point at which a fracture is initiated is described by the Kirsch equations and the tensional limit of the formation whereas the Leak-Off Point, as it is observed in a Leak-Off Test, is the point at which a fracture will become conductive to the drilling fluid. Therefore, Leak-Off Tests have to be investigated with keeping the drilling fluid properties in mind. The results might not be valid any longer as the fluid system is changed. After a fracture has been initiated at the wellbore wall, the stress regime, as described by Kirsch's equations does not influence fracture propagation. Minimum horizontal stress and fracture mechanics apply, describing the stress state at the fracture tip, and therefore fracture propagation.

As already the fracture created in a Leak-Off Test is significant and no permanent weakening of the wellbore's pressure containment is expected, Extended Leak-Off Tests might be a better option. Of course the fracture created in an Extended Leak-Off Test will be even larger but as one can see on the data presented, also Extended Leak-Off Tests can be repeated in several cycles without any significant reduction in the maximum pressure reached. Therefore, one can conclude that also Extended Leak-Off Test do not influence the wellbore pressure containment permanently. As in Extended Leak-Off Tests the pressure is increased until no further increase can be achieved, the real limit of the formation is measured. Furthermore, Extended Leak-Off Tests enable the estimation of the main principal stress magnitude, providing additional information on the situation downhole.

Further conclusions:

- The literature research showed that especially the expressions "Leak-Off Test" is often used as a general term for all kinds of different Formation Strength Test. Deviations in nomenclature exist and might lead to confusion.

- The linear behavior in Formation Strength Tests is mainly depended on the compressibility of the drilling fluid used. Especially oil based drilling fluids show significant compressibility. It has to noted that results of oil based and water based drilling fluids can differentiate significantly.

- Doubt raises on some theories explain why the recognition of cement channels in Leak-Off Test plots. Reason is that Formation Strength Test are influenced by many factors whereas most of them are unknown or at least of high uncertainty.

- A guideline for performing Formation Strength Test has been presented including operational guidelines as well as recommendations for equipment and proper arrangement of the equipment.

- Volumetric analysis of the Leak-Off Tests shows relatively low leak-off volumes. In the literature, test data with substantially larger Leak-Off Volumes can be found whereas detailed information of the wellbore geometry is often not available.

- Further pressure increase after fracture initiation cannot be explained by the stress distribution around the wellbore. Leak-Off Volume and therefore fracture volume suggest that a fracture reaches the undisturbed stress field shortly after fracture

initiation. It should be always keep in mind that a fractures width is very small, and substantial volume can only be achieved by large fracture length as fracture height is more or less fixed.

- Formation Strength Test should be performed with care and should be properly prepared and recorded to ensure data quality and simplify evaluation.

APPENDICES

Appendix A Casing Expansion Eq.

The general equation for stresses in a tube, which is restricted in longitudinal expansion, can be written as the following (Meier & Ermanni, 2010) assuming tension to be positive and compression to be negative:

$$\sigma_\theta = \frac{\chi^2 \cdot (P_i - P_e)}{1 - \chi^2} + (P_i - P_e) \cdot \frac{\chi^2}{(1 - \chi^2) \cdot \left(\frac{R}{R_o}\right)^2}$$

$$\sigma_r = \frac{\chi^2 \cdot (P_i - P_e)}{1 - \chi^2} - (P_i - P_e) \cdot \frac{\chi^2}{(1 - \chi^2) \cdot \left(\frac{R}{R_o}\right)^2}$$

$$\sigma_z = \nu(\sigma_\theta + \sigma_r)$$

and $\chi \quad = \left(\frac{R_i}{R_o}\right)$

The equation is derived from the general differential equation describing all forces acting on an infinite small volume of the pipe body and assuming plain strain conditions. As the change in volume, respectively the change in strain is of interest, which is caused by a change in stress the equations can be written as the following by substituting σ_θ by $\Delta\sigma_\theta$, σ_r by $\Delta\sigma_r$, σ_z by $\Delta\sigma_z$, P_i by ΔP_i and P_e by ΔP_e whereas $\Delta P_e = 0$ assuming no changes in external pressure:

$$\Delta\sigma_\theta(R) = \frac{{R_i}^2 \cdot \Delta P_i}{R_o^2 - R_i^2} + \Delta P_i \cdot \frac{R_o^2 \cdot R_i^2}{R_o^2 - R_i^2} \cdot \left(\frac{1}{R^2}\right)$$

$$\Delta\sigma_r(R) = \frac{{R_i}^2 \cdot \Delta P_i}{R_o^2 - R_i^2} - \Delta P_i \cdot \frac{R_o^2 \cdot R_i^2}{R_o^2 - R_i^2} \cdot \left(\frac{1}{R^2}\right)$$

$$\sigma_z = \nu(\sigma_\theta + \sigma_r)$$

The Correlation between stress and strain, for plain strain conditions, is described by Hook's Law for three dimensions:

$$\varepsilon_z = \frac{1}{E} \cdot \left(\Delta\sigma_z - \nu \cdot (\Delta\sigma_\theta + \Delta\sigma_r)\right) = 0$$

$$\varepsilon_\theta(R) = \frac{1}{E} \cdot (\Delta\sigma_\theta - \nu \cdot (\Delta\sigma_r + \Delta\sigma_z))$$

$$\varepsilon_r(R) = \frac{1}{E} \cdot (\Delta\sigma_r - \nu \cdot (\Delta\sigma_z + \Delta\sigma_\theta))$$

The change in volume can be determined directly from the tangential strain at the inside of the casing. To calculate the strain on the inside of the casing, R is substituted by R_i and the following equations are derived:

$$\Delta\sigma_\theta(R) = \frac{{R_i}^2 \cdot \Delta P_i}{R_o^2 - R_i^2} + \Delta P_i \cdot \frac{R_o^2 \cdot R_i^2}{R_o^2 - R_i^2} \cdot \left(\frac{1}{R_i^2}\right)$$

$$\Delta\sigma_\theta = \frac{{R_i}^2 \cdot \Delta P_i}{R_o^2 - R_i^2} + \Delta P_i \cdot \frac{R_o^2}{R_o^2 - R_i^2}$$

$$\boxed{\Delta\sigma_\theta = \Delta P_i \cdot \frac{{R_i}^2 + R_o^2}{R_o^2 - R_i^2}}$$

$\Delta\sigma_\theta$ is a positive value as it describes a tensional stress which is defined to be positive.

$$\Delta\sigma_r(R) = \frac{{R_i}^2 \cdot \Delta P_i}{R_o^2 - R_i^2} - \Delta P_i \cdot \frac{R_o^2 \cdot R_i^2}{R_o^2 - R_i^2} \cdot \left(\frac{1}{R_i^2}\right)$$

$$\Delta\sigma_r = \frac{{R_i}^2 \cdot \Delta P_i}{R_o^2 - R_i^2} - \Delta P_i \cdot \frac{R_o^2}{R_o^2 - R_i^2}$$

$$\boxed{\Delta\sigma_r = \Delta P_i \cdot \frac{{R_i}^2 - R_o^2}{R_o^2 - R_i^2} = -\Delta P_i}$$

$\Delta\sigma_r$ on the other hand side is negative as it describes a compressional stress which is defined to be negative.

$$\boxed{\sigma_z = \nu(\sigma_\theta + \sigma_r) = \nu\left(\Delta P_i \cdot \frac{{R_i}^2 + R_o^2}{R_o^2 - R_i^2} - \Delta P_i\right) = \nu \cdot \Delta P_i \left(\frac{{R_i}^2 + R_o^2}{R_o^2 - R_i^2} - 1\right)}$$

Hence,

$$\varepsilon_\theta(R) = \frac{1}{E} \cdot (\Delta\sigma_\theta - \nu \cdot (\Delta\sigma_r + \Delta\sigma_z))$$

$$\varepsilon_\theta(R = R_i) = \frac{1}{E} \cdot \left(\Delta P_i \cdot \frac{{R_i}^2 + R_o^2}{R_o^2 - R_i^2} - \nu \cdot \left(-\Delta P_i + \nu \cdot \Delta P_i \left(\frac{{R_i}^2 + R_o^2}{R_o^2 - R_i^2} - 1\right)\right)\right)$$

$$\varepsilon_\theta(R = R_i) = \frac{\Delta P_i}{E} \cdot \left(\frac{{R_i}^2 + R_o^2}{R_o^2 - R_i^2} \cdot (1 - \nu^2) + (\nu + \nu^2) \right)$$

The differential volume caused by tangential strain is calculated by the following equation:

$$\Delta V = \pi \cdot L_c \cdot \left((R_i + \Delta r)^2 - R_i^2 \right)$$

$$\Delta r = R_i \cdot \varepsilon_\theta$$

$$\Delta V = \pi \cdot L_c \cdot \left((R_i + R_i \cdot \varepsilon_\theta)^2 - R_i^2 \right)$$

$$\Delta V = \pi \cdot L_c \cdot R_i^2 \cdot (2\varepsilon_\theta + {\varepsilon_\theta}^2)$$

As ε_θ is small, ${\varepsilon_\theta}^2$ would be even smaller and is therefore neglected for the calculations of the differential volume caused by a change in inside pressure represented by the following equation. This gives a positive volume as the volume increase is the result of a tensional stress:

$$\Delta V = 2 \cdot \pi \cdot L_c \cdot R_i^2 \cdot \varepsilon_\theta$$

$$\Delta V = 2 \cdot \pi \cdot L_c \cdot R_i^2 \cdot \frac{\Delta P_i}{E} \cdot \left(\frac{{R_i}^2 + R_o^2}{R_o^2 - R_i^2} \cdot (1 - \nu^2) + (\nu + \nu^2) \right)$$

Appendix B Mud Compressibility Eq.

The compressibility of a fluid can be determined from the isothermal compressibility equation.

$$c = \left(-\frac{1}{V}\frac{\partial V}{\partial P}\right)_T$$

The subscripted T is dropped as for the short period of time during a Leak-Off Test temperature of the drilling fluid is assumed not to change. The minus sign tells that an increase in pressure results in a decreasing volume. In this case the compressed volume is replaced by volume pumped into the well and the minus sign can therefore be dropped.

$$c = \frac{1}{V}\frac{\partial V}{\partial P}$$

Separating variables and integration will lead to the exact solution of the isothermal compressibility equation:

$$c \cdot \int \partial P = \int \frac{\partial V}{V}$$

$$c \cdot \Delta P = \ln|V| + K$$

Solving for the boundary condition $V(\Delta P = 0) = V_0$:

$$0 = \ln|V_0| + K \rightarrow K = -\ln|V_0|$$

$$c \cdot \Delta P = \ln|V| - \ln|V_0|$$

$$c \cdot \Delta P = \ln\left|\frac{V}{V_0}\right|$$

with $V=V_0+\Delta V$

$$c \cdot \Delta P = \ln\left|\frac{V_0 + \Delta V}{V_0}\right|$$

$$\boxed{c \cdot \Delta P = \ln\left|1 + \frac{\Delta V}{V_0}\right|}$$

As this exact solution is not very helpful in the most cases an approximate solution can be derived by using the relationship of series expansion of logarithmic functions:

$$\ln|1+x| \cong x - \frac{1}{2}\cdot x^2 + \frac{1}{3}\cdot x^3 - \frac{1}{4}\cdot x^4 + \cdots$$

Leading to the following expression:

$$\mathrm{c}\cdot\Delta\mathrm{P} = \ln\left|1+\frac{\Delta\mathrm{V}}{V_0}\right| \cong \frac{\Delta\mathrm{V}}{V_0} - \frac{1}{2}\cdot\left(\frac{\Delta\mathrm{V}}{V_0}\right)^2 + \frac{1}{3}\cdot\left(\frac{\Delta\mathrm{V}}{V_0}\right)^3 - \frac{1}{4}\cdot\left(\frac{\Delta\mathrm{V}}{V_0}\right)^4 + \cdots$$

As the differential volume is small compared to the original volume due to the low compressibility of fluids the term $\frac{\Delta\mathrm{V}}{V_0}$ is small. Hence, all following terms are very small and can be neglected leading to the approximate solution of the isothermal compressibility equation:

$$\mathrm{c}\cdot\Delta\mathrm{P} = \frac{\Delta\mathrm{V}}{V_0}$$

$$\boxed{\Delta\mathrm{V} = V_0\cdot\mathrm{c}\cdot\Delta\mathrm{P}}$$

Appendix C Borehole Expansion Eq.

For elastic borehole expansion the same equations as used for casing expansion are used. The borehole is considered to be a tube restricted in longitudinal expansion of infinite outer radius. The same equation used for the calculation of the casing deformation is used but assuming the outside radius to infinite:

$$\Delta\sigma_\theta = \Delta P_i \cdot \frac{{R_i}^2 + R_o^2}{R_o^2 - R_i^2}$$

$$\lim_{R_o \to \infty} \left(\frac{R_o^2 + {R_i}^2}{R_o^2 - R_i^2} \right) = 1$$

$$\Delta\sigma_\theta = \Delta P_i$$

The equation for the radial stress does not change:

$$\Delta\sigma_r = \Delta P_i \cdot \frac{{R_i}^2 - R_o^2}{R_o^2 - R_i^2} = -\Delta P_i$$

The longitudinal stress turns out to be zero:

$$\sigma_z = \nu(\sigma_\theta + \sigma_r) = 0$$

Substituting the derived expressions into Hook's Law leads to the following equation for strain in tangential direction at the borehole wall:

$$\varepsilon_\theta(R) = \frac{1}{E} \cdot (\Delta\sigma_\theta - \nu \cdot (\Delta\sigma_r + \Delta\sigma_z))$$

$$\varepsilon_\theta(R = R_i) = -\frac{1}{E} \cdot \left(\Delta P_i - \nu \cdot (-\Delta P_i)\right)$$

$$\varepsilon_\theta(R = R_i) = \frac{\Delta P_i}{E} \cdot (1 + \nu)$$

The differential volume caused by tangential strain is calculated by the following equation:

$$\Delta V = \pi \cdot L_c \cdot R_i^2 \cdot (2\varepsilon_\theta + {\varepsilon_\theta}^2)$$

As ε_θ is small, ${\varepsilon_\theta}^2$ would be even smaller and is therefore neglected for the calculations of the differential volume caused by a change in inside Pressure

$$\Delta V = 2 \cdot \pi \cdot L_c \cdot R_i^2 \cdot \varepsilon_\theta$$

$$\Delta V = 2 \cdot \pi \cdot L_{OH} \cdot R_w^2 \cdot \frac{\Delta P_i}{E} \cdot (1 + \nu)$$

Appendix D Insitu Stress Distribution around the wellbore (Kirsch Eq.)

The insitu stress distribution around the wellbore as shown in Figure 59 is described by a set of equations commonly known as Kirsch Equations (Kirsch, 1898). The equation describing the effective tangential stress is presented below:

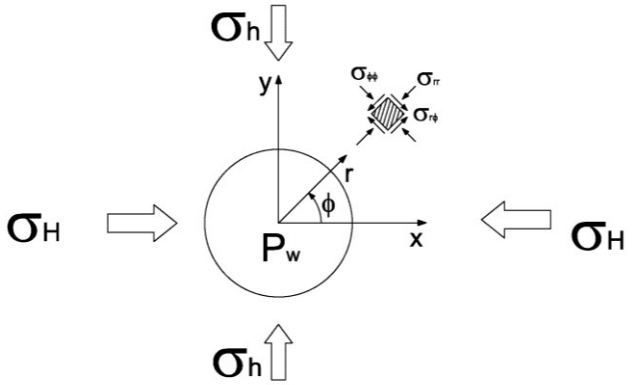

Figure 59 – Stress distribution around the wellbore

$$\sigma_{tan,eff}(\theta,r) = \frac{1}{2}(\sigma_H + \sigma_h)\left(1 + \frac{R_w^2}{R}\right) - \frac{1}{2}(\sigma_H - \sigma_h)\left(1 + 3\frac{R_w^4}{R^4}\right) \cdot \cos(2\theta) - P_w \cdot \frac{R_w^2}{R^2} - P_o$$

The radius of interest is apparently the borehole wall where r = r_w leading to the following formulation:

$$\sigma_{tan,eff}(\theta, r = r_w) = (\sigma_H + \sigma_h) - 2(\sigma_H - \sigma_h)\cos(2\theta) - P_i - P_o$$

Tensional Failure:

Tensional failure will occur in direction of the maximum horizontal stress θ = 0° or θ = 180° hence cos(2θ) = 1 leading to the following simplification:

$$\sigma_{tan,eff}(\theta = 0°, r = r_w) = (\sigma_H + \sigma_h) - 2(\sigma_H - \sigma_h) - P_i - P_o$$

$$\sigma_{tan,eff} = 3\sigma_h - \sigma_H - P_i - P_o$$

A fracture will be initiated as soon as the effective tangential stress will exceed the tensile strength of the formation at the borehole wall. Note that compressive stress is declared positive and tensional stress negative. The tensional strength refers to a limit in tensional stress and is therefore negative.

$$\sigma_{tan,eff} = 3\sigma_h - \sigma_H - P_i - P_o$$

$$\sigma_{tan,eff} = 3\sigma_h - \sigma_H - P_i - P_o \leq -\sigma_T$$

Therefore, the fracture initiation pressure is the wellbore pressure fulfilling the failure criteria mentioned above:

$$P_i = 3\sigma_h - \sigma_H - P_o + \sigma_T$$

The wellbore pressure at which fracture initiation occurs is usually termed Leak-Off Pressure (LOP)

$$LOP = 3\sigma_h - \sigma_H - P_o + \sigma_T$$

If the stress contrast β describing the relation of minimum horizontal stress to maximum horizontal stress is introduced the following equation can be derived:

$$\beta = \frac{\sigma_H}{\sigma_h}$$

$$LOP = 3\sigma_h - \sigma_H - P_o + \sigma_T$$

$$LOP = (3 - \beta) \cdot \sigma_h - P_o + \sigma_T$$

Compressional Failure:

Compressional failure will occur on minimum horizontal stress azimuth, θ = 90° or θ = 270° hence cos(2θ) = -1 leading to the following simplification:

$$\sigma_{tan,eff}(\theta = 90°, r = r_w) = (\sigma_H + \sigma_h) + 2(\sigma_H - \sigma_h) - P_i - P_o$$

$$\sigma_{tan,eff} = 3\sigma_H - \sigma_h - P_i - P_o$$

The limit for compressive failure would be a limit in compressive stress σ_c to allow for a certain breakout width.

$$\sigma_{tan,eff} = 3\sigma_H - \sigma_h - P_i - P_o$$

$$\sigma_{tan,eff} = 3\sigma_H - \sigma_h - P_i - P_o \leq \sigma_C$$

Therefore, the breakout initiation pressure is the wellbore pressure fulfilling the failure criteria mentioned above:

$$P_i = 3\sigma_H - \sigma_h - P_o - \sigma_C$$

The wellbore pressure at which break out overcome the allowed break out width is termed break out limit (BOL):

$$BOL = 3\sigma_h - \sigma_H - P_o - \sigma_C$$

Again, the stress contrast β describing the relation of minimum horizontal stress to maximum horizontal stress is introduced the following equation can be derived:

$$\beta = \frac{\sigma_H}{\sigma_h}$$

$$BOL = 3\sigma_H - \sigma_h - P_o - \sigma_C$$

$$BOL = (3\beta - 1) \cdot \sigma_h - P_o - \sigma_C$$

Mud weight window for wellbore stability:

For wellbore stability, the wellbore pressure should not exceed the pressure at which tensile failure would occur and should not be below the pressure at which the allowed breakout width is exceeded. Too high pressure results in tensional failure (fracture) whereas too low pressure results in compressional failure (breakouts).

$$(3\beta - 1) \cdot \sigma_h - P_o - \sigma_C \leq P_i \leq (3 - \beta) \cdot \sigma_h - P_o + \sigma_T$$

From this equation it can be seen that an increase in rock strength (compressional and/or tensional) will result in a larger window of hole stability as one would expect. The tensional limit rises with increasing tensional strength whereas the compressive limit is lowered by a higher compressive limit.

Furthermore, a higher anisotropy results in a higher stress contrast b will narrow down the window of hole stability. The tensional limit will be lowered and the compressional limit will be increased. This means that a compressional failure will occur already at a higher pressure and tensional failure at a lower pressure.

Appendix E Leak-Off Test Data

Well A – Dobermannsdorf 2

LOT					
Well	Dobermannsdorf 2 (Dob2)			**Date**	9.11.2010
Test TD	561 m	**Casing Shoe**	556 m	**Drilled TD**	558 m
Open-hole	5 m	**Ex. Formation**	3 m	**DW**	12 ¼ in
Completion	13 3/8 in / 54,4 ppf / J55			**Cycles**	1

Cycle	LOP [bar]	LOV [liter]	Pmax [bar]	SSIP [bar]
1	85	6	90,5	81

Table 9 – Summary LOT Dobermannsdorf 2 (1)

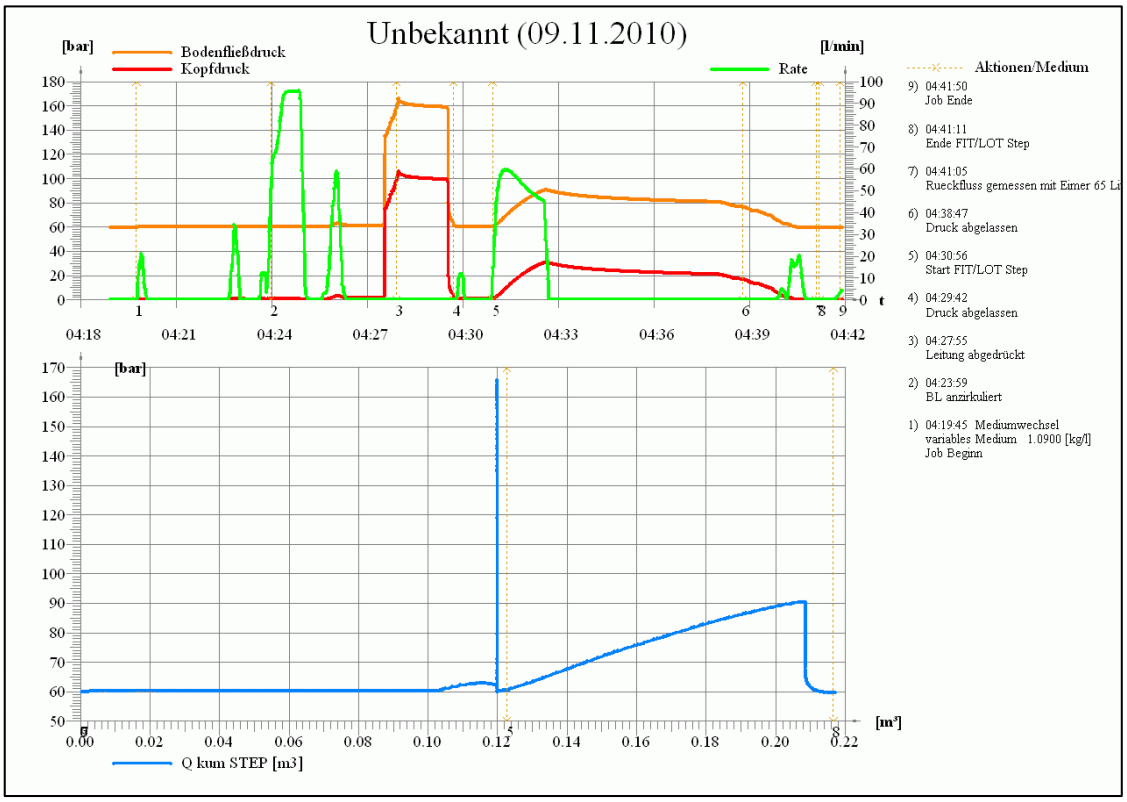

Figure 60 – LOT Record Dobermannsdorf 2 (1)

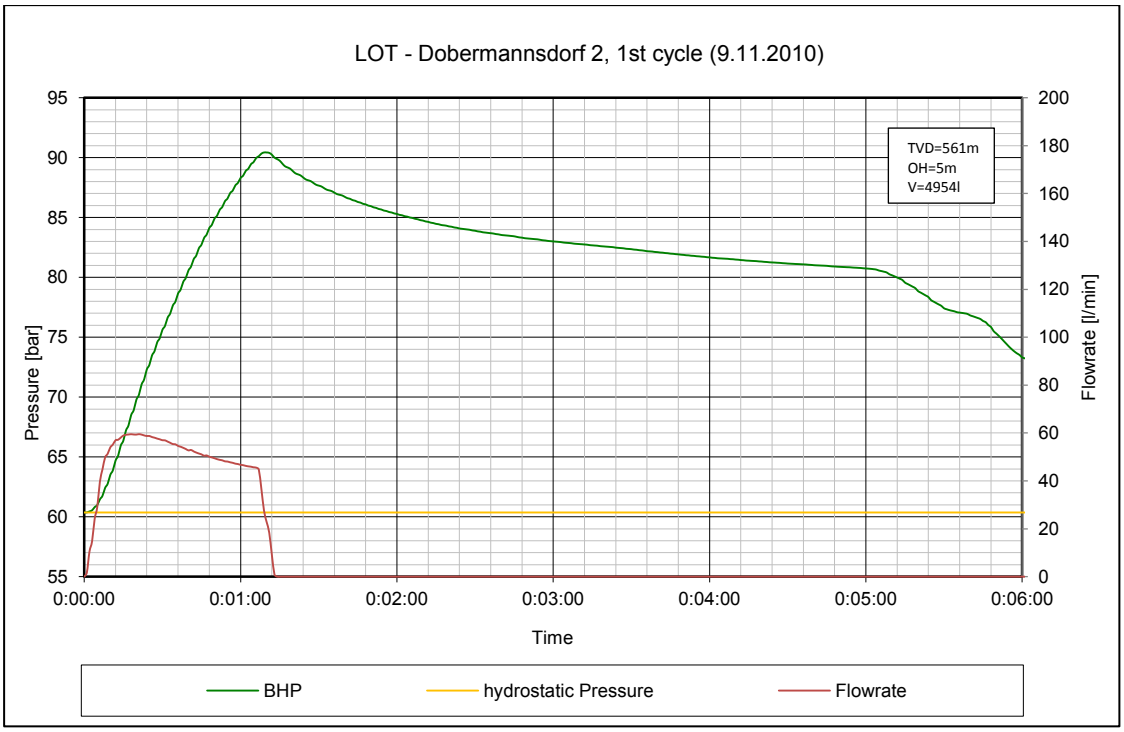

Figure 61 – LOT Dobermannsdorf 2, Pressure vs. Time, 1st cycle

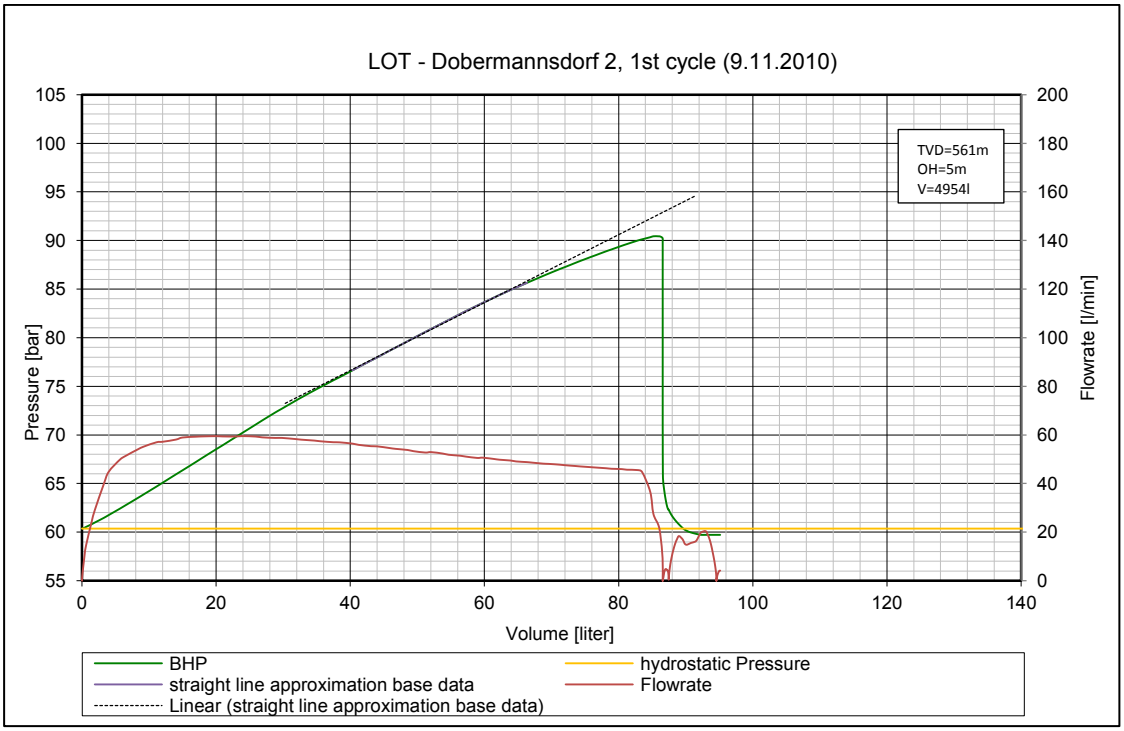

Figure 62 – LOT Dobermannsdorf 2, Pressure vs. Volume, 1st cycle

LOT					
Well	Dobermannsdorf 2 (Dob2)			**Date**	15.11.2010
Test TD	1225 m	**Casing Shoe**	1219 m	**Drilled TD**	1222 m
Open-hole	6 m	**Ex. Formation**	3 m	**DW**	8 ½ in
Completion	9 5/8 in / 36 ppf / J55			**Cycles**	1

Cycle	LOP [bar]	LOV [liter]	Pmax [bar]	SSIP [bar]
1	256	8	269	244
2	248	16	266	246

Table 10 – Summary LOT Dobermannsdorf 2 (2)

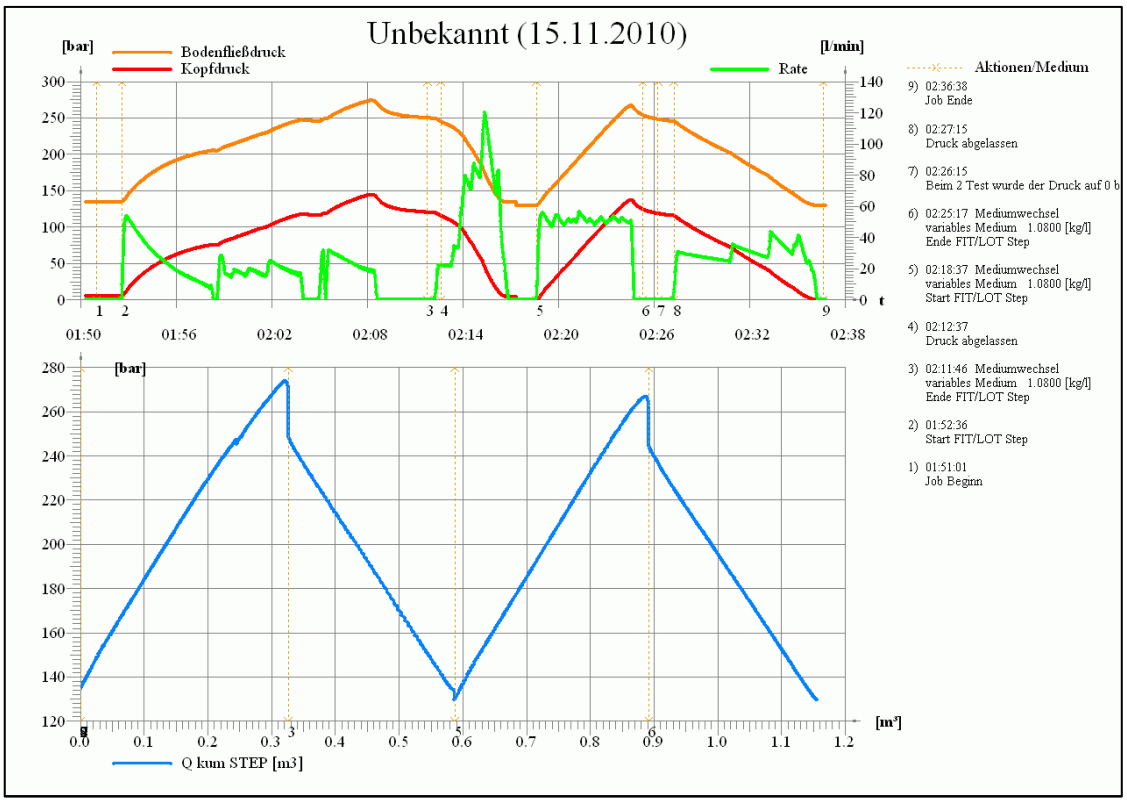

Figure 63 – LOT Record Dobermannsdorf 2 (2)

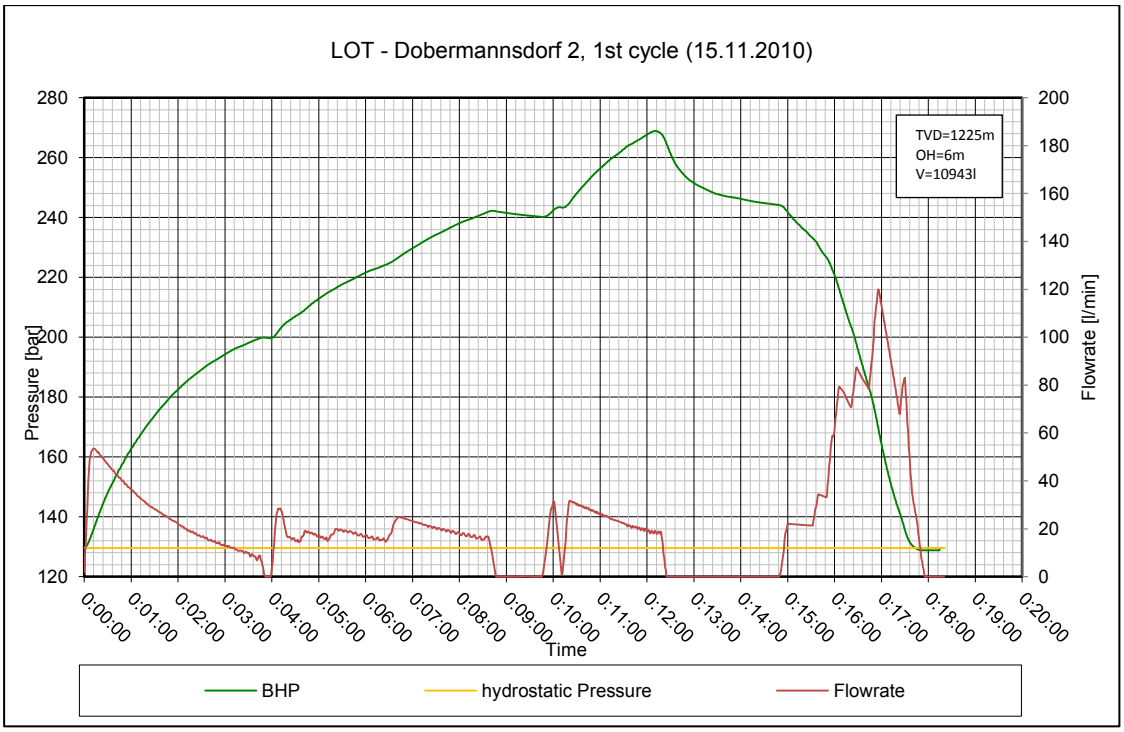

Figure 64 – LOT Dobermannsdorf 2, Pressure vs. Time, 1st cycle

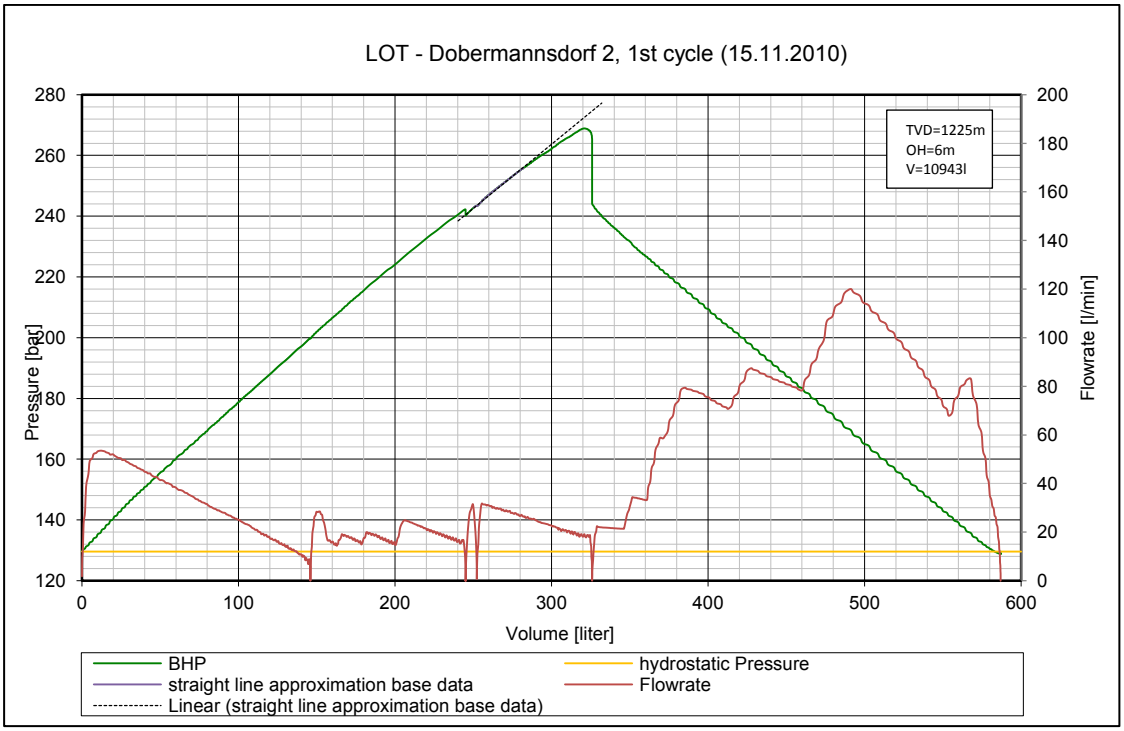

Figure 65 – LOT Dobermannsdorf 2, Pressure vs. Volume, 1st cycle

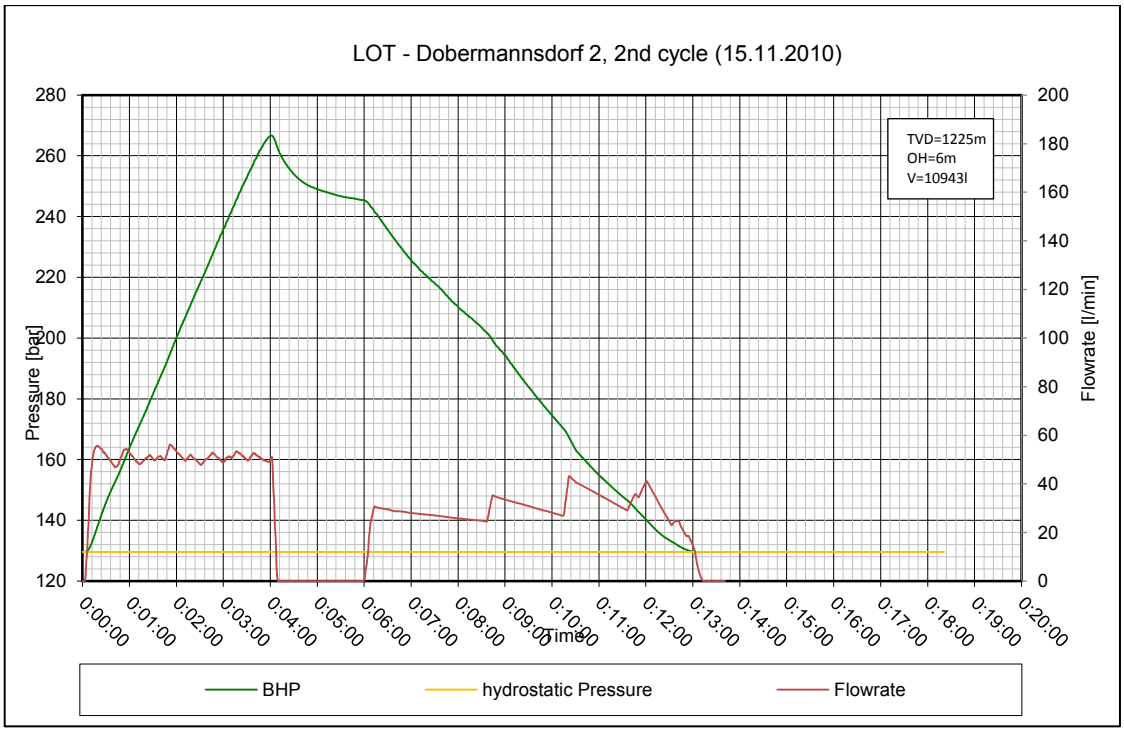

Figure 66 – LOT Dobermannsdorf 2, Pressure vs. Time, 2nd cycle

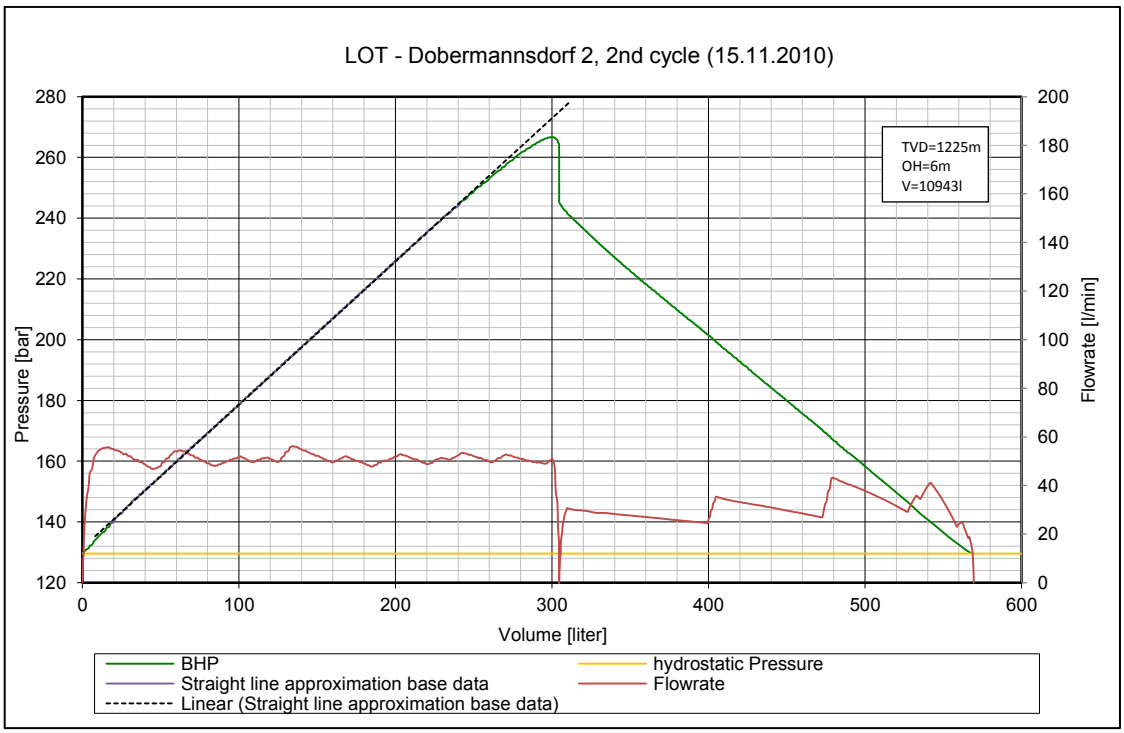

Figure 67 – LOT Dobermannsdorf 2, Pressure vs. Volume, 2nd cycle

Well B – Ebenthal 20

LOT					
Well	Ebenthal 20 (Eb20)			**Date**	25.8.2010
Test TD	995 m	**Casing Shoe**	990 m	**Drilled TD**	992 m
Open-hole	5 m	**Ex. Formation**	3 m	**DW**	8 ½ in
Completion	9 5/8in / 36ppf / J55			**Cycles**	2

Cycle	LOP [bar]	LOV [liter]	Pmax [bar]	SSIP [bar]
1	228	8	226	163
2	160	12	175	162

Table 11 – Summary LOT Ebenthal 20

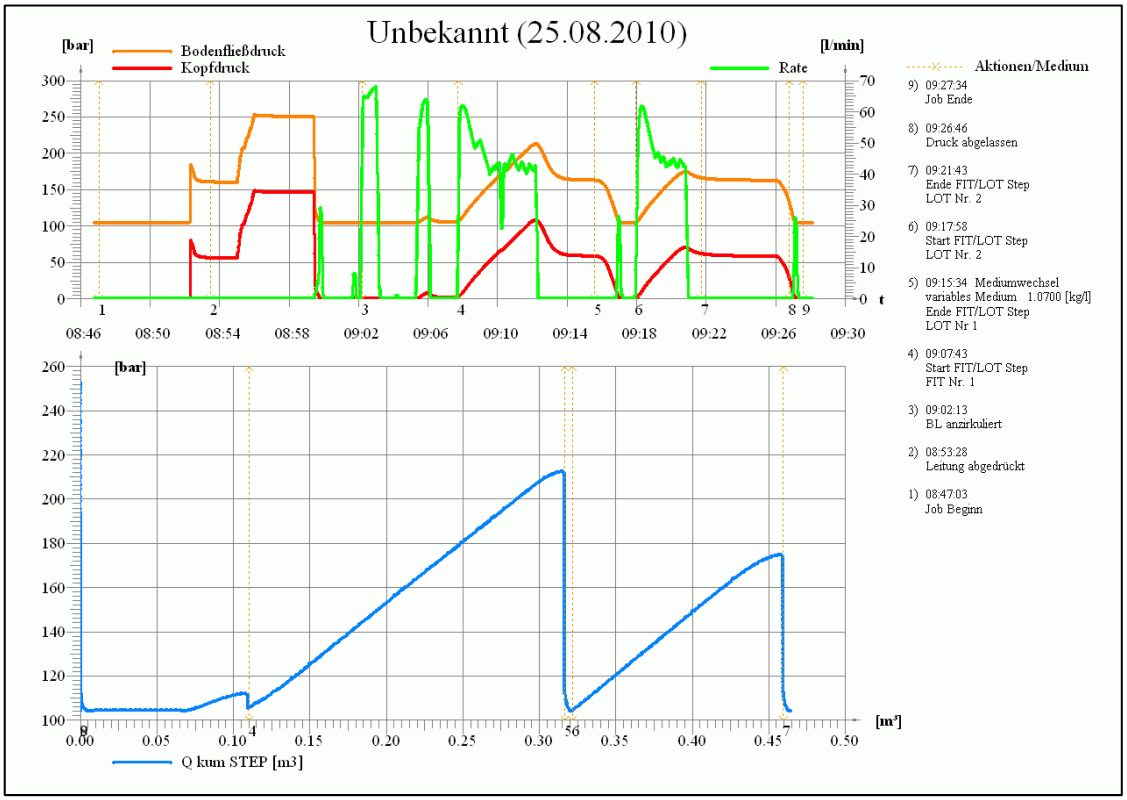

Figure 68 – LOT Record Ebenthal 20

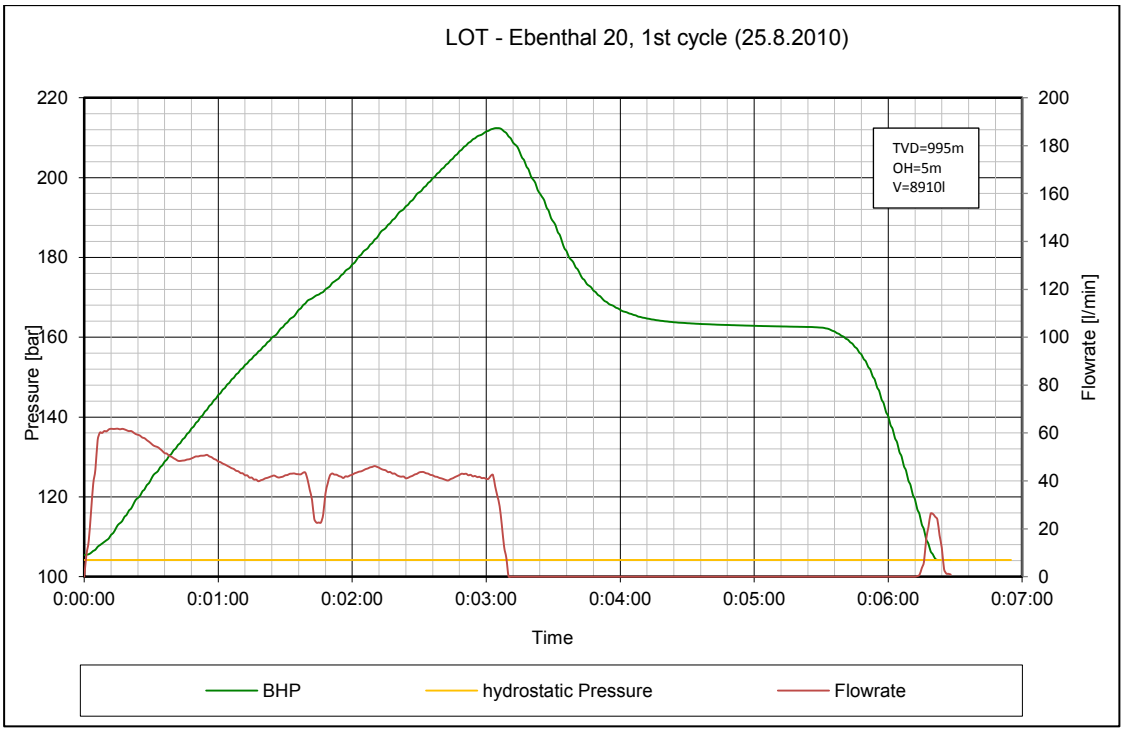

Figure 69 – LOT Ebenthal 20, Pressure vs. Time, 1st cycle

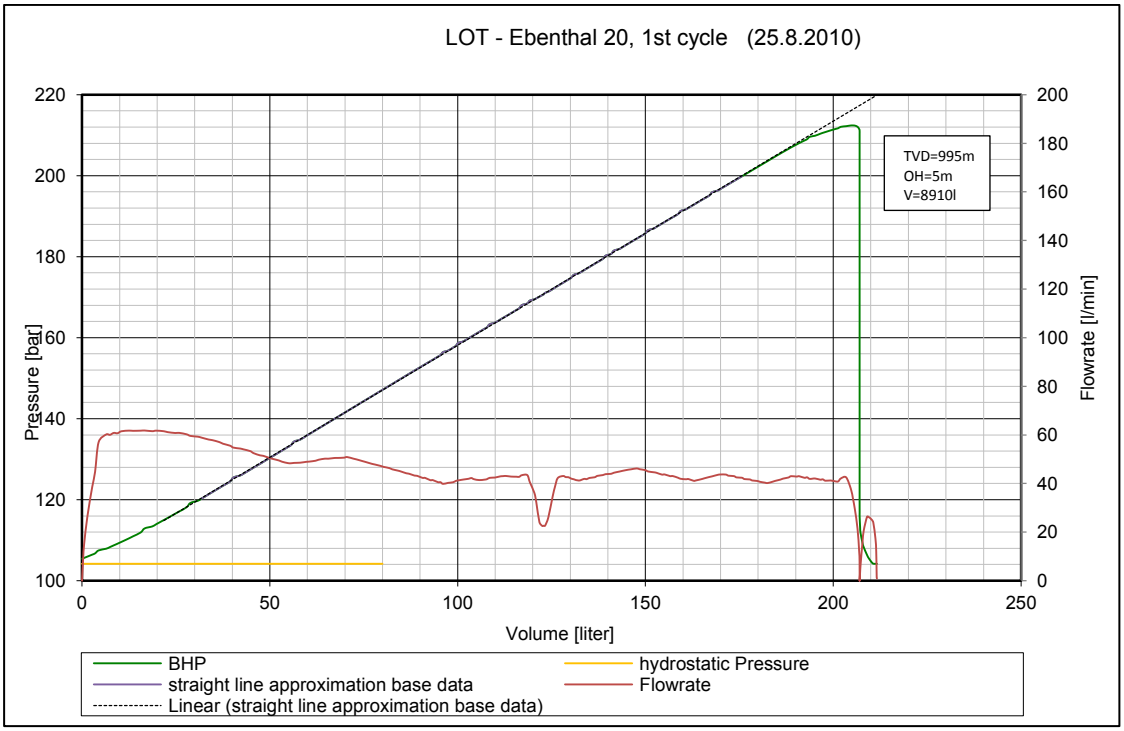

Figure 70 – LOT Ebenthal 20, Pressure vs. Volume, 1st cycle

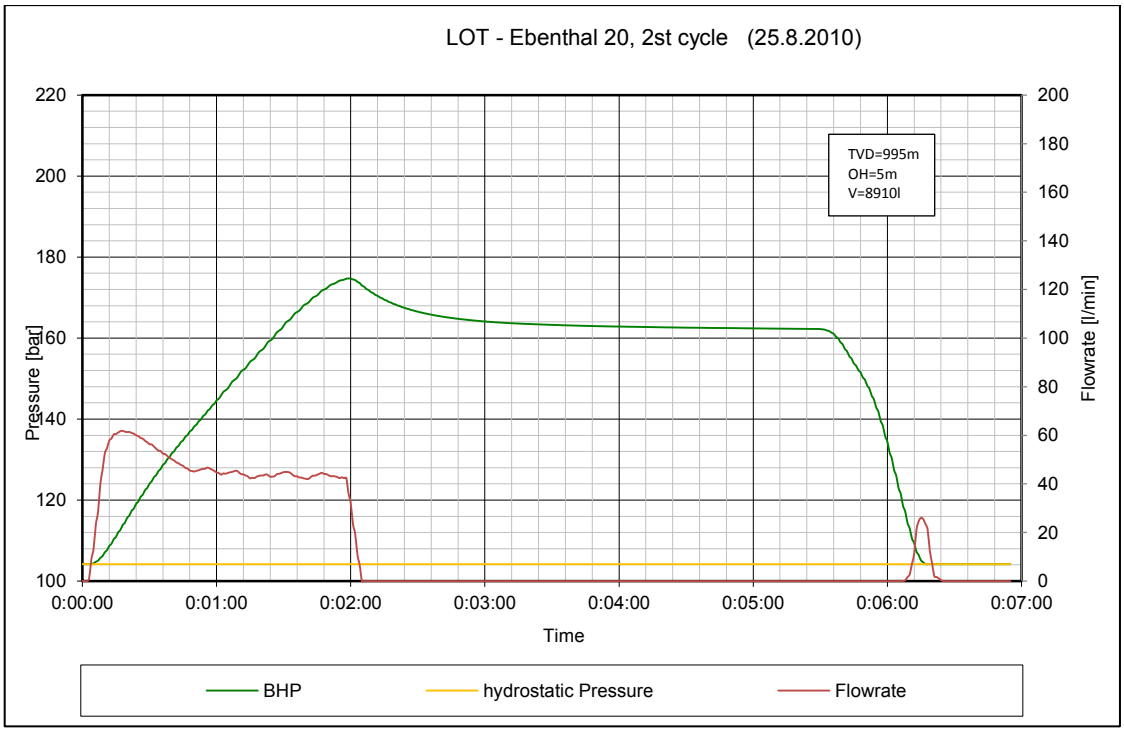

Figure 71 – LOT Ebenthal 20, Pressure vs. Time, 2nd cycle

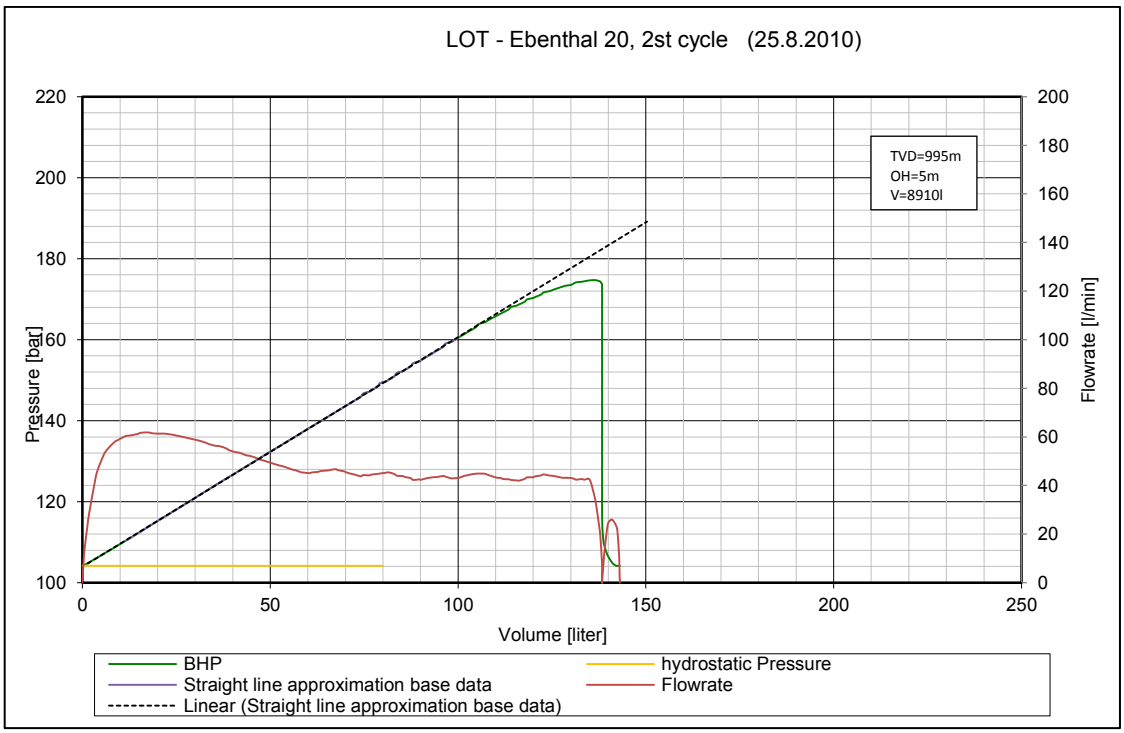

Figure 72 – LOT Ebenthal 20, Pressure vs. Volume, 2nd cycle

Well C – Erdpress 9

LOT					
Well	Erdpress 9 (Erd9)			**Date**	20.2.2010
Test TD	513 m	**Casing Shoe**	508 m	**Drilled TD**	510 m
Open-hole	5 m	**Ex. Formation**	3 m	**DW**	8 ½ in
Completion	9 5/8 in / 36ppf / J55			**Cycles**	2

Cycle	LOP [bar]	LOV [liter]	Pmax [bar]	SSIP [bar]
1	87	4	93	81
2	84	6	91,5	84

Table 12 – Summary LOT Erdpress 9

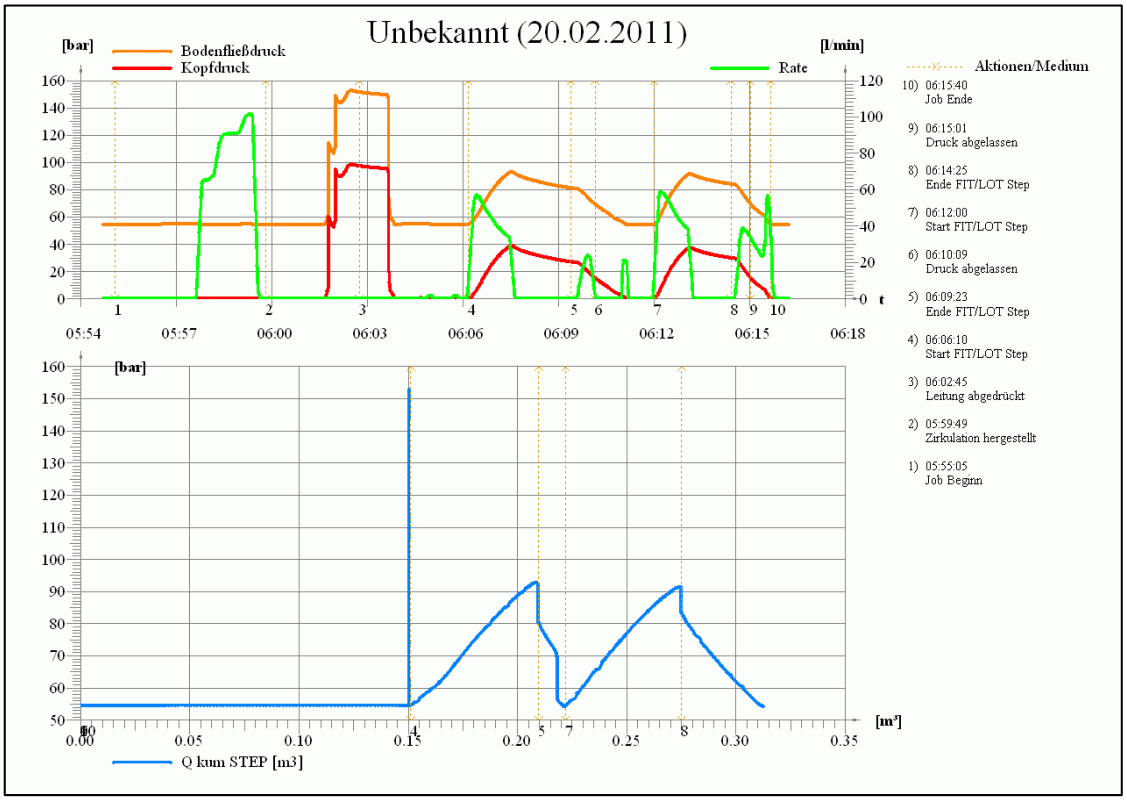

Figure 73 - LOT Record Erdpress 9

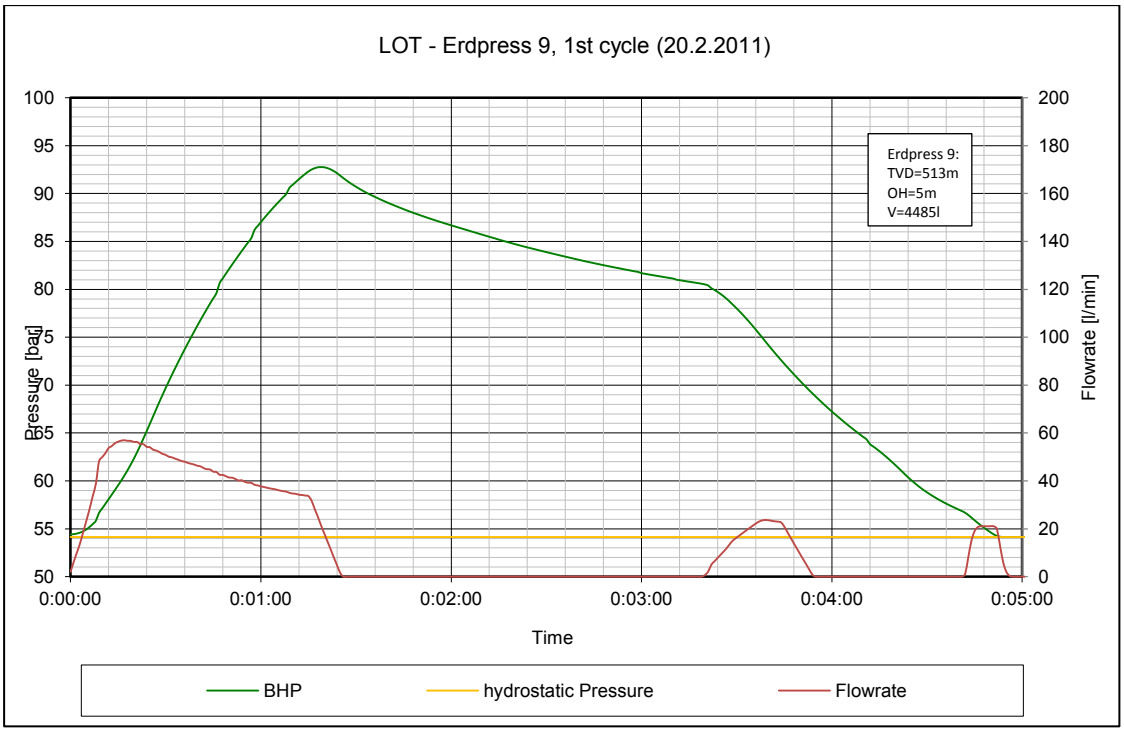

Figure 74 – LOT Erdpress 9, Pressure vs. Time, 1st cycle

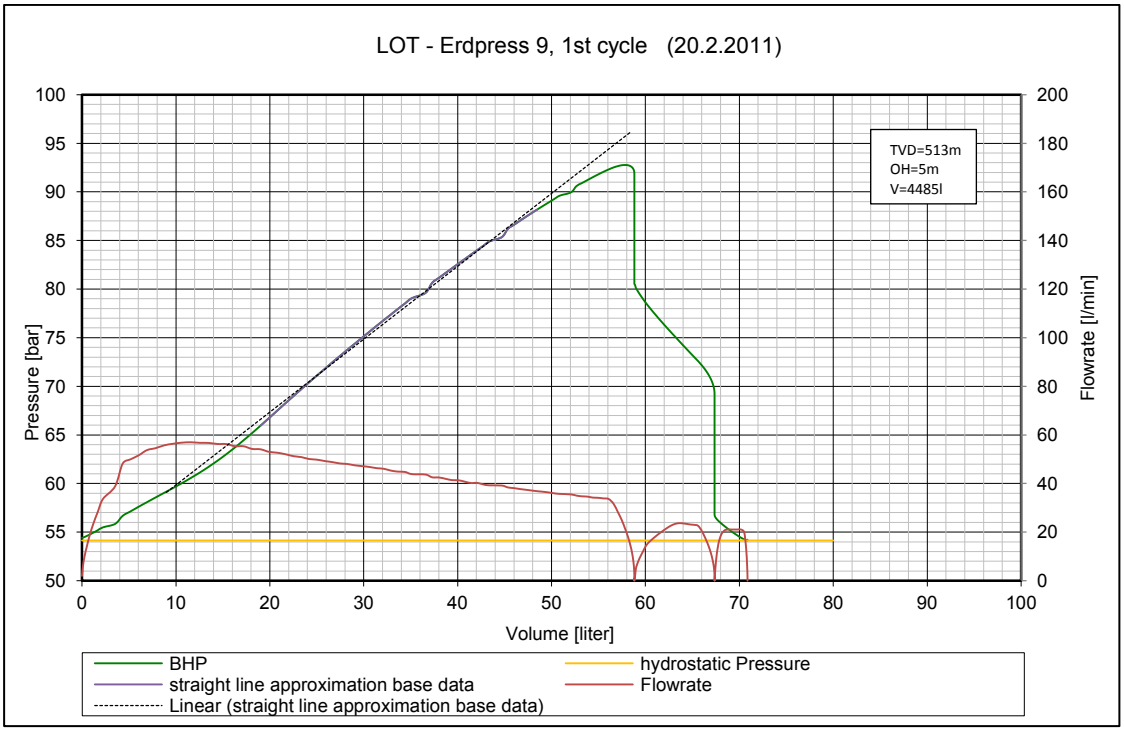

Figure 75 – LOT Erdpress 9, Pressure vs. Volume, 1st cycle

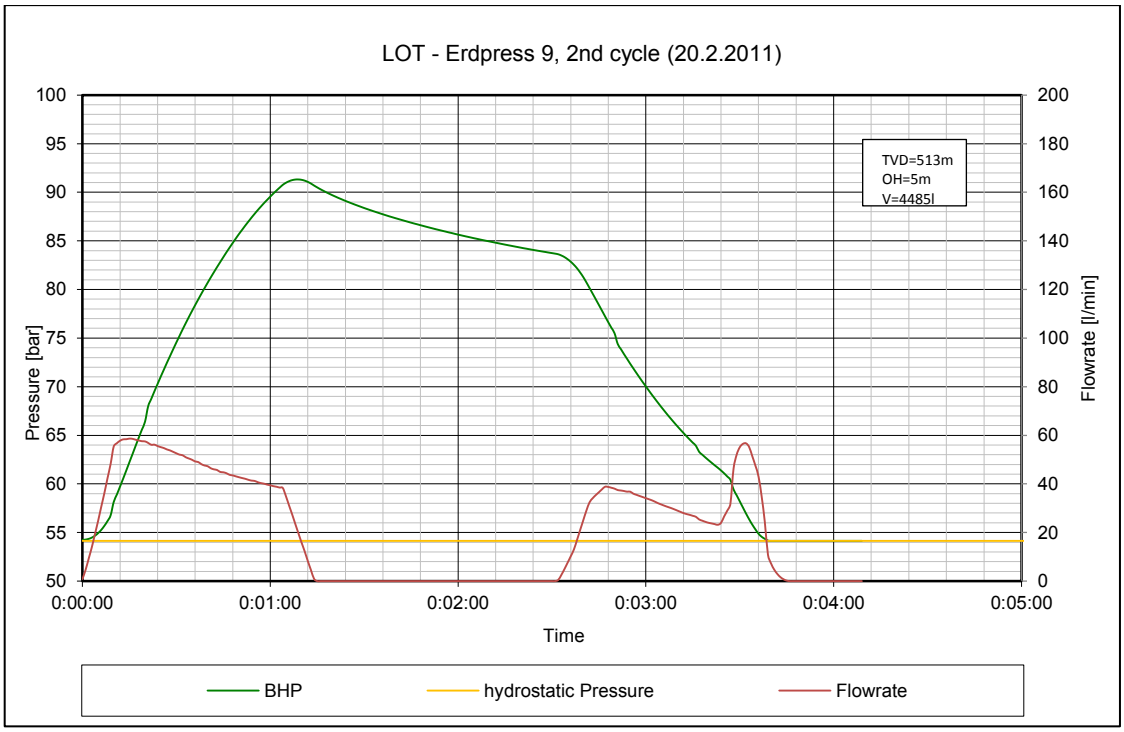

Figure 76 – LOT Erdpress 9, Pressure vs. Time, 2nd cycle

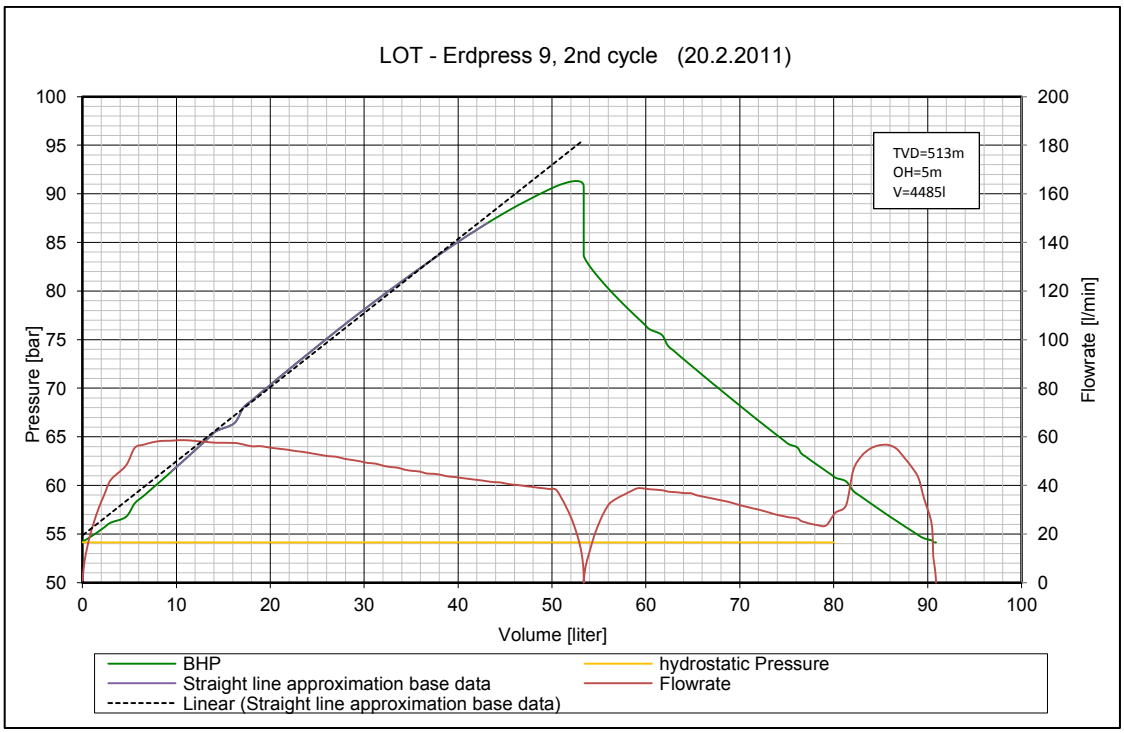

Figure 77 – LOT Erdpress 9, Pressure vs. Volume, 2nd cycle

Well D – Erdpress 10

LOT					
Well	Erdpress 10 (Erd10)			**Date**	15.3.2011
Test TD	548 m	**Casing Shoe**	543 m	**Drilled TD**	545 m
Open-hole	5 m	**Ex. Formation**	3 m	**DW**	8 ½ in
Completion	9 5/8 in / 36ppf / J55			**Cycles**	2

Cycle	LOP [bar]	LOV [liter]	Pmax [bar]	SSIP [bar]
1	90	6	94,5	86
2	91	8	100	91

Table 13 – Summary LOT Erdpress 10

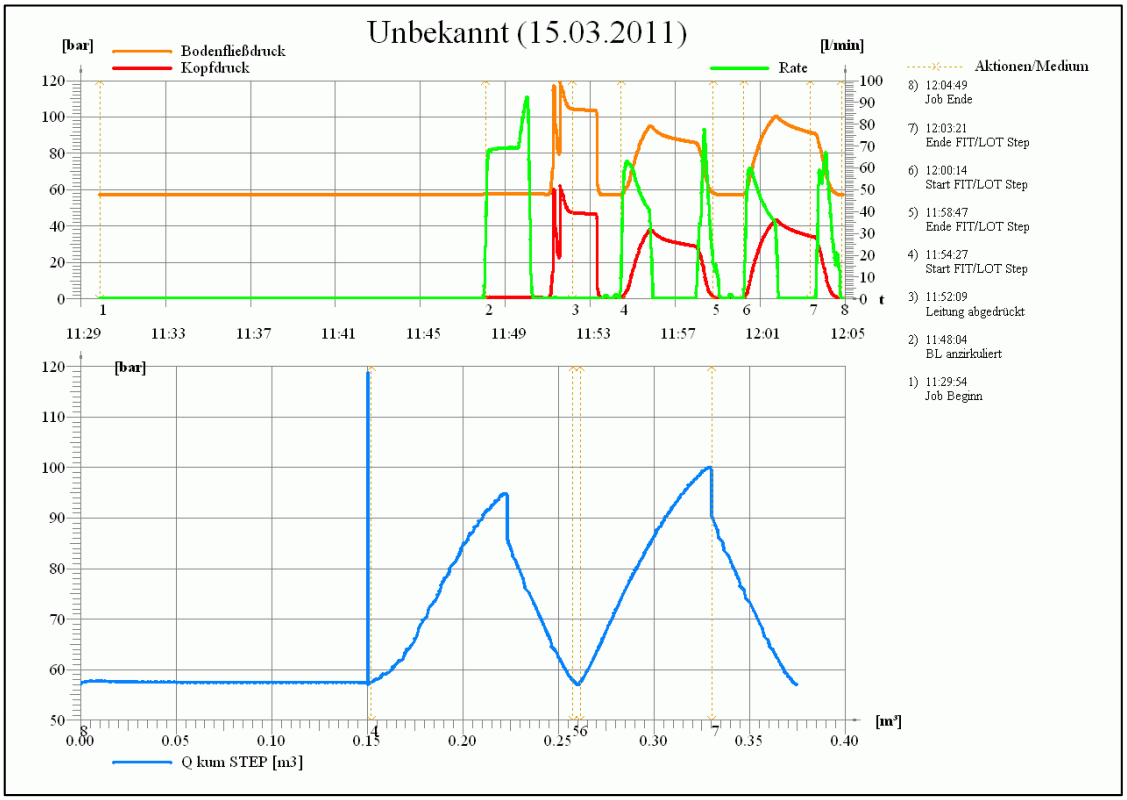

Figure 78 - LOT Record Erdpress 10

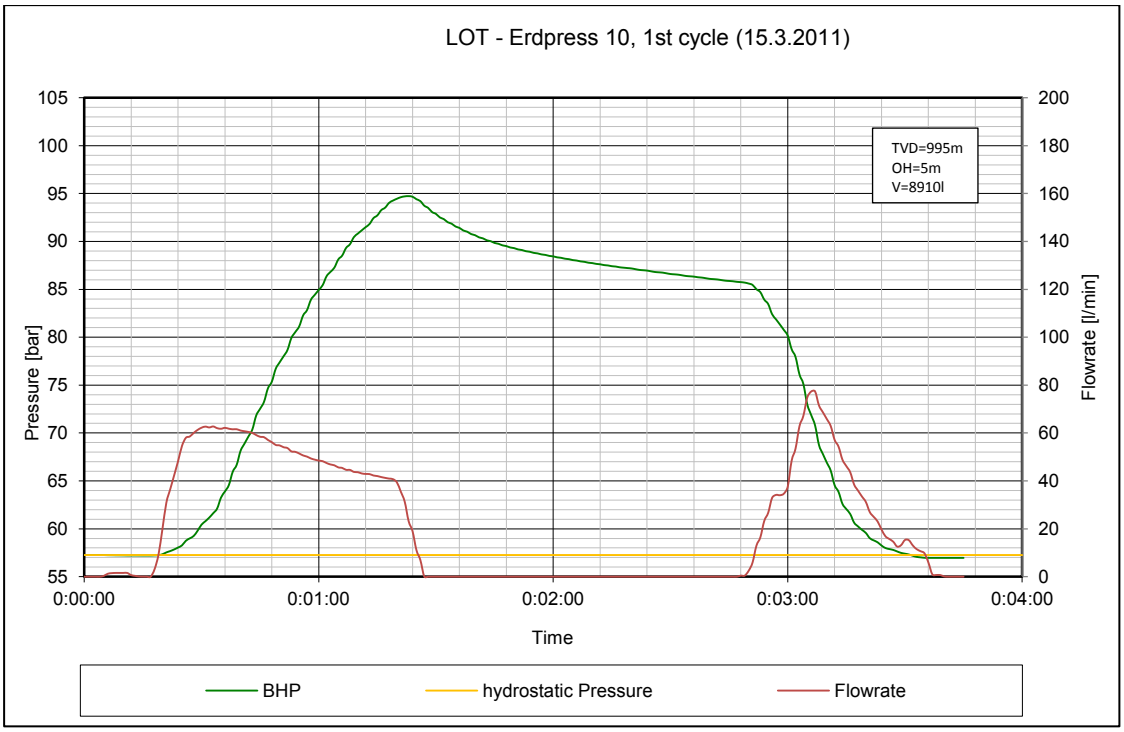

Figure 79 – LOT Erdpress 10, Pressure vs. Time, 1st cycle

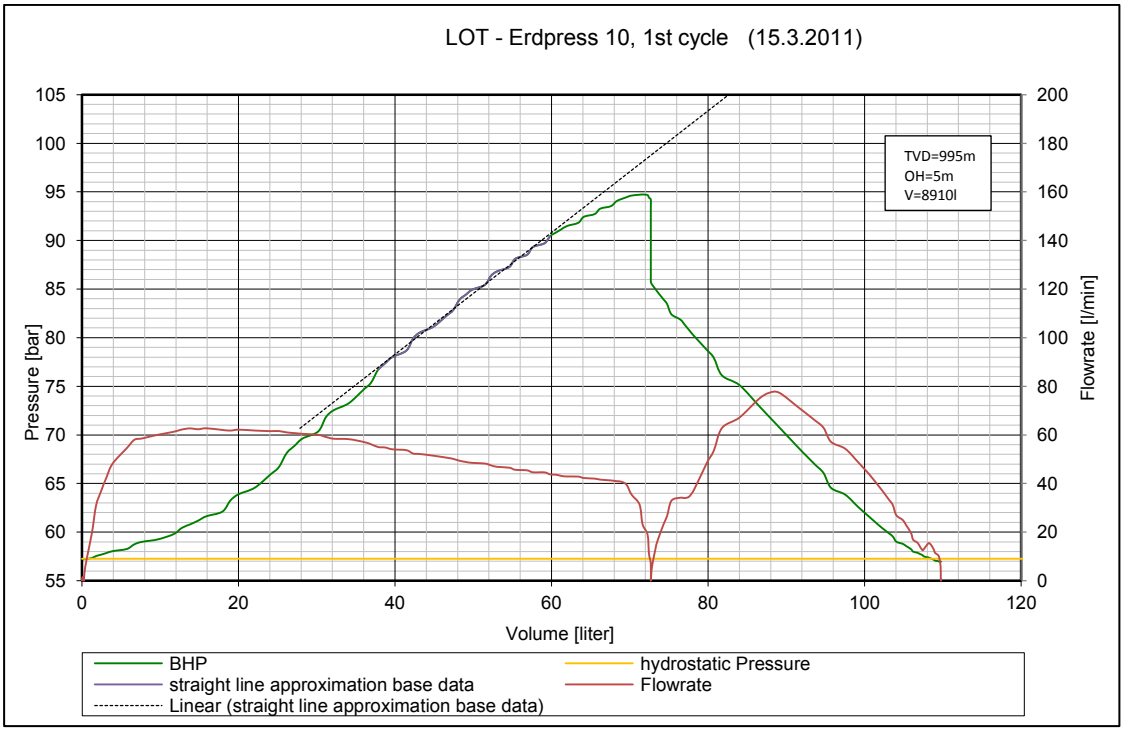

Figure 80 – LOT Erdpress 10, Pressure vs. Volume, 1st cycle

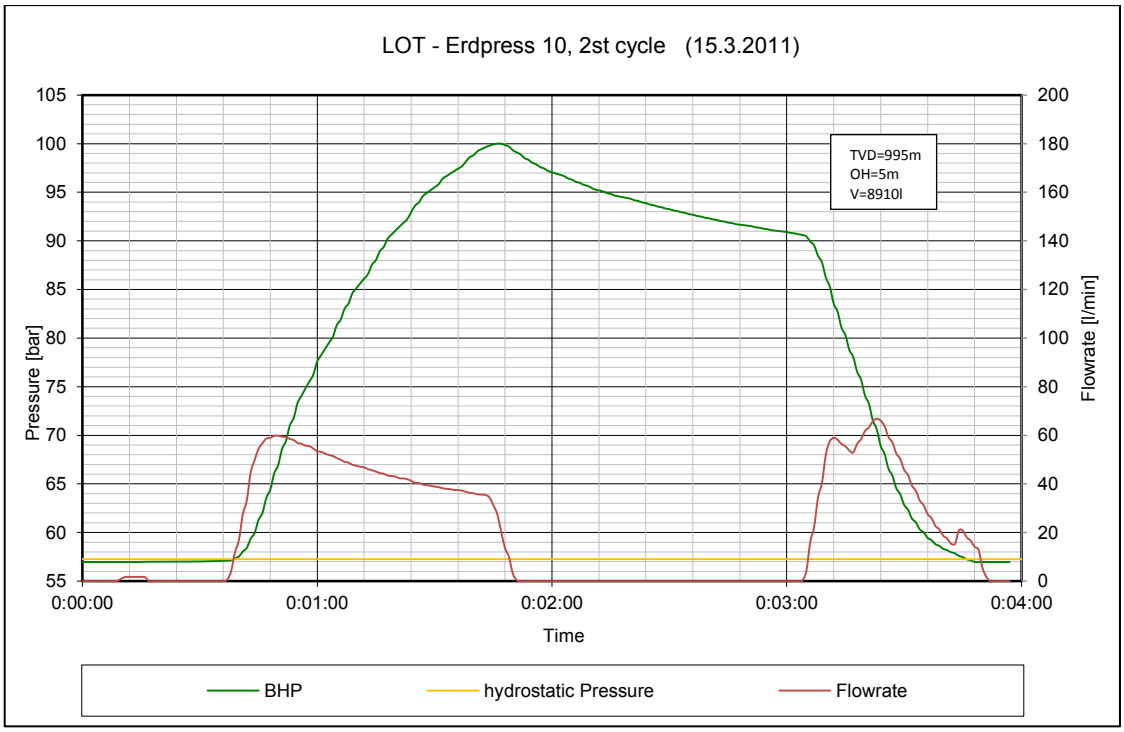

Figure 81 – LOT Erdpress 10, Pressure vs. Time, 2nd cycle

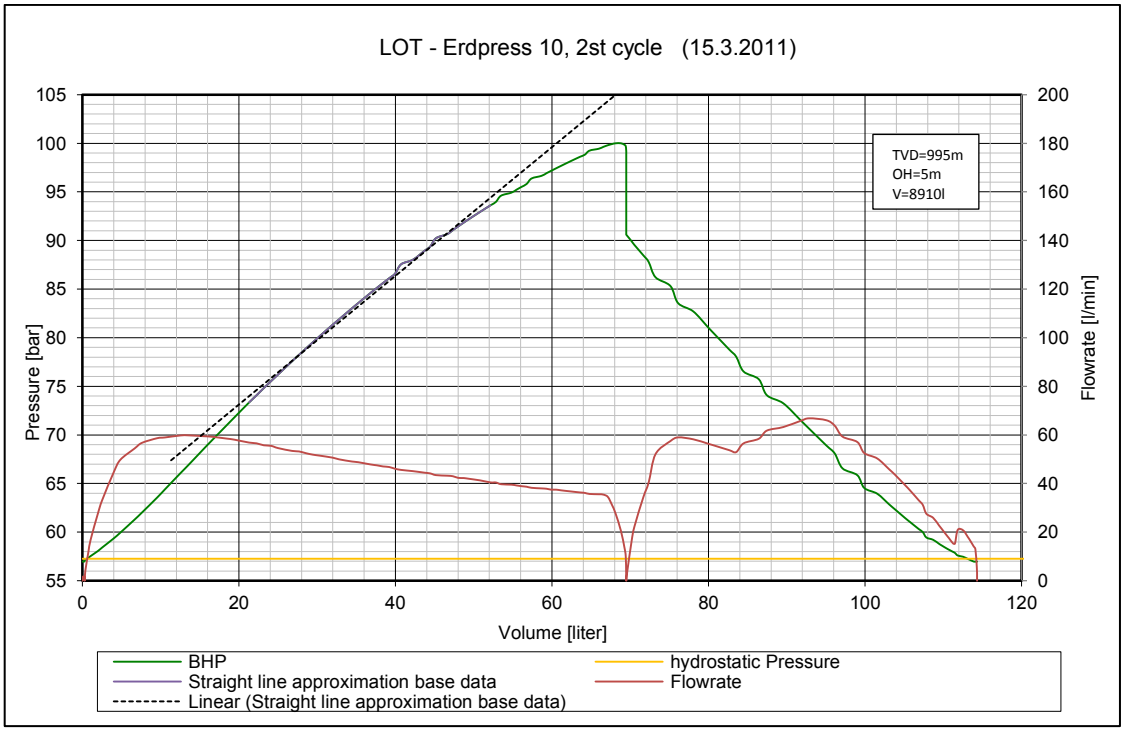

Figure 82 – LOT Erdpress 10, Pressure vs. Volume, 2nd cycle

Well E – Erdpress 12

LOT					
Well	Erdpress 12 (Erd12)			**Date**	20.2.2010
Test TD	510 m	**Casing Shoe**	505 m	**Drilled TD**	507 m
Open-hole	5 m	**Ex. Formation**	3 m	**DW**	8 ½ in
Completion	9 5/8 in / 36ppf / J55			**Cycles**	2

Cycle	LOP [bar]	LOV [liter]	Pmax [bar]	SSIP [bar]
2	82	16	96	89

Table 14 – Summary LOT Erdpress 12

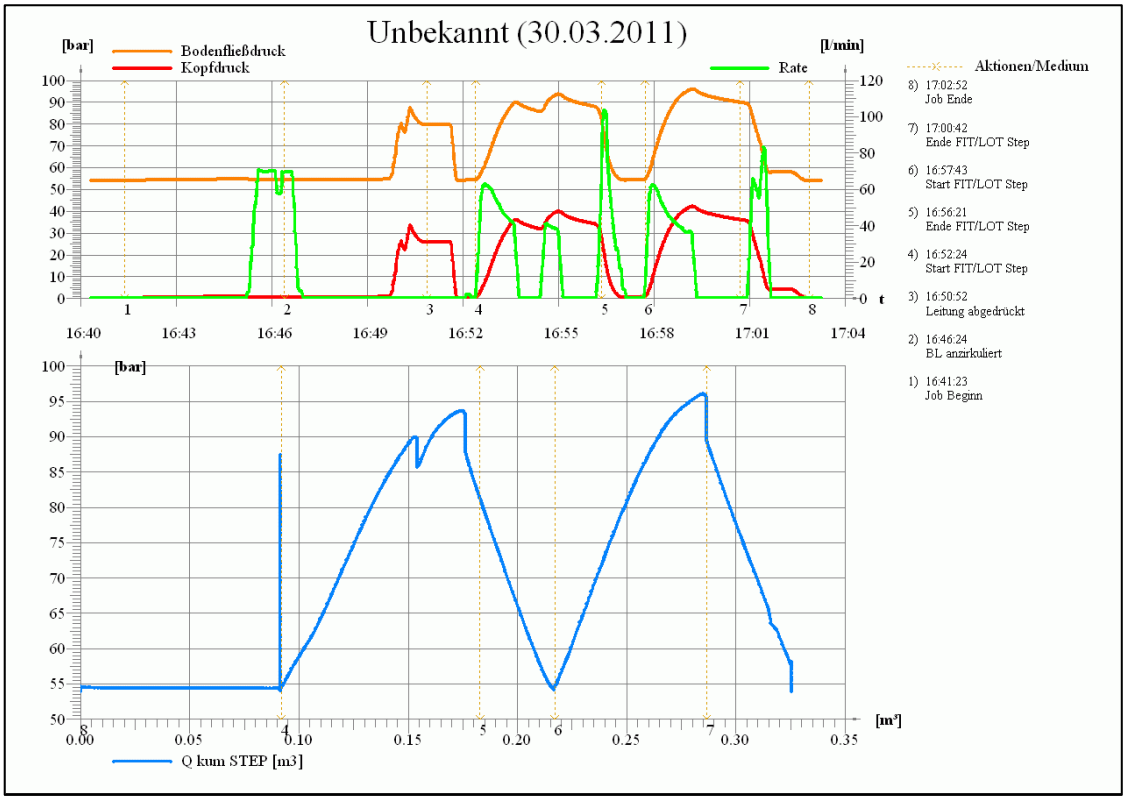

Figure 83 - LOT Record Erdpress 12

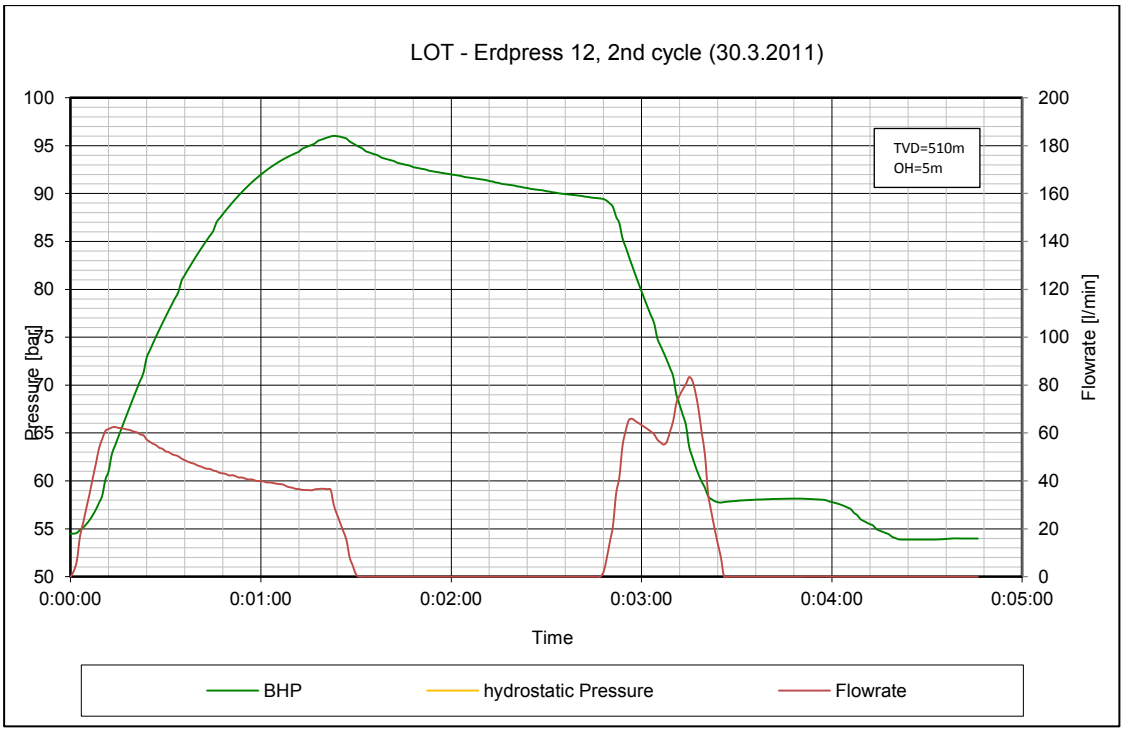

Figure 84 – LOT Erdpress 12, Pressure vs. Time, 2nd cycle

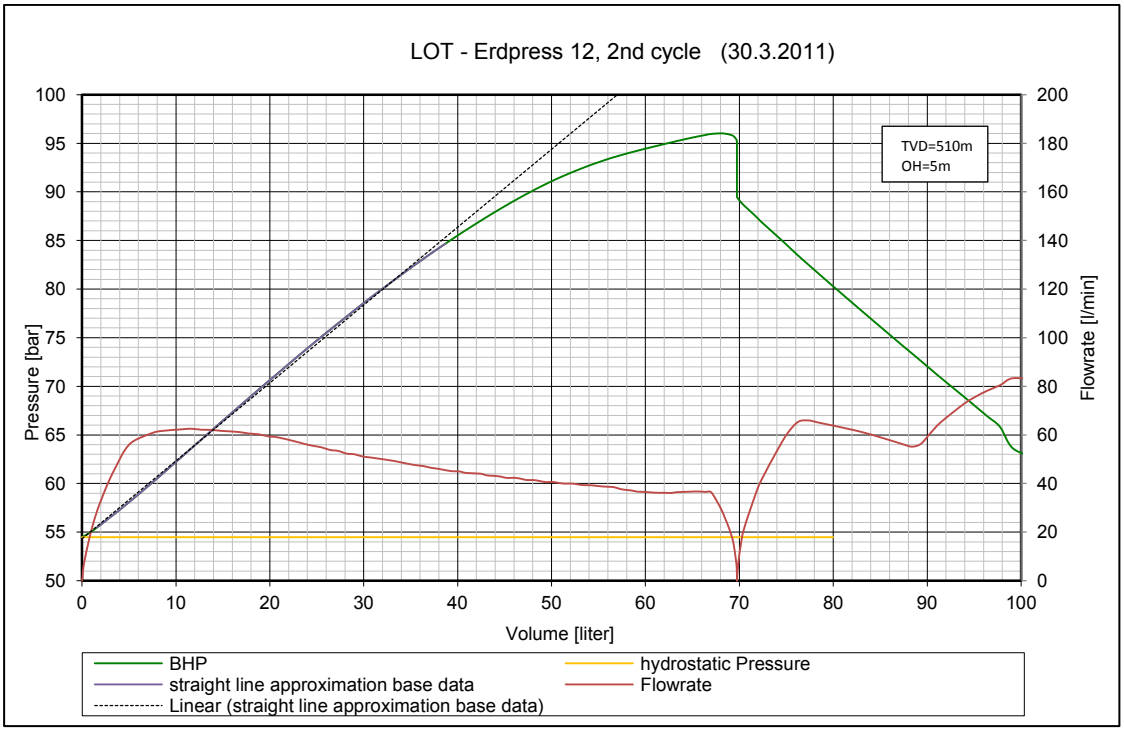

Figure 85 – LOT Erdpress 12, Pressure vs. Volume, 2nd cycle

Well F – Hauskirchen 86

LOT					
Well	Hauskirchen 86 (Hau86)			**Date**	22.9.2010
Test TD	555 m	**Casing Shoe**	550 m	**Drilled TD**	552 m
Open-hole	5 m	**Ex. Formation**	3 m	**DW**	8 ½ in
Completion	9 5/8 in / 36 ppf / J55			**Cycles**	3

Cycle	LOP [bar]	LOV [liter]	Pmax [bar]	SSIP [bar]
1	90	14	98	79
2	91	10	94	82
3	91	100	94	83

Table 15 – Summary LOT Hauskirchen 86

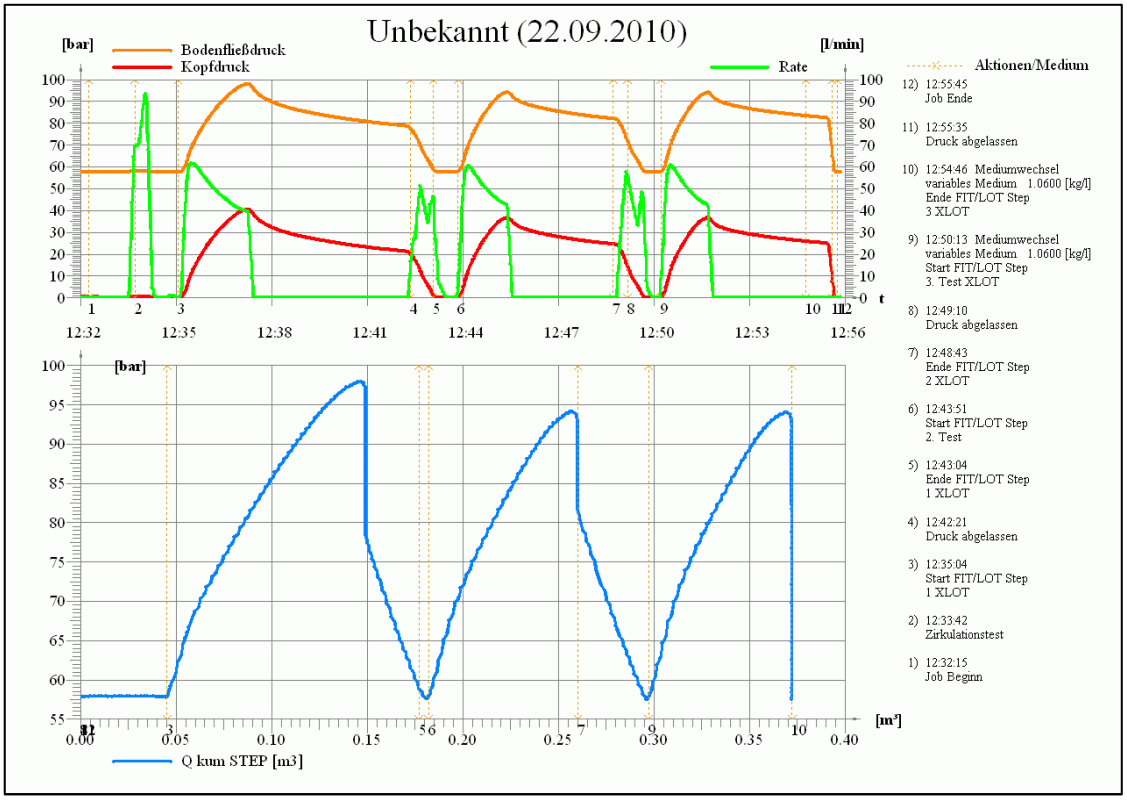

Figure 86 - LOT Record Hauskirchen 86

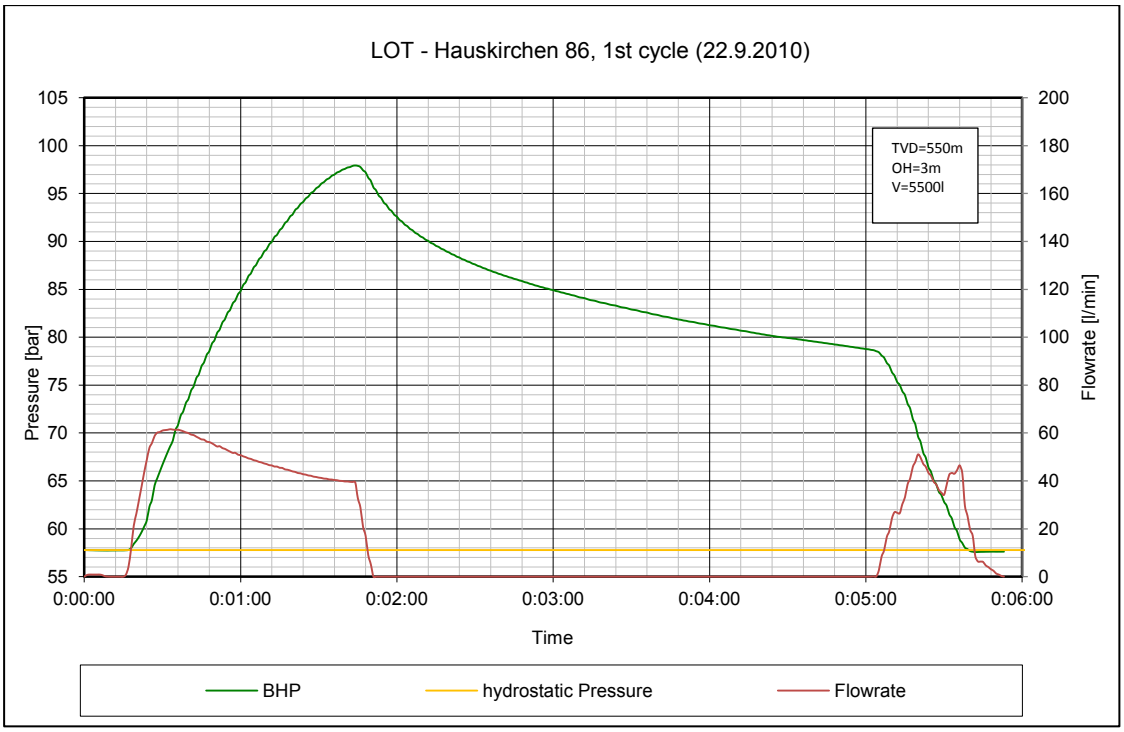

Figure 87 – LOT Hauskirchen 86, Pressure vs. Time, 1st cycle

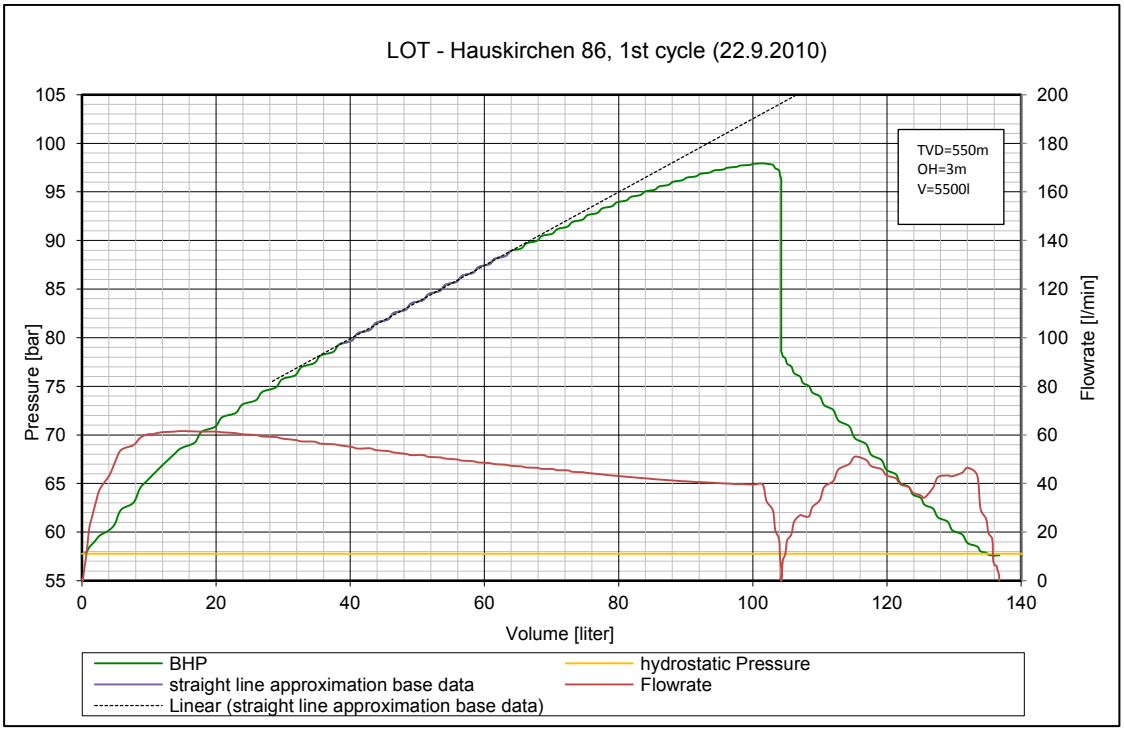

Figure 88 – LOT Hauskirchen 86, Pressure vs. Volume, 1st cycle

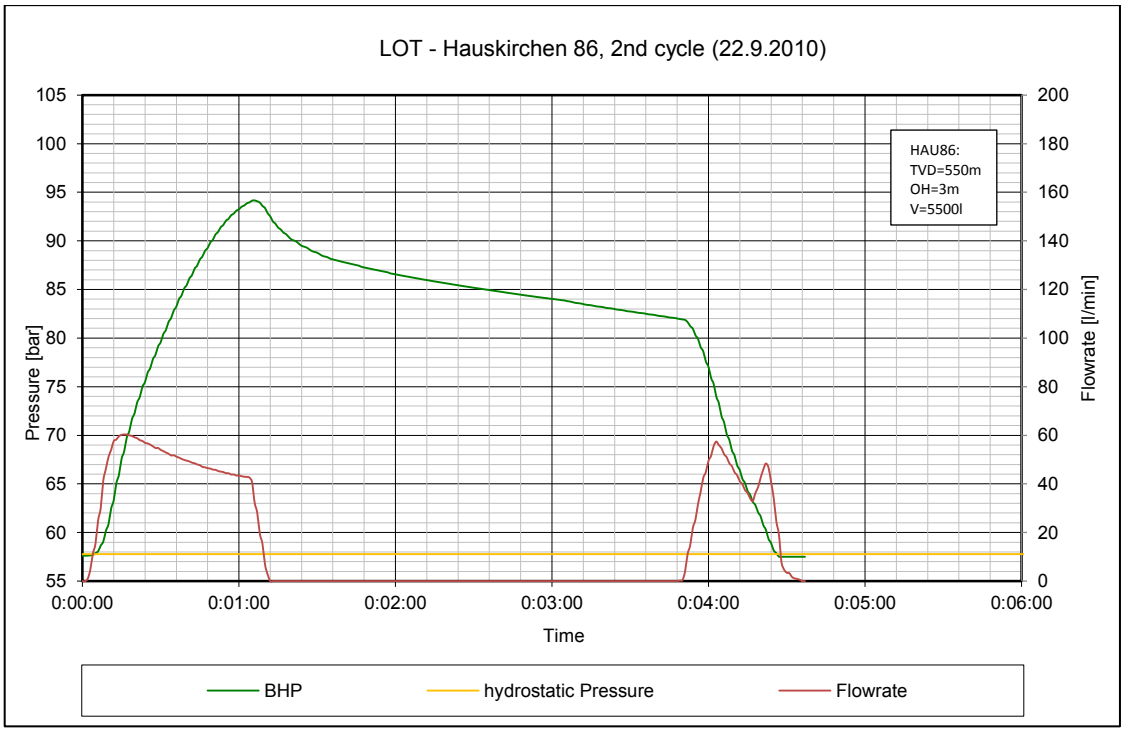

Figure 89 – LOT Hauskirchen 86, Pressure vs. Time, 2nd cycle

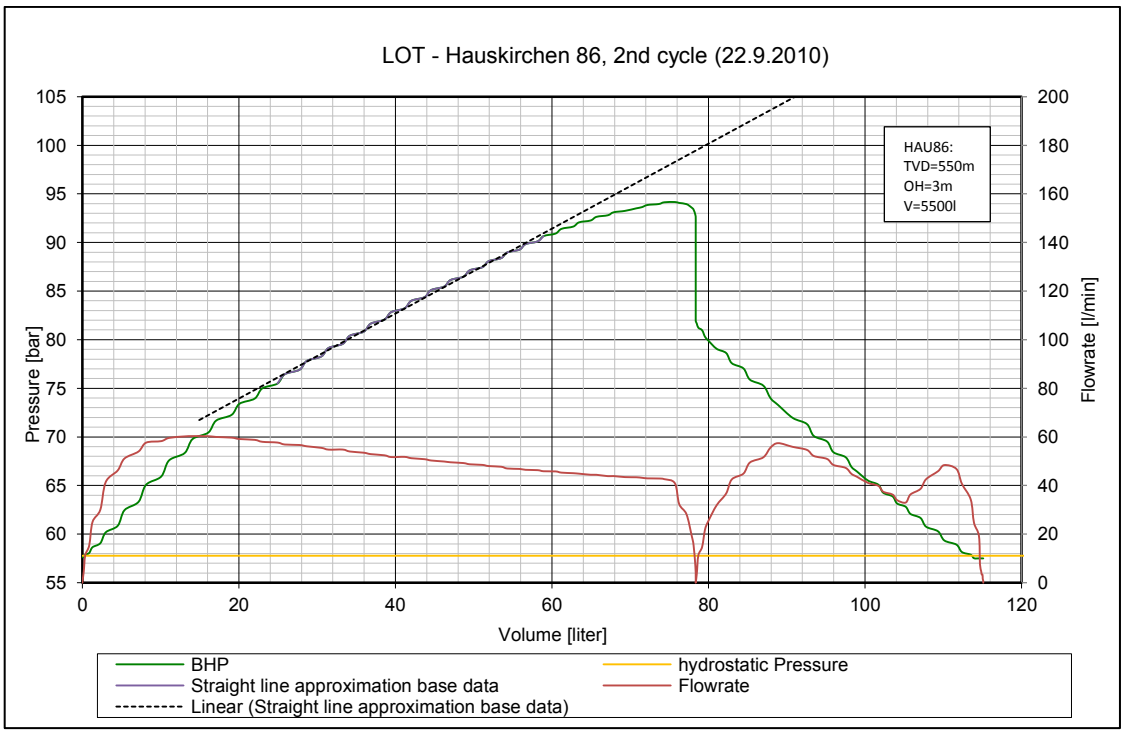

Figure 90 – LOT Hauskirchen 86, Pressure vs. Volume, 2nd cycle

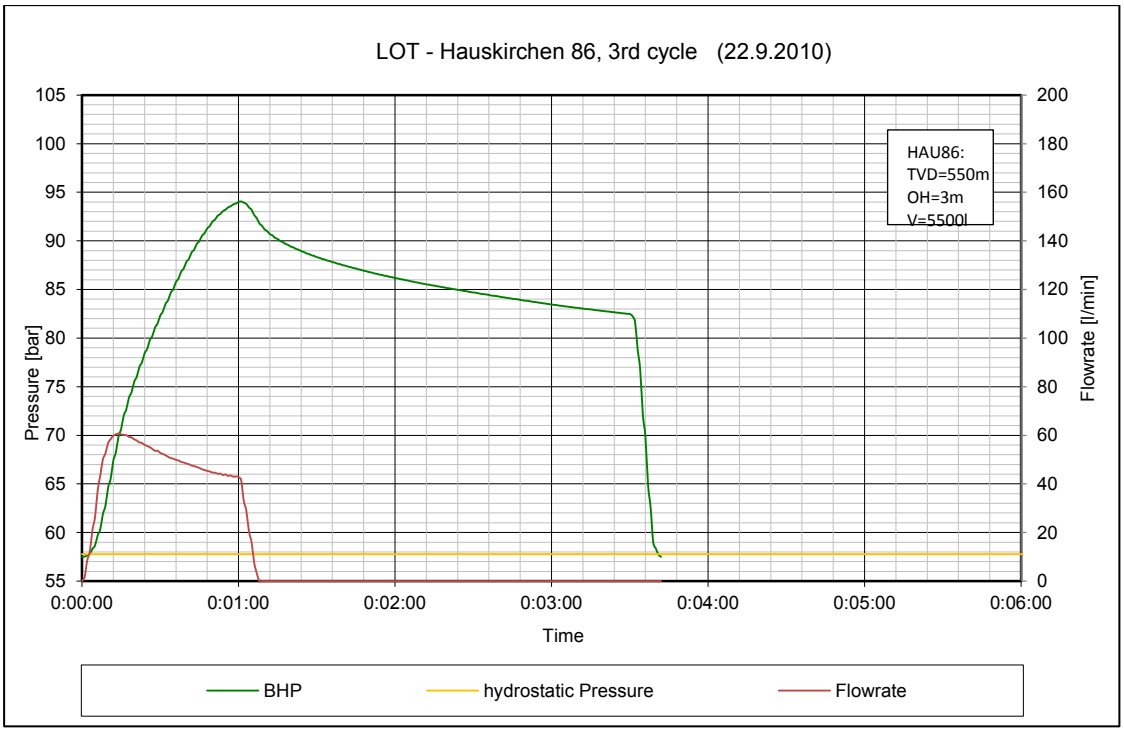

Figure 91 – LOT Hauskirchen 86, Pressure vs. Time, 3rd cycle

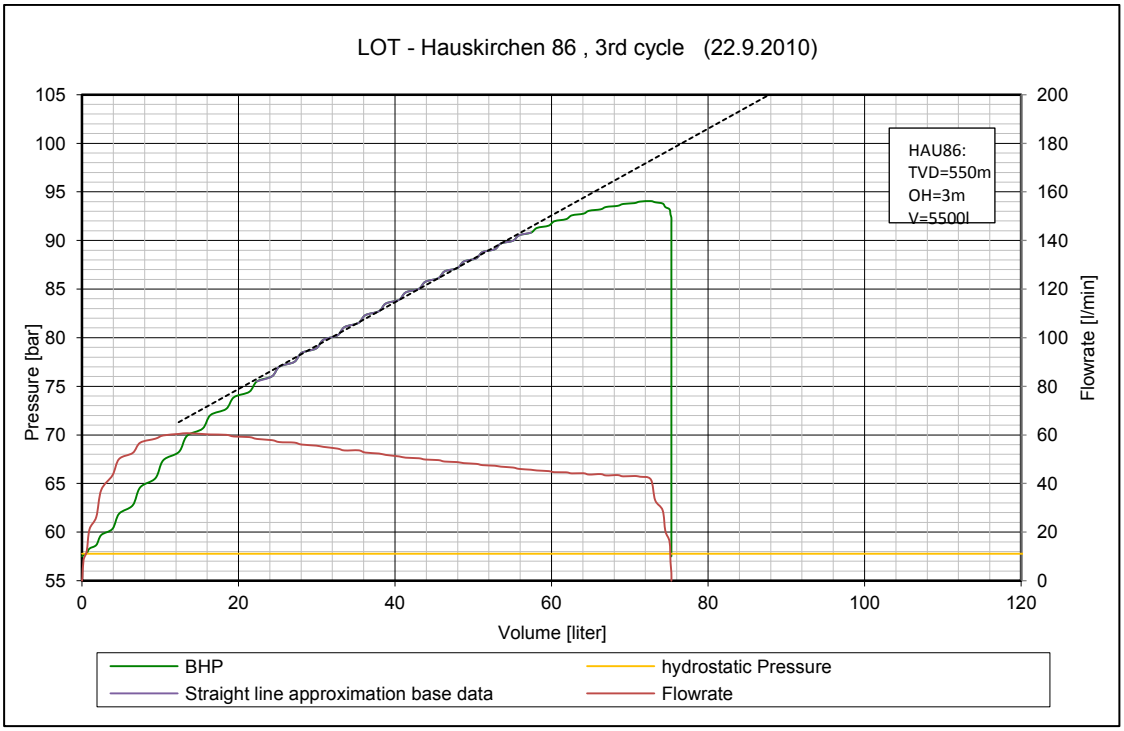

Figure 92 – LOT Hauskirchen 86, Pressure vs. Volume, 3rd cycle

Well G – Poysbrunn 3

LOT					
Well	Poysbrunn (PoBr3)			**Date**	21.12.2010
Test TD	635 m	**Casing Shoe**	630 m	**Drilled TD**	632 m
Open-hole	5 m	**Ex. Formation**	3 m	**DW**	8 ½ in
Completion	9 5/8 in / 36ppf / J55			**Cycles**	2

Cycle	LOP [bar]	LOV [liter]	Pmax [bar]	SSIP [bar]
1	168	6	180	156
2	160	12	174	156

Table 16 – Summary LOT Poysbrunn 3

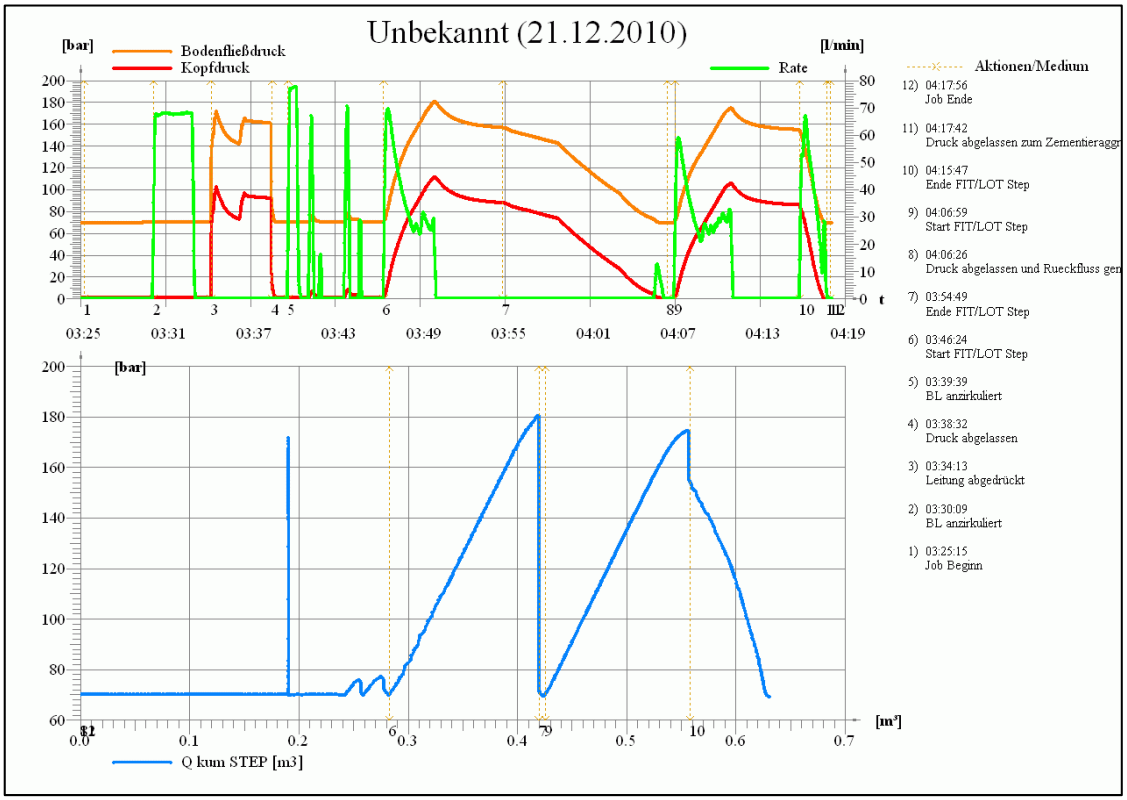

Figure 93 - LOT Record Poysbrunn 3

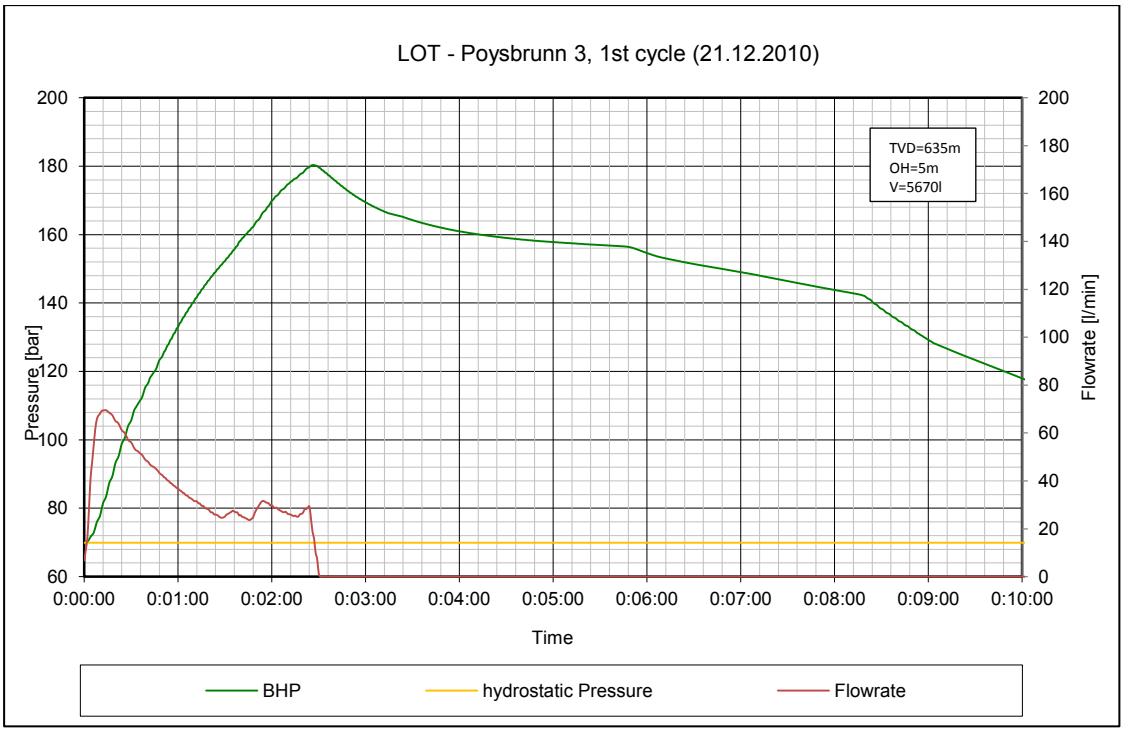

Figure 94 – LOT Poysbrunn 3, Pressure vs. Time, 1st cycle

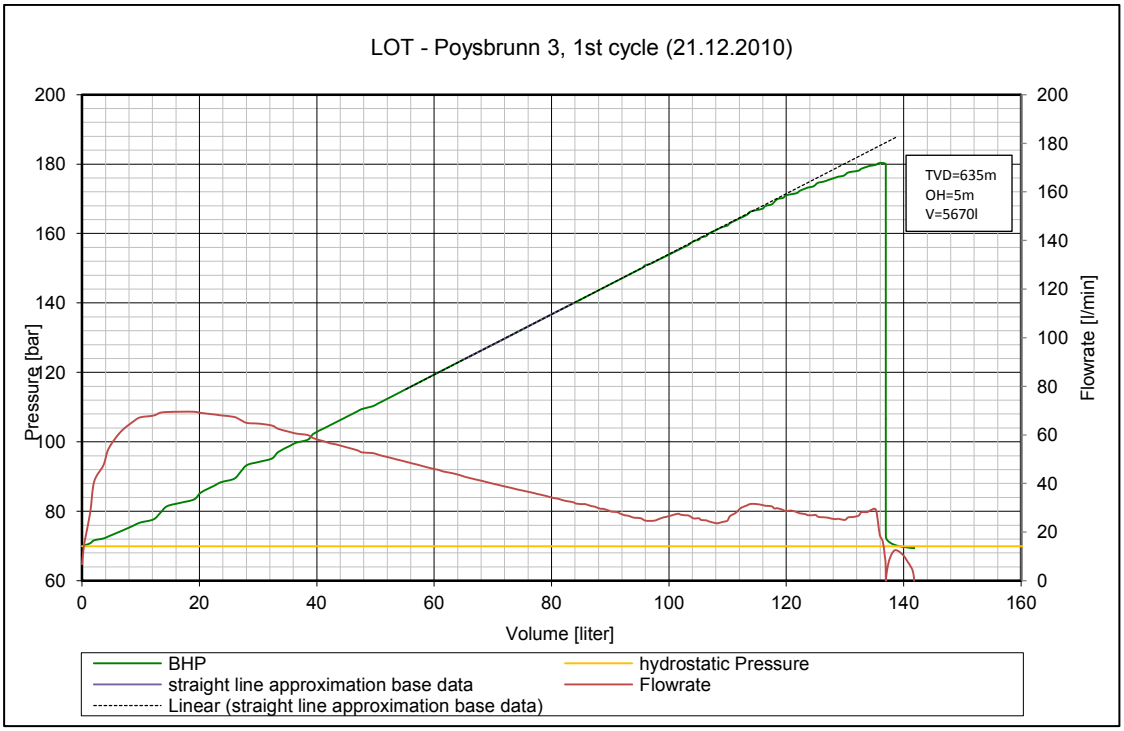

Figure 95 – LOT Poysbrunn 3, Pressure vs. Volume, 1st cycle

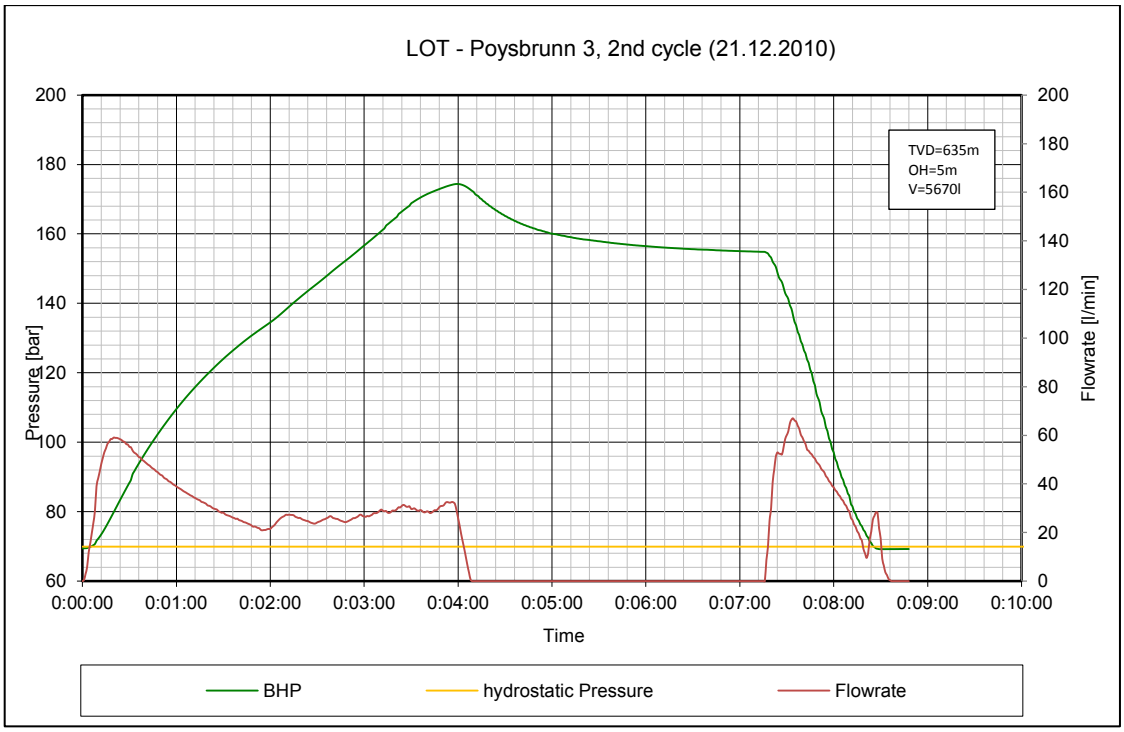

Figure 96 – LOT Poysbrunn 3, Pressure vs. Time, 2nd cycle

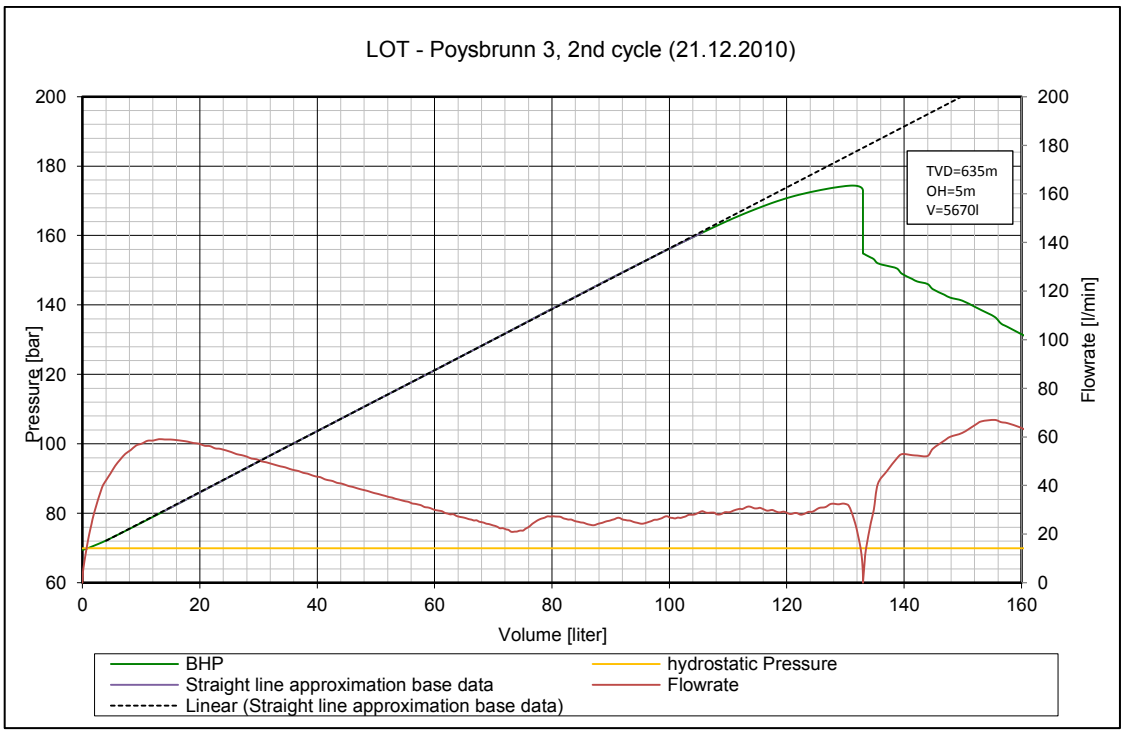

Figure 97 – LOT Poysbrunn 3, Pressure vs. Volume, 2nd cycle

Well H – Roseldorf 22

LOT					
Well	Roseldorf 22 (Ro22)			**Date**	19.10.2010
Test TD	491 m	**Casing Shoe**	486 m	**Drilled TD**	488 m
Open-hole	5 m	**Ex. Formation**	3 m	**DW**	8 ½ in
Completion	9 5/8 in / 36 ppf / J55			**Cycles**	1

Cycle	LOP [bar]	LOV [liter]	Pmax [bar]	SSIP [bar]
1	104	1,5	111	106

Table 17 – Summary LOT Roseldorf 22

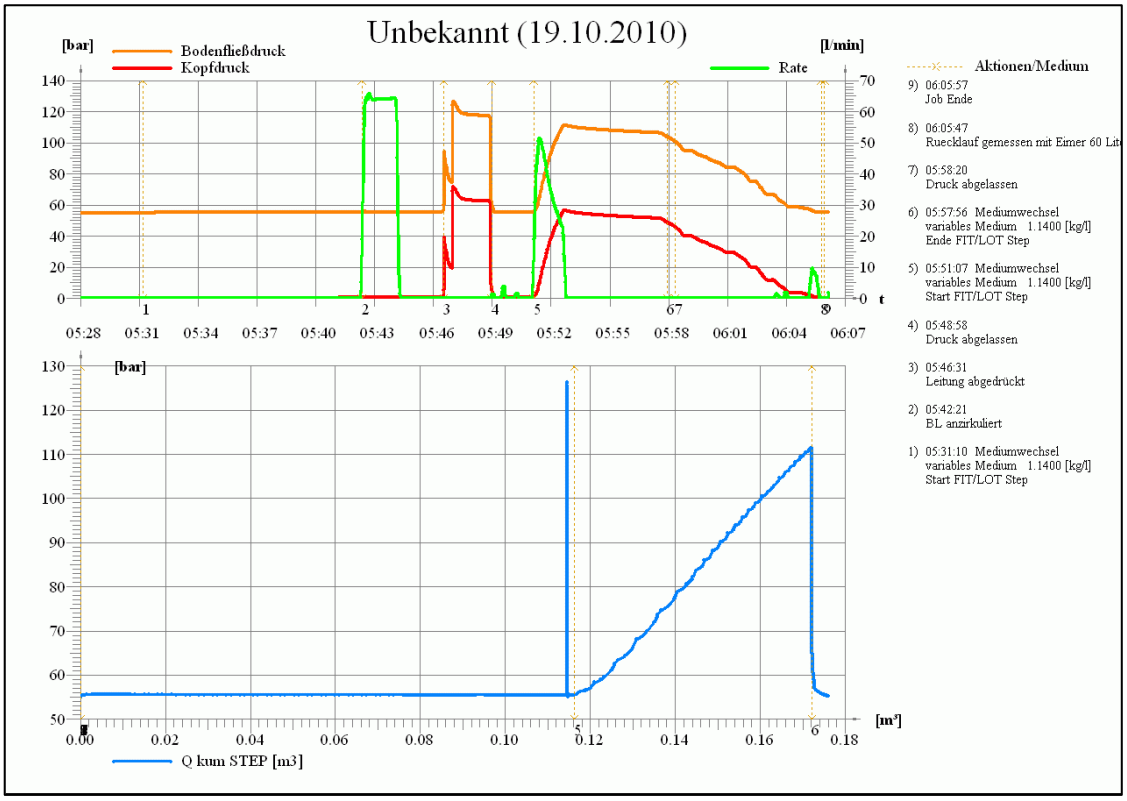

Figure 98 - LOT Record Roseldorf 22

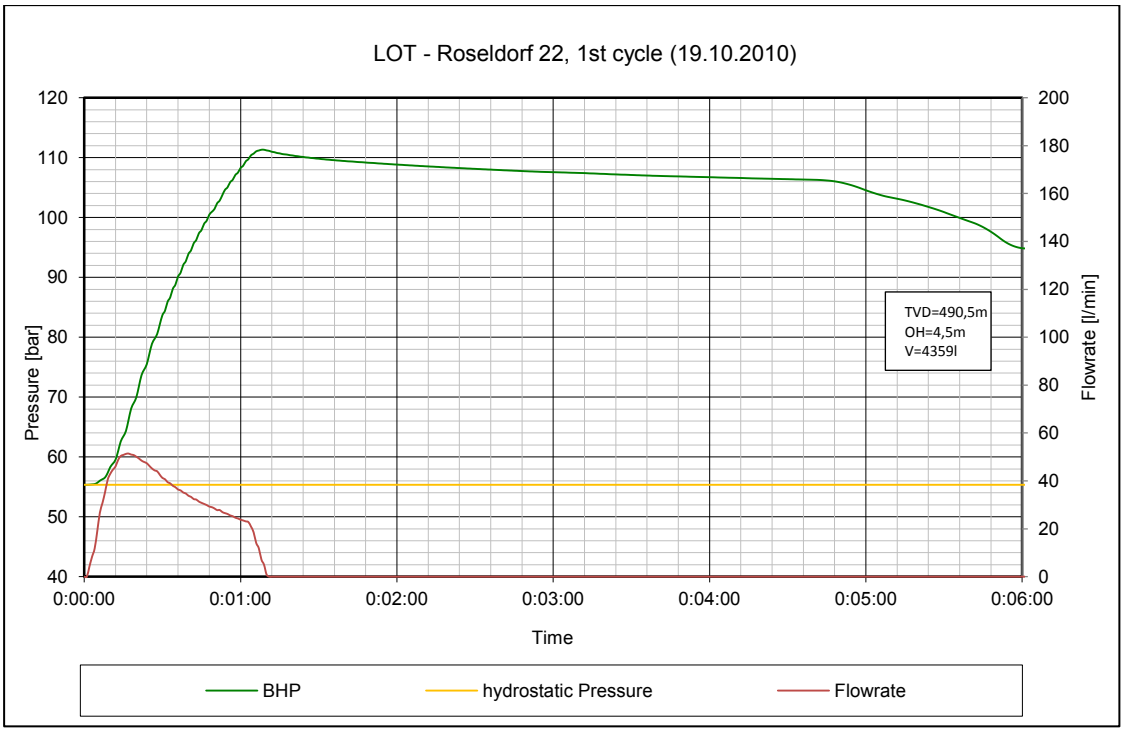

Figure 99 – LOT Roseldorf 22, Pressure vs. Time, 1st cycle

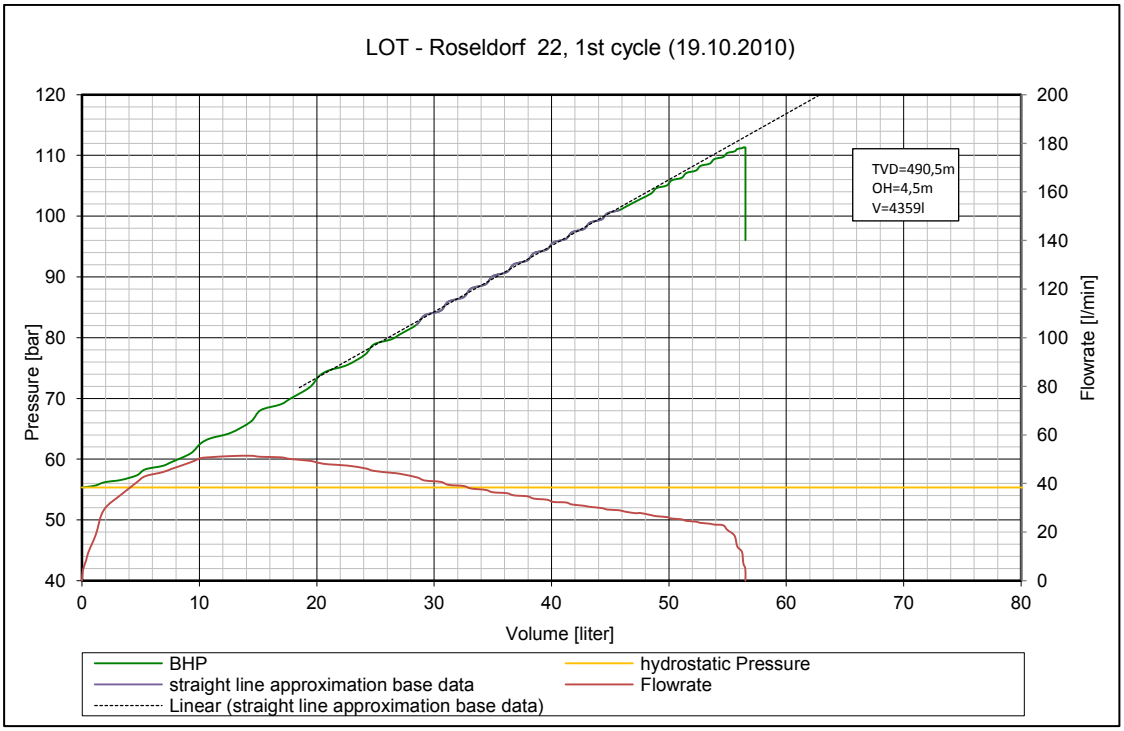

Figure 100 – LOT Roseldorf 22, Pressure vs. Volume, 1st cycle

Appendix F Extended Leak-Off Test Data

Rabensburg 12

In this Example an extended Leak-Off Test is presented where no pressure drop prior to propagating the fracture far into the formation can be observed.

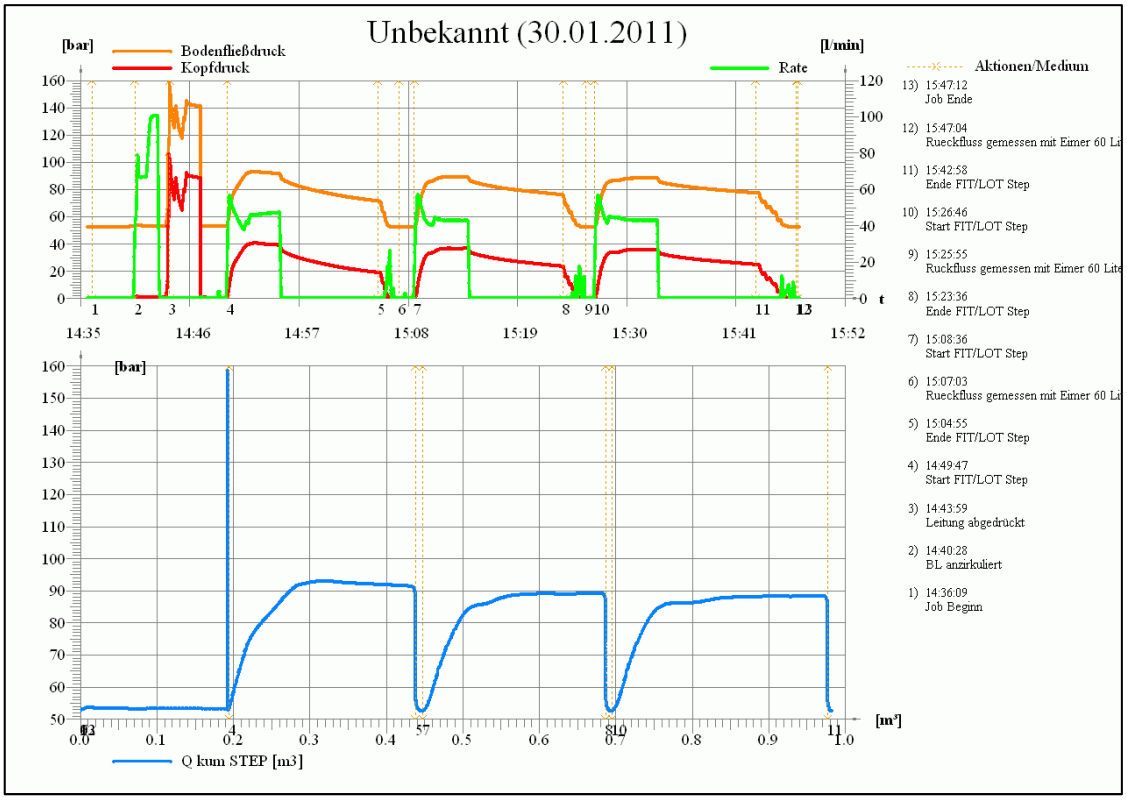

Figure 101 – xLOT Record Rabensburg 12

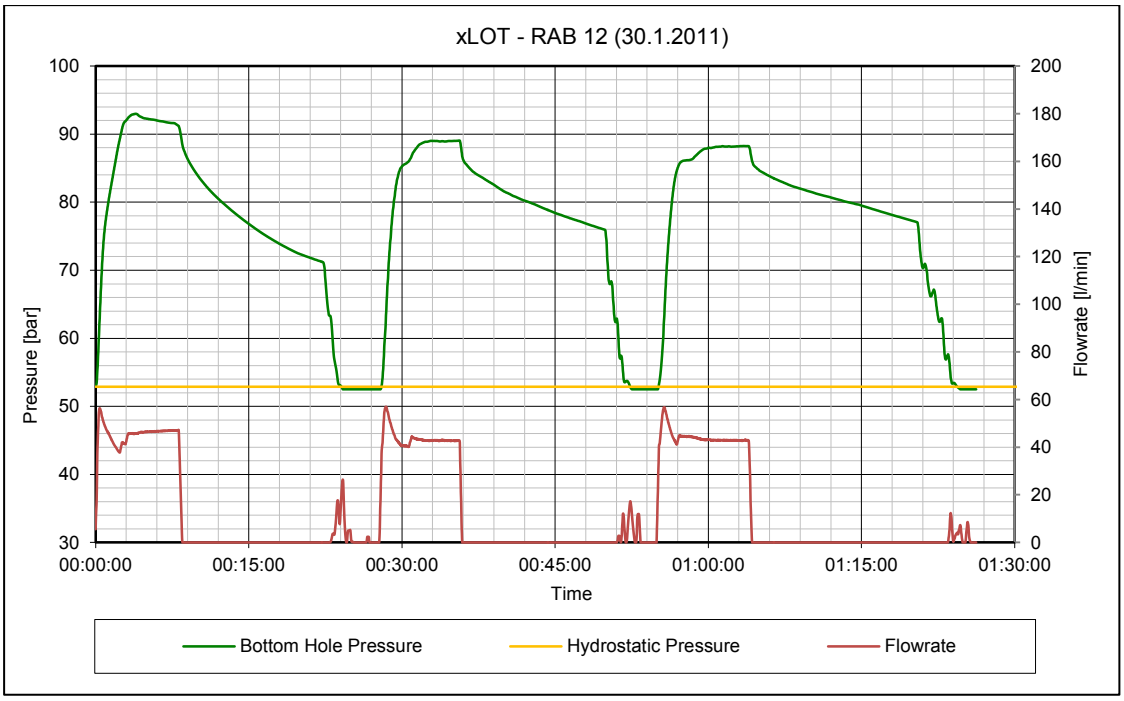

Figure 102 – xLOT Rabensburg 12, Pressure vs. Time

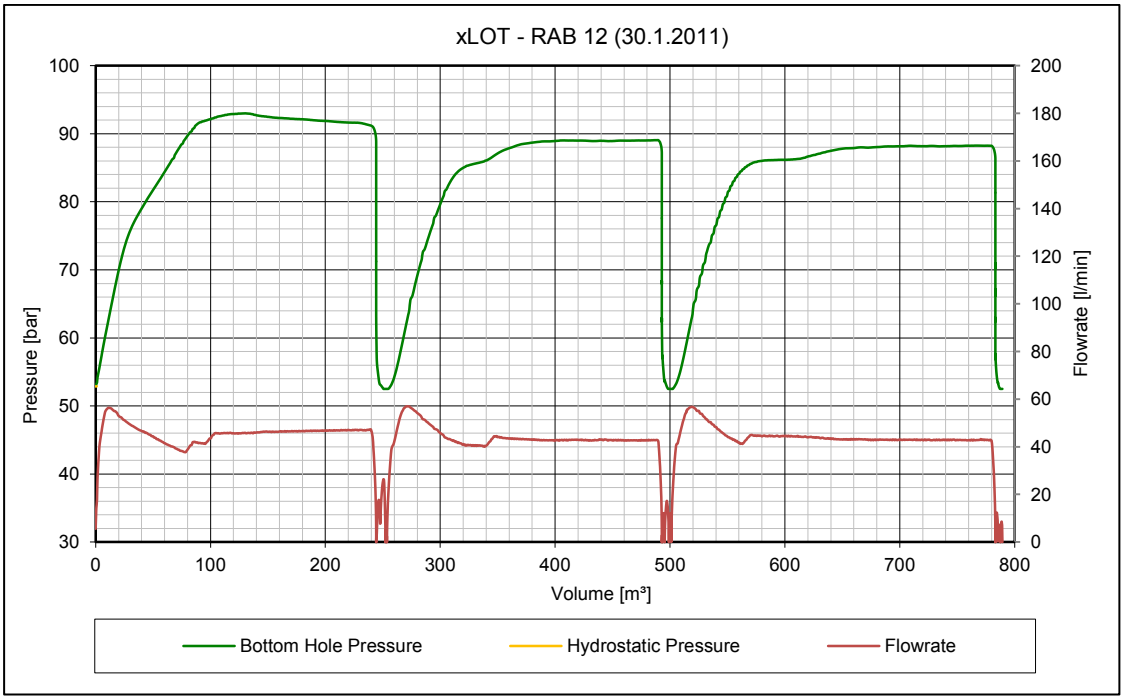

Figure 103 – xLOT Rabensburg 12, Pressure vs. Volume

Schönkirchen C2

In this Example, in contrast to the extended Leak-Off Test presented previously, a drop in pressure can be seen as a fracture is created.

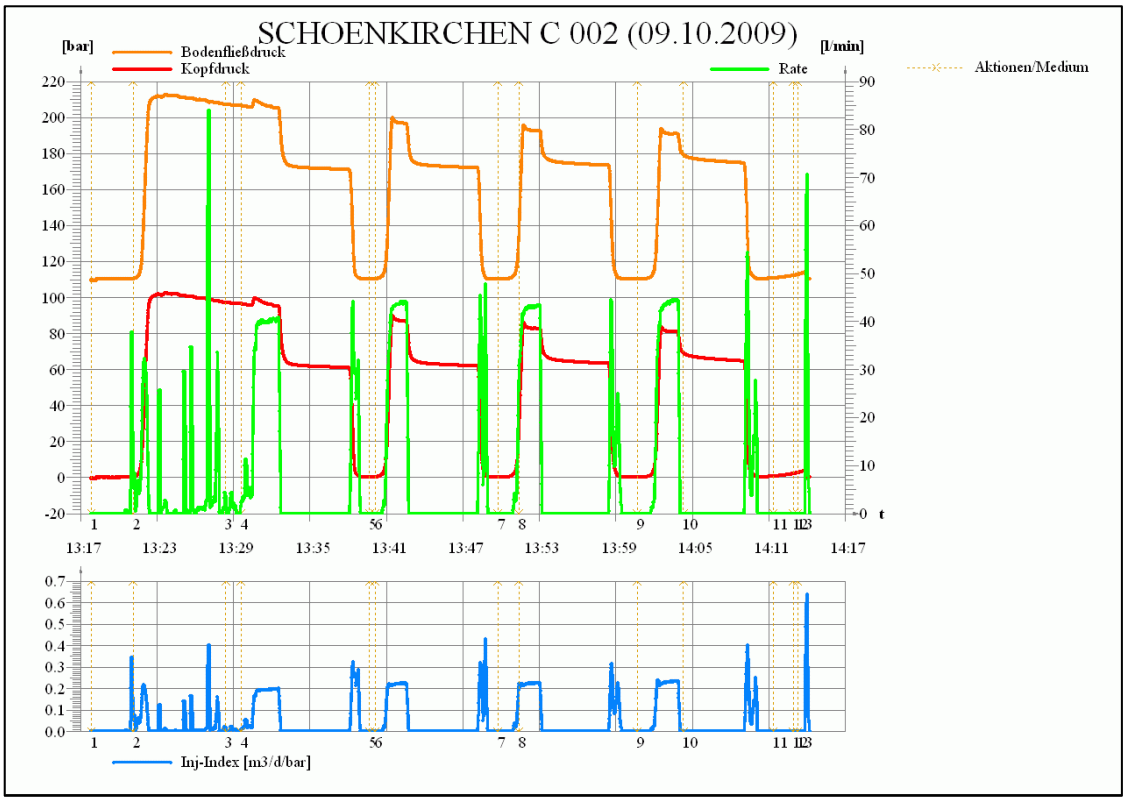

Figure 104 – xLOT Record Schönkirchen C2

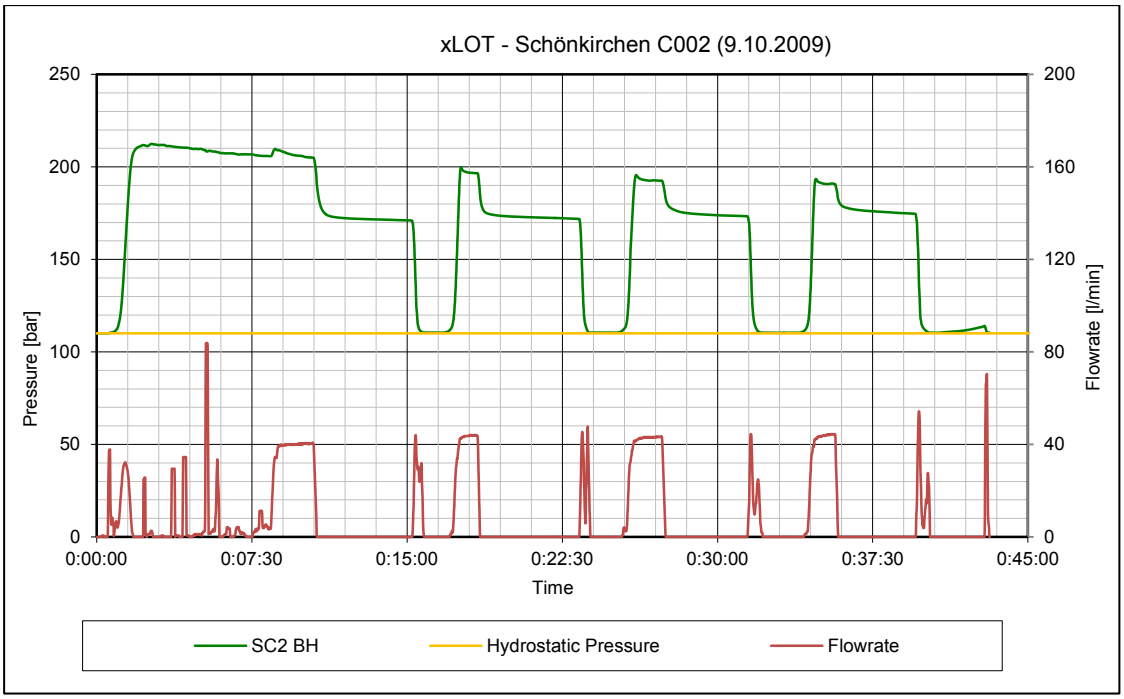

Figure 105– xLOT Schönkirchen C002, Pressure vs. Time

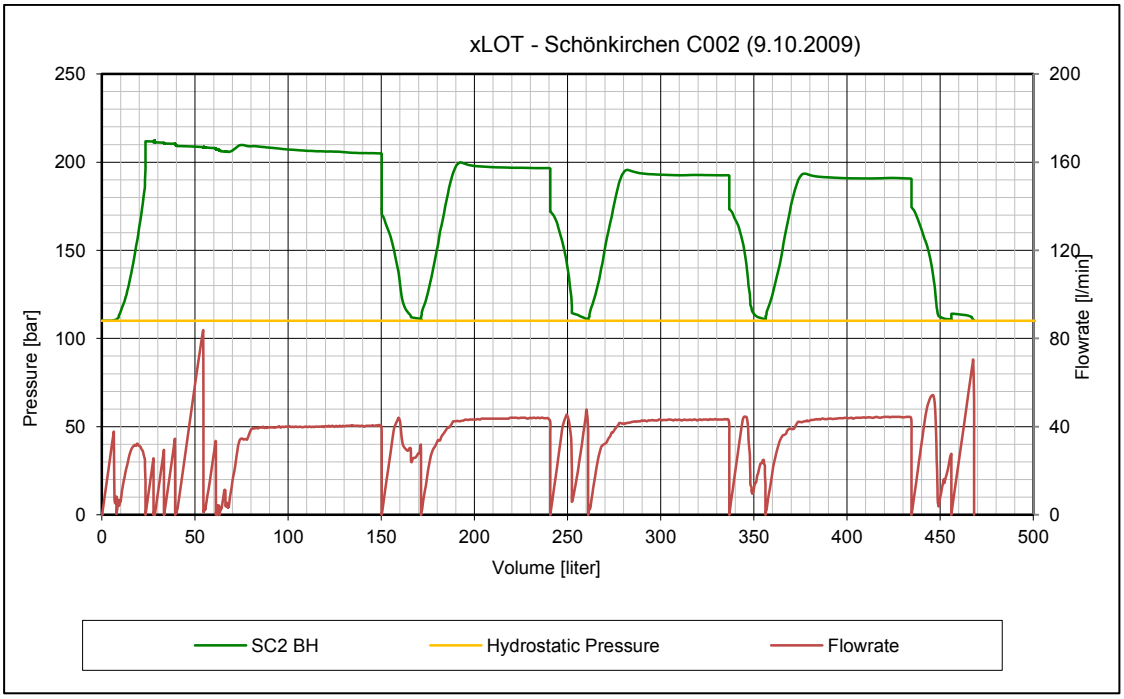

Figure 106 – xLOT Schönkirchen C002, Pressure vs. Volume

Table of Figures

List of Tables

Nomenclature & Abbreviations

A	Area	[m²]
a	Crack half length	[m]
BOL	Break out limit	[MPa]
c_{mud}	Compressibility factor of drilling mud	[1/ MPa]
c_{Oil}	Compressibility factor of oil	[1/ MPa]
c_{Solids}	Compressibility factor of solids	[1/ MPa]
cwater	Compressibility factor of water	[1/Mpa]
D_W	Wellbore diameter	[m]
E	Young's Modulus of steel	[MPa]
E_f	Young's Modulus of the formation	[MPa]
FBP	Formation Breakdown Pressure	[MPa]
FIP	Fracture Initiation Pressure	[MPa]
FIT	Formation Integrity Test	-
FPP	Fracture Propagation Pressure	[MPa]
FRP	Fracture Reopening Pressure	[MPa]
G_I	Energy release rate (mode I)	[Nm]
G_{IC}	Critical energy release rate (mode I)	[Nm]
H	Fracture height	[m]
h_{mc}	Filter cake thickness	[cm]
ISIP	Instantaneous shut-in pressure	[MPa]
k	Permeability	[Darcy]
K_I	Stress intensity factor (opening mode I)	[MPa $m^{1/2}$]
K_{IC}	Fracture toughness (opening mode I)	[MPa $m^{1/2}$]
L_c	Length of the casing string (not cemented)	[m]
L_{OH}	Length of the open-hole section	[m]
LOP	Leak-Off Pressure	[MPa]

LOT	Leak-Off Test	-
LOV	Leak-Off Volume	[liter]
LP	Limit pressure	[MPa]
P	Pressure	[MPa]
P_{FI}	Fracture initiation pressure	[MPa]
P_i	Internal pressure	[MPa]
P_o	External pressure	[MPa]
R	Radial coordinate	[m]
R_i	Inside radius	[m]
R_o	Outside radius	[m]
R_w	Wellbore radius	[m]
s	Thickness of the plastic zone	[m]
S_1, S_2, S_3	Principal stresses	[MPa]
S_{oil}	Oil saturation	[-]
SSIP	Stabilized shut-in pressure	[MPa]
S_{solids}	Solids saturation	[-]
S_{water}	Mud saturation	[-]
T	Temperature	[K]
t	Time	[s]
TOC	Top of cement	[m]
U_m	Mechanical energy	[Nm]
U_s	Surface energy	[Nm]
V	Volume	[m³]
V_0	Initial volume	[m³]
V_{csg}	Volume of the casing	[m³]
V_{mud}	Volume of the drilling fluid	[m³]
W	Fracture width	[m]
x	Coordinate in fracture growth direction	[m]
xLOT	Extended Leak-Off Test	-
Y	Yield stress of initial wellbore failure	[MPa]
Y_g	Geometry factor	[-]

α_{mud}	Thermal expansion coefficient of drilling mud	[1/K]
β	Stress contrast	[-]
ε_r	radial strain	[-]
ε_z	horizontal strain	[-]
ε_σ	tangential strain	[-]
ϕ	Angle	[deg]
γ_s	Surface energy per unit area	[Nm]
ν	Poisson's ratio	[-]
σ_c	Compressional limit	[MPa]
σ_H	Maximum horizontal stress	[MPa]
σ_h	Minimum horizontal stress	[MPa]
σ_r	Radial stress	[MPa]
σ_t	Tensional limit	[MPa]
σ_z	Horizontal stress	[MPa]
σ_ϕ	Hoop stress	[MPa]

Si Metric Conversion Table

bbl	×	1.589	E – 01	=	m^3
in	×	2.54*	E – 02	=	m
ft	×	3.048*	E – 00	=	m
psi	×	6.894	E - 03	=	Pa

*Conversion factor is exact

Bibliography

Aadnoy, B. S., Vahid, M., & Hareland, G. (2009). Fracture Mechanics Interpretation of Leak-Off Tests. *presented at the 2009 Kuwait International Petroleum Conference, Kuwait City, Kuwait, 14 - 16 December.* SPE 126452.

Aadnoy, B., & Mesfin, B. (2004). elasto-plastic fracturing model for wellbore stability using non-penetrating fluids. *Journal of Petroleum Science and Engineering 45*, S. 179-192.

Altun, G., Langlinais, J., & Bourgoyne, A. T. (June 2001). Application of a New Model to Analyze Leak-Off Tests. *SPE Drilling & Completion*, S. 108 - 116.

Arzmüller, G., Buchta, S., Ralbovský, E., & Wessely, G. (2006). The Vienna Basin. In J. Golonka, & F. Picha, *The Carpathians and their foreland: Geology and hydrocarbon resources* (S. 191-204). AAPG Memoir 84.

Backers, T. (2004). *Fracture Toughness Determination and Micromechanics of Rock Under Mode I and Mode II Loading.* Potsdam, Germany: University of Potsdam.

Barree, R., & Winterfeld, P. (1998). Effects of Shear Planes and Interfacial Slippage on Fracture Growth and Treating Pressure. *presented at the SPE Annual Technical Conference and Exhibition held in New Orleans, Louisiana, USA, 27 - 30 September.* SPE 48926.

Bourgoyne, A. T., Millheim, K. K., Chenevert, M. E., & Young, F. S. (1986). *Applied Drilling Engineering.* Richardson, TX, USA: Society of Petroleum Engineers.

Brudy, M., & Raaen, A. M. (2001). Pump in / flow back test Reduce the Estimate of Horizontal In-Situ Stress Significantly. *presented at the SPE Annual Technical Conference and Exhibition, New Orleans, Lousiana 30.Sept - 3.Oct.* SPE 71367.

de Aguiar Almeidar, M. (1986). *Computer aided analysis of Formation Pressure Integrety Tests used in Oil Well Drilling.* Louisiana, USA: Louisiana State University.

Gabolde, G., & Nguyen, J.-P. (1999). *Drilling Data Handbook - 7th Edition.* Paris: Editions Technip.

Halliburton. (2010). *www.halliburton.com*. Retrieved March 17, 2011, from http://www.halliburton.com/ps

Harzhauser, M., Daxner-Höck, G., & Piller, W. E. (2004). An integrated stratigraphy of the Pannonian (Late Miocene) in the Vienna Basin. *Austrian Journal of Earth Sciences, Volume 95/96*.

Heger, A., & Spörker, H. F. (2011). Understanding XLOT's. *presented at the SPE/IADC Drilling Conference and Exhibition, Amsterdam, The Netherlannds, 1-3 March.* IADC/SPE 140028.

Kirsch, E. G. (1898). Die Theorie der Elastizität und die Bedürfnisse der Festigkeitslehre. *Zeitschrift des Vereines deutscher Ingenieure, 42*, S. 797–807.

Lee, D., Birchwood, R., & Bratton, T. (2004). Leak-Off Test Interpretation and Modeling with Application to Geomechanics. *presented at the 6th North America Rock Mechanics Symposium held in Houston, Texas, USA, 5 - 9 June.* ARMA/NARMS 04-547.

Lin, W., Yamamoto, K., Ito, H., Masago, H., & Kawamura, Y. (2008). Estimation of Minimum Principal Stress from an Extended Leak-off Test Onboard the Chikyu Drilling Vessel and Suggestions for Future Test Procedures. *Scientific Drilling, No. 6, July*, 43 - 47.

Meier, M., & Ermanni, P. (September 2010). *Dimensionieren 1 - Skript zur Vorlesung 151-0303-00L.* Zürich, Switzerland: ETH Zürich.

Meng, C., & de Parter, C. (2011). Hydraulic Fracture Propagation in Pre-Fractured Natural Rock. *presented at the SPE Hydraulic Fracturing Technology Conference and Exhibition held in The Woodlands, Texas, USA, 24 - 26 January.* SPE 140429.

Park, N. (2006). *Discrete Element Modeling of Rock Fracture Behaviour: Fracture Toughness and time-dependent fracture growth.* Austin, TX, USA: University of Texas at Austin.

Postler, D. P. (1997). Pressure Integrety Test Interpretation. *presented at the annual Technical Conference and Exhibition, Amsterdam, The Netherlands, 4. - 6. March.* SPE 37589.

Raaen, A. M., Skomedal, E., Kjorholt, H., Markestad, P., & Økland, P. (8. April 2001). Stress determination from hydraulic fractureing tests - the system stiffness approach. *International Journal of Rock Mechanics & Mining Sciences 38*, S. 529–541.

Rezmer-Cooper, I. M., Rambow, F. H., Arasteh, M., Hashem, M. N., Swanson, B., & Gzara, K. (2000). Real-Time Formation Integrity Tests Using Downhole Data. *presentation at the 2000 IADC/SPE Drilling Conference, New Orleans, Louisiana, 23–25 February*. IADC/SPE 59123.

van Oort, E., & Vargo, R. (2007). Improving Formation Strength Tests and Their Interpretation. *presented at the SPE/IADC Drilling Conference, Amsterdam, The Netherlands, 20 - 22 February.* SPE/IADC 105193.

Wijesinghe, A. M. (1987). *Extended Analysis of Constant-Height Hydraulic Fractures for the Estimation of In-Situ Crack-Opening Modulus from Bottomhole Pressure Records.* Livemore: Lawrence Livermore National Laboratory.

Zihai, S. (2009). *Crack Analysis in Structural Concrete - Theory and Application.* Burlington, USA: Elsevier Ltd.

Zoback, M. D. (2008). *Reservoir Geomechanics.* New York, NY, USA: Cambridge University Press.